AWARD NUMBER: W81XWH-16-1-0064

TITLE: Inside-Out Immunotherapy: Preventing Metastatic Breast Cancer Recurrence via Nanoparticle-Directed Modulation of the Tumor Microenvironment

PRINCIPAL INVESTIGATOR: Rebecca S. Cook, Ph.D.

CONTRACTING ORGANIZATION: Vanderbilt University

REPORT DATE: SEPTEMBER 2020

TYPE OF REPORT: Final

PREPARED FOR: U.S. Army Medical Research and Development Command
Fort Detrick, Maryland 21702-5012

REPORT DOCUMENTATION PAGE

Form Approved
OMB No. 0704-0188

1. REPORT DATE	**2. REPORT TYPE**	**3. DATES COVERED**
SEPTEMBER 2020	Final	**15MAY2016 - 14MAY2020**

4. TITLE AND SUBTITLE;

Inside-Out Immunotherapy: Preventing Metastatic Breast Cancer Recurrence via Nanoparticle-Directed Modulation of the Tumor Microenvironment

5a. CONTRACT NUMBER
W81XWH-16-1-0064

5b. GRANT NUMBER
BC150791P1

5c. PROGRAM ELEMENT NUMBER

6. AUTHOR(S)

Rebecca S. Cook

E-Mail: rebecca.cook@vanderbilt.edu

5d. PROJECT NUMBER

5e. TASK NUMBER

5f. WORK UNIT NUMBER

7. PERFORMING ORGANIZATION NAME(S) AND ADDRESS(ES)

Vanderbilt University
Nashville TN 37232

8. PERFORMING ORGANIZATION REPORT NUMBER

9. SPONSORING / MONITORING AGENCY NAME(S) AND ADDRESS(ES)

U.S. Army Medical Research and Development Command
Fort Detrick, Maryland 21702-5012

10. SPONSOR/MONITOR'S ACRONYM(S)

11. SPONSOR/MONITOR'S REPORT NUMBER(S)

12. DISTRIBUTION / AVAILABILITY STATEMENT

Approved for Public Release; Distribution Unlimited

13. SUPPLEMENTARY NOTES

14. ABSTRACT

Purpose. We proposed to design and validate immunotherapeutic nanoparticles (IT-NPs) for precise immunomodulation of the tumor microenvironment. Our hypothesis is that that activation of RIG-I in combination with intra-tumoral silencing of TGF-beta receptor 2 will induce systemic antitumor immunity for eradicating local disease, distant disease, and future recurrences.

Scope: We proposed to (1) develop IT-NPs for intra-tumoral delivery breast tumors (led by Initiating PI Wilson); (2) evaluate the effect of local RIG-I activation in breast cancer cells and in the breast TME in immunocompetent mice (led by Partnering PI Cook); and (3) demonstrate that IT-NPs induce breast tumor regression, eliminate metastatic tumors, and prevent future metastatic recurrence using mouse breast cancer models (Wilson and Cook together).

Major Findings: 1.) The RIG-1 mimetic (5'ppp-HP20) potently activates Type I inflammatory cytokines in human and mouse breast cancer cells; 2.) The RIG-1 mimetic fails to induce inflammation in breast cancer cells with genomic loss of *DDX58*, the gene encoding RIG-1. 3.) The RIG-I mimetic induces pyroptotic cell death in breast cancer cells; 4.) Intra-tumoral IT-NP delivery of RIG-I mimetic decreased growth and metastasis of breast cancers in immune-competent mice.

Significance.1.) RIG-I mimetic induced inflammatory cytokines and pyroptosis (an immunogenic cell death), which will maximize anti-tumor immune responses while reducing tumor cell burden directly. 2.) Tumor *DDX58* can be used to predict response (or lack of response) to RIG-I mimetics.

15. SUBJECT TERMS
RIG-I, Nanoparticle, Breast Cancer, Metastasis, Tumor growth, Anti-tumor immunity, Immunotherapy, Gene silencing

16. SECURITY CLASSIFICATION OF:			**17. LIMITATION OF ABSTRACT**	**18. NUMBER OF PAGES**	**19a. NAME OF RESPONSIBLE PERSON**
a. REPORT	**b. ABSTRACT**	**c. THIS PAGE**			USAMRMC
Unclassified	Unclassified	Unclassified	UU	62	**19b. TELEPHONE NUMBER** *(include area code)*

1. **INTRODUCTION:** This project pursues a new approach to preventing metastatic breast cancer recurrence through the development of a novel immunotherapeutic technology that generates antitumor immunity via reprograming of the tumor microenvironment (TME). Our approach is based on sustained intratumoral release of multifunctional immunotherapeutic nanoparticles (IT-NPs) that precisely re-shape the TME through coordinated immunostimulation and blockade of immunosuppression. IT-NPs promote efficient cytosolic delivery of novel RNA therapeutics designed to activate antitumor innate immunity via the retinoic acid-inducible gene I (RIG-I) pathway while concurrently silencing key immunosuppressive pathways, including TGF-β signaling. The ***overall objective*** of this grant is to develop injectable IT-NP delivery platform that allows for precise immunomodulation of the TME, and to investigate how the dynamics of TME reprogramming influence tumor growth and induction of anti-tumor immunity. We ***hypothesize*** that activation of RIG-I combined with silencing of TGF-β receptor 2 (TβR2) will increase the immunogenicity of the TME, resulting in induction of local and systemic anti-tumor immunity and immune memory that can eliminate local and disease and prevent future recurrence.

2. KEYWORDS: RIG-I, Nanoparticle, Breast Cancer, Metastasis, Tumor growth, Anti-tumor immunity, Immunotherapy, Gene silencing

3. ACCOMPLISHMENTS:

What were the major goals of the project? The overall goal of this project is to prevent metastatic breast cancer recurrence through the development of a novel *in situ* vaccination strategy for generating antitumor immunity and immune memory. To accomplish this, we are designing and validating an injectable IT-NP delivery platform that allows for precise immunomodulation of the TME. We are pursuing the following Specific Aims:

Aim 1: Develop an injectable delivery platform for sustained and tunable release of immunotherapeutic nanoparticles (IT-NPs) to breast tumors.

Aim 2: Evaluate the effect of local TβR2 silencing and RIG-I activation on the breast tumor microenvironment in an immunocompetent murine model of metastatic breast cancer.

Aim 3: Demonstrate the efficacy of local and temporally regulated immunomodulation of the breast TME in mediating breast tumor regression, eliminating established breast cancer metastases, and preventing future metastatic recurrence of breast cancer.

The following Tasks from the Statement of Work are color coded to represent Tasks led by the Initiating PI John Wilson (in gray) or Partnering PI Rebecca Cook (in blue). Those tasks which represent significant intercalation of efforts from the Initiating PI and Partnering PI are indicated in green.

<u>Specific Aim 1:</u> Develop a platform for controlled, sustained and tunable release of immunotherapeutic nanoparticles (IT-NPs) to breast tumors.

Major Task 1: Synthesize and characterize "smart" nanoparticles for cytosolic delivery of 5'ppp-TβR2 siRNA

Subtask 1: Synthesize "smart" polymeric nanoparticles, characterize polymer molecular weight and polydispersity, and measure particle size by dynamic light scattering. **Months 1-2.**

Status: These projects were completed in Year 1 (see Y1 progress report, 2017).

Subtask 2: Screen TβR2 siRNA sequences in mammary tumor epithelial cells from MMTV-PyMT mice, macrophages, and dendritic cells (DCs) to select one with an IC50 of 10 nM or less. **Months 2-4.**

Status: These projects were completed in Year 1 (see Y1 progress report, 2017).

Subtask 3: Synthesize 2-3 mg 5'ppp-siTβR2 and control sequences. Demonstrate TβR2 knockdown and RIG-I-dependent IFN-β secretion in primary mammary tumor epithelial cells, macrophages, and DCs. **Months 4-5.**

Status: These projects were completed in Year 1 (see Y1 progress report, 2017).

Major Task 2: Develop PLGA micro-particles for controlled release of IT-NPs.

Subtask 1: Use a water-in-oil-in-water emulsion method to load IT-NPs into 5-10 μm PLGA microparticles formulated with 0, 1.25, 2.5, and 5 wt% trehalose to control release kinetics. Characterize microparticle size, polydispersity, and porosity via TEM and SEM. **Months 3-6.**

Status: These projects were completed in Year 1 (see Y1 progress report, 2017).

Subtask 2: Determine microparticle IT-NP loading capacity and encapsulation efficiency and measure the *in vitro* release kinetics of IT-NPs from microparticles fabricated with different amounts of trehelose. Fit with transport models to determine half-maximal release for each formulation. **Months 6-8.**

Status: These projects were completed in Year 1 (see Y1 progress report, 2017).

Subtask 3: Compare the siRNA silencing and RIG-I activity of IT-NPs released from microparticles to freshly-prepared IT-NPs. **Months 6-8.**

Status: These projects were completed in Year 2 (see Y2 progress report, 2018).

Major Task 3: Characterize the intratumoral retention time of IT-NPs from microspheres delivered to TME.

Subtask 1: Using the *MMTV-PyVmT* syngeneic mammary tumor model, perform preliminary dosing (0.1-1 mg.kg RNA) and safety studies. Monitor animals for local and systemic side effects and quantify TβR2 knockdown as an initial validation of delivery. **Months 8-12.**

Status: These experiments were completed in Y1 using a 3pRNA RIG-I ligand complexed to free IT-NPs (see Y1 progress report, 2017).

Subtask 2. Administer IT-NP release depots into tumors and quantify local IT-NP retention as a function of time using whose animal fluorescent imaging. **Months 8-12.**

Status: These projects were completed in Year 2 (see Y2 progress report, 2018).

<u>Specific Aim 2</u>: Evaluate the effect of local TβR2 silencing and RIG-I activation on the breast tumor microenvironment.

Major Task 1: Characterize the tissue- and cell-level biodistribution of intratumorally administered IT-NPs.

Subtask 1: Characterize the cellular uptake of IT-NPs by tumor cell and leukocytes in the TME and TDLN at 24 h, 96h, 1wk, 2wk, and 1 month using flow cytometric analyses. **Months 8-12.**

Status: These experiments were completed in Year 3 (see Y3 progress report, 2019

Subtask 2: Characterize systemic IT-NP biodistribution in the blood, liver, lung, kidney, heart, and spleen using whole organ fluorescent imaging. **Months 12-15.**

Status: These projects were completed in Year 2 (see Y2 progress report, 2018).

Major Task 2: Quantify local TβR2 knockdown and RIG-I mediated type-I IFN production in vivo.

Subtask 1: Quantify TβR2 expression in tumor at 24h, 96h, 1 wk, 2 wks, and 1 month. Western analysis for phospho-Smad2/3 and total Smad2/3 will be performed. Flow cytometric analysis will be used to quantify TβR2 expression by breast cancer cells, macrophages, dendritic cells, and MDSCs. **Months 15-20**.

Status: These projects were completed in Year 2 (see Y2 progress report, 2018).

Subtask 2: Quantify IFN-α/β induction in tumor and TDLN homogenates via RT-PCR and/or ELISA at 24h, 96h, 1 week, 2 weeks and 1 month. Western analysis for phospho-IRF3 will be performed to confirm induction of IFN signaling. **Months 15-20.**

Status: These projects were completed in Year 2 (see Y2 progress report, 2018).

Major Task 3: Characterize the effect of local IT-NP delivery on local leukocyte populations and cytokine profiles

Subtask 1: Assess leukocyte populations in tumors. Antibody panels to identify macrophages, MDSCs, DCs, NK cells, CD8+ T cells, CD4+ T cells, and regulatory T cells will be used to monitor changes in cellular infiltrate 24h, 96h, 1 week, 2 weeks and month post particle administration. **Months 20-26.**

Status: These studies were completed in Year 3 (see Y3 progress report, 2019).

Subtask 2: Measure cytokine levels (including IL-4, IL-1α/β, IL-10, IL-6, IL-12, IL-2, INF-γ, TGF-β, and TNF-α) in tumor and TDLN lysates using cytokine arrays, and RT-PCR. **Months 20-26.**

Status: These studies were completed in Year 3 (see Y3 progress report, 2019)

Specific Aim 3. Demonstrate the efficacy of local and temporally regulated modulation of the breast TME in mediating breast tumor regression, eliminating established breast cancer metastases, and preventing future metastatic recurrence of breast cancer.

Major Task 1: Evaluate the efficacy of local IT-NP delivery in preventing tumor growth and metastasis and protection from re-challenge in an orthotopic model.

Subtask 1: Administer microparticles for IT-NP into mammary tumors, monitoring tumor volume throughout treatment and measuring tumor metastases upon sacrifice at treatment day 28. **Months 24-36.**

Status: These studies were completed in Year 3 (see Y3 progress report, 2019).

Subtask 2: Re-challenge mice receiving IT-NP formulations that inhibit tumor growth and metastasis for three months with luciferase-expressing tumor cells. **Months 30-36.**

Status: These studies were completed in Year 3 (see Y3 progress report, 2019).

Major Task 2: Evaluate the efficacy of local IT-NP delivery in two spontaneous breast cancer models.

Subtask 1: Administer optimized IT-NP depots into 200 mm^3 primary breast tumors in MMTV-PyMT mice. Measure tumor growth, metastasis, and survival. **Months 30-36.**

Status: These studies were completed in Year 3 (see Y3 progress report, 2019).

Subtask 2: Administer optimized IT-NP depots into 200 mm^3 primary breast tumors in MMTV-Neu mice. Measure tumor growth, metastasis, and survival. **Months 30-36.**

Status: These studies were completed in Year 3 (see Y3 progress report, 2019)..

What was accomplished under these goals?

Our findings are published in peer-review journals. PDF versions of the published reports are included as Appendix materials.

What opportunities for training and professional development has the project provided?

Five graduate students, **Max Jacobson** and **Christian Palmer** in the lab of the Initiating PI John Wilson, and **Michelle Williams** and **David Elion** from the lab of the partnering PI Rebecca Cook, and one post-doctoral research fellow, **Dr. Thomas Werfel** from the Cook Lab, worked on aspects of this project. Each student gained valuable experience in studying cell-based assays to assess RIG-I signaling, cell death, and

expression analysis. Each graduate student regularly presented results at group meetings. In addition, Mr. Jacobson has mastered polymer synthesis and nanoparticle fabrication and characterization, and has gained experience in characterizing innate immune responses. This project also involved a postdoctoral fellow in the Wilson Lab, **Dr. Sema Sevimli** who expanded upon her training in polymer chemistry with complementary expertise in design and optimization of microparticle depots for controlled release. Additionally, Dr. Sevimli received co-mentorship from Dr. Cook in breast cancer biology and evaluating nanoparticle therapeutics and delivery depots in animal models of breast cancer. All trainees regularly presented results at group meetings, and Mr. Jacobson, Mr. Elion, and Dr. Sevimli were regular attendees and contributors at a monthly project planning meeting held between the Wilson, Cook, and Duvall groups. Two undergraduate students, **Linus Lee** (Vanderbilt University School of Engineering) and **Bushra Rahman** (Vanderbilt University, College of Arts and Sciences) participated in RIG-I research projects. These two undergraduate students and three graduate students listed above learned basic research skills and data analysis. Further, graduate student mentoring of undergraduates will build valuable mentoring, project management, and communication skills that will serve them throughout their careers. Finally, both Drs. Cook and Wilson worked with the Vanderbilt School for Science and Math, a Vanderbilt Community Outreach program to build STEM-focused opportunities for underserved/under-represented high school students in the Metro Nashville area, to recruit and train promising high school students. Dr. Cook used this project as a backdrop for this immersive summer experience.

How were the results disseminated to communities of interest?

These results have been published (Elion et al., *Cancer Research*, 2018; Palmer et al., *Bioconjug. Chem.*, 2018; Jacobson et al., *Biomat. Sci.*, 2018). presented at Cook lab meeting (11-2018 and 4-2019), and at Balko-Cook lab meeting (3-2019). These data were presented at the Microenvironmental Influences in Cancer Training Grant Scientific Forum at Vanderbilt University (June 2018), and the Cancer Biology Graduate Program Science Hour (October, 2018). These results were presented at the Vanderbilt-Ingram Cancer Center Retreat (May 2019).

What do you plan to do during the next reporting period to accomplish the goals?

Nothing to Report

4. **IMPACT:** *Describe distinctive contributions, major accomplishments, innovations, successes, or any change in practice or behavior that has come about as a result of the project relative to:*

a. **What was the impact on the development of the principal discipline(s) of the project?**

Our findings have led to the initial development of a new class of nanoparticle-based therapeutics that activate anti-tumor innate immunity while concurrently silencing mediators of immunosuppression. Because siRNA can be designed against virtually any target, this approach has broad potential for impact in cancer immunotherapy.

We have developed a novel "nano-in-micro" depot technology for sustained release of IT-NPs, which offers a new opportunity for sustaining anti-viral sensing and/or gene silencing in local immunotherapy applications.

These findings demonstrate that synthetic RIG-I agonists potently and specifically stimulate RIG-I signaling in breast cancer cells in culture and in vivo.

These findings demonstrate that a nanoparticle-based approach for RIG-I activation in vivo decreases breast tumor growth.

These findings show that RIG-I signaling induces breast cancer cell death through a tumor cell intrinsic pathway.

These findings demonstrate that IT-NPs that activate RIG-I potently increase the number of leukocytes that infiltrate breast tumors.

These findings show that IT-NPs that activate RIG-I modulate cytokines and chemokines in breast tumors, and increase expression of MHC-I on breast tumor cells.

These findings demonstrate that the number of lung metastases is reduced in tumor-bearing mice.

b. **What was the impact on other disciplines?**

This approach can be applied to a multitude of other cancers, as RIG-I is expressed in an abundance of cell types. Thus, multiple cancers could be screened using RIG-I agonists for response to RIG-I activation.

The PLGA depot technology has broad applicability for local gene silencing applications.

Sustained release of IT-NPs can also be leveraged for antigen-specific vaccine applications in both cancer and infectious disease.

The duration of viral infection and type-I interferon production can have a significant impact on the magnitude and phenotype of an immune response. The IT-NP depot technology may provide a tool for modulating the kinetics of viral sensing and understanding how this influences immunity.

IT-NPs enable efficient delivery of bi-functional 3p-siRNA designed for gene silencing and activation of RIG-I. This platform can be modified to silence a diversity of gene targets, leading to the design of novel immunotherapeutics and vaccine adjuvants..

c. **What was the impact on technology transfer?**

i. A provisional patent application describing a new class of environmentally-responsive RIG-I ligand was filed.:

d. **What was the impact on society beyond science and technology?**

We anticipate that the findings presented herein will be applied toward therapeutic treatment of patients with breast cancer. Additionally, IT-NPs and controlled release formations have broad potential as cancer immunotherapeutics and as vaccine careers.

5. CHANGES/PROBLEMS:

a. Changes in approach and reasons for change

As introduced in our Year 1 progress report, upon realizing how little was reported in the literature regarding the impact of RIG-I signaling in breast cancer cells, we initiated investigations to understand RIG-I activation in the context of breast tumor cells per se. In order to interpret the data of the proposed experiments with more rigor, we required an initial basis of understanding of how breast cancer cells might react to RIG-I activation, specifically in the absence of tumor infiltrating leukocytes. This avenue of research made a substantial contribution to the field of breast cancer biology and to the field of immunotherapy, providing key observations that most breast cancers, but not all breast cancers, express RIG-I, and thus patients will need to be selected carefully prior to treatment with a RIG-I mimetic once these preclinical studies progress to clinical studies. Further, the observation that RIG-I signaling induces programmed cell death in breast cancer cells provides an added layer of therapeutic value to the use of RIG-I mimetics in treatment-resistant breast cancers. Finally, our finding that pyroptosis, rather than instrinsic apoptosis, is the mechanism underlying programmed cell death of breast cancer cells upon RIG-I induction provides a safeguard against the generation of immune tolerance, as is often seen following intrinsic apoptosis. Instead, pyroptosis is potentially immunogenic, and may cooperate with inflammatory cytokines and tumor-infiltrating leukocytes to bolster therapeutic anti-tumor immunity in breast cancer patients. .

b. Actual or anticipated problems or delays and actions or plans to resolve them

Nothing to report.

c. Changes that had a significant impact on expenditures

Nothing to report

d. Significant changes in use or care of human subjects, vertebrate animals, biohazards, and/or select agents

i. Nothing to report.

e. Significant changes in use or care of human subjects

N/A

f. Significant changes in use or care of vertebrate animals.

Nothing to report

g. Significant changes in use of biohazards and/or select agents

Nothing to report

6. PRODUCTS:

a. Publications

Journal publications.

Garland KM, Sevimli S, Kilchrist KV, Duvall CL, Cook RS, Wilson JT.. Microparticle Depots for Controlled and Sustained Release of Endosomolytic Nanoparticles. ***Cell Mol Bioeng.*** 2019 May 3;12(5):429-442. doi: 10.1007/s12195-019-00571-6. eCollection 2019 Oct

Elion DL, Cook RS. Activation of RIG-I signaling to increase the pro-inflammatory phenotype of a tumor. ***Oncotarget.*** 2019 Mar 22;10(24):2338-2339. doi: 10.18632/oncotarget.26729. eCollection 2019 Mar 22

Elion DL, Jacobson ME, Hicks DJ, Rahman B, Sanchez V, Gonzales-Ericsson PI, Fedorova O, Pyle AM, Wilson JT, Cook RS. Therapeutically Active RIG-I Agonist Induces Immunogenic Tumor Cell Killing in Breast Cancers. ***Cancer Res.*** 2018 Nov 1;78(21):6183-6195. doi: 10.1158/0008-5472.CAN-18-0730. Epub 2018 Sep 17

Elion DL, Cook RS. Genetic and Phenotypic Diversification of Heterogeneous Tumor Populations. ***Trends Mol Med.*** 2018 Aug;24(8):655-656. doi: 10.1016/j.molmed.2018.06.003. Epub 2018 Jun 28

Elion DL, Cook RS. Harnessing RIG-I and intrinsic immunity in the tumor microenvironment for therapeutic cancer treatment. ***Oncotarget.*** 2018 Jun 22;9(48):29007-29017. doi: 10.18632/oncotarget.25626. eCollection 2018 Jun 22

Other publications, conference papers, and presentations.

Departments of Immunobiology and Molecular, Cellular and Developmental Biology, Yale University, New Haven, CT. *Engineering Smart Nanotechnologies for Immuno-Oncology: Harnessing Cytosolic Immune Surveillance Pathways for Cancer Immunotherapy.* Invited Seminar (Wilson JT).

Southeastern Immunology Symposium, Vanderbilt University, Nashville, TN, *Engineering therapeutic activation of RIG-I to promote multi-faceted tumor cell killing.* Poster Presentation

Engineering Immunity Symposium, Vanderbilt University, Nashville, TN. *Optimizing pH-Responsive Diblock Copolymer Compositions for Cytosolic Delivery of RIG-I Agonist.* Poster Presentation

Cancer Biology Training Consortium, Stevenson, WA, *RIG-I activates TRAIL signaling and inflammasome-mediated pyroptosis to promote tumor cell death in luminal breast cancers*. Poster Presentation

Annual Cancer Biology Retreat, Vanderbilt University, Nashville, TN, *RIG-I activation promotes multi-faceted tumor cell killing in luminal breast cancer.* Poster Presentation.

Meharry Medical College/ Vanderbilt Ingram Cancer Center/ Tennessee State University Cancer Partnership Annual Retreat (Health Disparities in Cancer Immunology and Immune Therapy), *Therapeutically active RIG-I agonists increase immunogenic tumor cell killing in breast cancer cells.* Poster Presentation

Website(s) or other Internet site(s)

nothing to report

Technologies or techniques

Intratumoral delivery of IT-NPs

Formulation methods for generating PLGA depots for IT-NP relase/delivery

Inventions, patent applications, and/or licenses

Nothing to report

Other Products

i. PLGA depots for IT-NP release (Intellectual property has not yet been filed on this invention)

Nanoparticles for cytosolic delivery of RIG-I ligands (Intellectual property has not yet been filed on this invention)

RIG-I prodrugs based on synthetic polymer overhangs (A provisional patent has been filed: **Wilson JT**, Palmer C. Retinoic acid-inducible gene I (RIG-I) prodrugs and methods of use thereof. Provisional patent 62615370 filed January 9, 2018.

PARTICIPANTS & OTHER COLLABORATING ORGANIZATIONS

b. **What individuals have worked on the project?**

Name:	*John T. Wilson*
Project Role:	*PI*
Researcher Identifier (e.g. ORCID ID):	*Unknown*
Nearest person month worked:	*2.5*
Contribution to Project:	*Guidance of graduate students, postdocs, and research staff in the work (particle development, tumor immunology)*

Name:	*Rebecca Cook*
Project Role:	*Partnering PI*
Researcher Identifier (e.g. ORCID ID):	*Unknown*
Nearest person month worked:	*2*
Contribution to Project:	*Guidance of graduate students, postdocs, and research staff in the work (cancer biology, tumor models, microenvironment)*

Name:	*Craig Duvall*
Project Role:	*Co-Investigator*
Researcher Identifier (e.g. ORCID ID):	*Unknown*
Nearest person month worked:	*1.5*
Contribution to Project:	*Guidance on depot development and characterization; support on IVIS imaging.*

Name:	*Max Jacobson*
Project Role:	*Graduate Student*
Researcher Identifier (e.g. ORCID ID):	*Unknown*
Nearest person month worked:	*12*

Contribution to Project:	*Mr. Jacobson synthesized polymers, generated IT-NP formulations, and investigated effects of IT-NP on breast cancer and immune cells.*
Funding Support:	*This project*

Name:	*Sema Sevimli*
Project Role:	*Postdoctoral Fellow*
Researcher Identifier (e.g. ORCID ID):	*Unknown*
Nearest person month worked:	*5*
Contribution to Project:	*Dr. Sevimli has lead efforts on PLGA depot formulation and evaluation of IT-NP in vitro and in vivo.*
Funding Support:	*Komen Foundation Postdoctoral Fellowship*

Name:	*Kyle Becker*
Project Role:	*Research Assistant II*
Researcher Identifier (e.g. ORCID ID):	*Unknown*
Nearest person month worked:	*3*
Contribution to Project:	*Mr. Becker provides full laboratory support for all culture and animal experiments performed in the Wilson Lab*
Funding Support:	*This project and other extramural support*

Name:	*Christian Palmer*
Project Role:	*Graduate Student*
Researcher Identifier (e.g. ORCID ID):	*Unknown*
Nearest person month worked:	*1*
Contribution to Project:	*Mr. Palmer contributed to the development of novel RNA immunotherapeutics for RIG-I activation*

Funding Support:	*Institutional and other extramural support*

Name:	*David Elion*
Project Role:	*Graduate Student*
Researcher Identifier (e.g. ORCID ID):	*Unknown*
Nearest person month worked:	*3*
Contribution to Project:	*Mr. Elion provided RT-qPCR analysis of breast cancer cell lines transfected with 5'ppp-HP20 and HP20.*
Funding Support:	*Tumor Microenvironmental Influences in Cancer T32 Training Grant*

Name:	*Michelle Williams*
Project Role:	*Graduate Student*
Researcher Identifier (e.g. ORCID ID):	*Unknown*
Nearest person month worked:	*1*
Contribution to Project:	*Ms. WIlliams provided western analysis of breast cancer cell lines transfected with 5'ppp-HP20 and HP20.*
Funding Support:	*NCI F31 Fellowship*

Name:	*Linus Lee*
Project Role:	*Undergraduate Student*
Researcher Identifier (e.g. ORCID ID):	*Unknown*
Nearest person month worked:	*<1*
Contribution to Project:	*Mr. Lee provided cell culture support for breast cancer cell lines.*
Funding Support:	*N/A*

Name:	*Bushra Rahman*
Project Role:	*Undergraduate Student*
Researcher Identifier (e.g. ORCID ID):	*Unknown*
Nearest person month worked:	*>1*
Contribution to Project:	*Ms. Rahman provided qRT-PCR support for cells transfected with 5'ppp-HP20 and HP20.*
Funding Support:	*Biomedical Engineering Scholarship*

Name:	*Selvia Waghu*
Project Role:	*High School Student*
Researcher Identifier (e.g. ORCID ID):	*Unknown*
Nearest person month worked:	*>1*
Contribution to Project:	*Ms. Waghu provided basic lab support and cell culture support.*
Funding Support:	*Vanderbilt School for Science and Math*

Name:	*Donna Hicks*
Project Role:	*Laboratory Manager*
Researcher Identifier (e.g. ORCID ID):	*Unknown*
Nearest person month worked:	*4*
Contribution to Project:	*Ms. Hicks provided full laboratory support and infrastructure for all cell culture, western, RT-qPCR, and aanimal modeling experimentation*
Funding Support:	*This grant*

c. **Has there been a change in the active other support of the PD/PI(s) or senior/key personnel since the last reporting period?**

The Initiating PI (Wilson) has been awarded additional grants since the last reporting period. These new grants are listed below and none have overlap with this grant.

Funding Agency: DoD CDMRP BCRP / Era of Hope Scholar Award
Title: "Translating immunotherapy to breast cancer: mechanisms, biomarkers, and rationally designed therapeutic combinations"
Performance Period: 07/01/2018-05/31/2022
Role: Co-I (PI: J. Balko)

Funding Agency / Mechanism: National Institutes of Health / R01
Title: "Neoantigen-Based Therapeutic Targeting of Head and Neck Cancers"
Performance Period: 07/01/18-06/30/23
Role: Co-I (Co-PI: S. Joyce and Y. Kim)

Funding Agency/ Mechanism: Veterans Administration / Merit Award
Title: "Vaccinating at Mucosal Surfaces with Nanoparticle Conjugated Antigen and Adjuvant"
Performance Period: 07/01/2018-05/31/2023
Level of Funding:
Role: Co-I (PI: S. Joyce)

Funding Agency / Mechanism: DoD CDMRP KCRP / Idea Development Award
Title: "Reinvigorating Anti-Tumor Immunity in Renal Cell Carcinoma with Nanoparticulate STING Agonists"
Performance Period: 10/01/2018-09/30/2021

d. **What other organizations were involved as partners?**

    i. Nothing to report

ii.

7. SPECIAL REPORTING REQUIREMENTS

a. **COLLABORATIVE AWARDS:**

The Initiating PI, Dr. John Wilson, has submitted his final report for this Partnering PI grant award.

b. **QUAD CHARTS:**

N/A

8. APPENDICES:

i. Garland KM, Sevimli S, Kilchrist KV, Duvall CL, Cook RS, Wilson JT.. Microparticle Depots for Controlled and Sustained Release of Endosomolytic Nanoparticles. ***Cell Mol Bioeng.*** 2019 May 3;12(5):429-442. doi: 10.1007/s12195-019-00571-6. eCollection 2019 Oct

ii. Elion DL, Cook RS. Activation of RIG-I signaling to increase the pro-inflammatory phenotype of a tumor. ***Oncotarget.*** 2019 Mar 22;10(24):2338-2339. doi: 10.18632/oncotarget.26729. eCollection 2019 Mar 22

iii. Elion DL, Jacobson ME, Hicks DJ, Rahman B, Sanchez V, Gonzales-Ericsson PI, Fedorova O, Pyle AM, Wilson JT, Cook RS. Therapeutically Active RIG-I Agonist Induces Immunogenic Tumor Cell Killing in Breast Cancers. ***Cancer Res.*** 2018 Nov 1;78(21):6183-6195. doi: 10.1158/0008-5472.CAN-18-0730. Epub 2018 Sep 17

iv. Elion DL, Cook RS. Harnessing RIG-I and intrinsic immunity in the tumor microenvironment for therapeutic cancer treatment. ***Oncotarget.*** 2018 Jun 22;9(48):29007-29017. doi: 10.18632/oncotarget.25626. eCollection 2018 Jun 22

Cellular and Molecular Bioengineering, Vol. 12, No. 5, October 2019 *(© 2019)* pp. 429–442
https://doi.org/10.1007/s12195-019-00571-6

Microparticle Depots for Controlled and Sustained Release of Endosomolytic Nanoparticles

Kyle M. Garland,[1] Sema Sevimli,[1] Kameron V. Kilchrist,[2] Craig L. Duvall,[2] Rebecca S. Cook,[3,4,5] and John T. Wilson [1,2,4,5]

[1]Department of Chemical and Biomolecular Engineering, Vanderbilt University, Nashville, TN, USA; [2]Department of Biomedical Engineering, Vanderbilt University, Nashville, TN, USA; [3]Department of Cell and Developmental Biology, Vanderbilt University, Nashville, TN, USA; [4]Cancer Biology Program, Vanderbilt University, Nashville, TN, USA; and [5]Vanderbilt-Ingram Cancer Center, Vanderbilt University Medical Center, Nashville, TN, USA

(Received 17 February 2019; accepted 22 April 2019; published online 3 May 2019)

Associate Editor Michael R. King oversaw the review of this article.

Abstract

Introduction—Nucleic acids have gained recognition as promising immunomodulatory therapeutics. However, their potential is limited by several drug delivery barriers, and there is a need for technologies that enhance intracellular delivery of nucleic acid drugs. Furthermore, controlled and sustained release is a significant concern, as the kinetics and localization of immunomodulators can influence resultant immune responses. Here, we describe the design and initial evaluation of poly(lactic-*co*-glycolic) acid (PLGA) microparticle (MP) depots for enhanced retention and sustained release of endosomolytic nanoparticles that enable the cytosolic delivery of nucleic acids.

Methods—Endosomolytic *p*[DMAEMA]$_{10kD}$-*bl*-[PAA$_{0.3}$-*co*-DMAEMA$_{0.3}$-*co*-BMA$_{0.4}$]$_{25kD}$ diblock copolymers were synthesized by reversible addition-fragmentation chain transfer polymerization. Polymers were electrostatically complexed with nucleic acids and resultant nanoparticles (NPs) were encapsulated in PLGA MPs. To modulate release kinetics, ammonium bicarbonate was added as a porogen. Release profiles were quantified *in vitro* and *in vivo via* quantification of fluorescently-labeled nucleic acid. Bioactivity of released NPs was assessed using small interfering RNA (siRNA) targeting luciferase as a representative nucleic acid cargo. MPs were incubated with luciferase-expressing 4T1 (4T1-LUC) breast cancer cells *in vitro* or administered intratumorally to 4T1-LUC breast tumors, and silencing *via* RNA interference was quantified *via* longitudinal luminescence imaging.

Results—Endosomolytic NPs complexed to siRNA were effectively loaded into PLGA MPs and release kinetics could be modulated *in vitro* and *in vivo via* control of MP porosity, with porous MPs exhibiting faster cargo release. *In vitro*, release of NPs from porous MP depots enabled sustained luciferase knockdown in 4T1 breast cancer cells over a five-day treatment period. Administered intratumorally, MPs

Address correspondence to John T. Wilson, Department of Chemical and Biomolecular Engineering, Vanderbilt University, Nashville, TN, USA. Electronic mail: john.t.wilson@vanderbilt.edu

John T. Wilson is an Assistant Professor of Chemical and Biomolecular Engineering and Biomedical Engineering at Vanderbilt University. He received his B.S. in Bioengineering from Oregon State University and his Ph.D. from the Georgia Institute of Technology in the laboratory of Professor Elliot L. Chaikof, where he was awarded a Whitaker Foundation Graduate Fellowship. He then joined the laboratory of Professor Patrick Stayton at the University of Washington with support of a Cancer Research Institute Postdoctoral Fellowship. He started his independent laboratory at Vanderbilt in January of 2014, where his group works at the interface of molecular engineering and immunology to innovate technologies to improve human health. His multidisciplinary research program is supported by productive and synergistic collaborations with oncologists, cancer biologists, immunologists, chemists, and other engineers. Since establishing his lab at Vanderbilt, he has been awarded the NSF CAREER Award, an 'A' Award from Alex's Lemonade Stand Foundation, a Melanoma Research Alliance Young Investigator Award, an Innovative Research Grant from Stand Up To Cancer, and has been named an Emerging Investigator by *Biomaterials Science*.

This article is part of the 2019 CMBE Young Innovators special issue.

Kyle Garland and Sema Sevimli contributed equally to this paper.

prolonged the retention of nucleic acid within the injected tumor, resulting in enhanced and sustained silencing of luciferase relative to a single bolus administration of NPs at an equivalent dose.
Conclusion—This work highlights the potential of PLGA MP depots as a platform for local release of endosomolytic polymer NPs that enhance the cytosolic delivery of nucleic acid therapeutics.

Keywords—Nucleic acid therapeutics, Local delivery, Intratumoral, Immunotherapy, RNA interference, Endosomal escape, PLGA, Biomaterial, Drug delivery depot.

ABBREVIATIONS

BMA	Butyl methacrylate
DCM	Dichloromethane
DMAEMA	Dimethylaminoethyl methacrylate
D-PDB	Poly[DMAEMA]$_{10kD}$-*block*-[PAA$_{0.3}$-*co*-DMAEMA$_{0.3}$-*co*-BMA$_{0.4}$]$_{25kD}$
ECT	4-Cyano-4-(ethylsulfanylthiocarbonyl) sulfanylpentanoic acid
MP	Microparticle
NP	Nanoparticle
PAA	Propylacrylic acid
PLGA	Poly(lactic-*co*-glycolic) acid
PVA	Polyvinyl alcohol
SEM	Scanning electron microscopy
V-70	2,2′-Azobis(4-methoxy-2,4-dimethyl valeronitrile)

INTRODUCTION

Nucleic acids have emerged as a promising class of immunotherapeutics with potential to treat numerous diseases, including infections, inflammation, autoimmunity, and cancer.[20,33,42,43,57,79,85] This broad and versatile class of biomacromolecular drugs can be leveraged to both activate and suppress the immune system. Notably, short-interfering RNA (siRNA) can be utilized to selectively inhibit expression of specific immunoregulatory proteins through RNA interference (RNAi),[26,57,68,76,79] allowing for precision tailoring of immune responses. Additionally, nucleic acids that chemically or structurally mimic pathogenic genetic material can be harnessed to activate the innate immune system by targeting various nucleic acid sensing pathways, which have evolved to detect viral or bacterial invasion.[13,20,33,42,43,84,85] Nucleic acids have been widely explored as adjuvants to bolster responses to vaccines,[70] and more recently as cancer immunotherapeutics that initiate inflammatory programs at tumor sites to stimulate antitumor immunity.[1,62] Despite their immense promise as immunomodulators, the clinical advancement of nucleic acid therapeutics has been relatively modest due to a multitude of challenges that hinder drug efficacy and/or patient safety.[11,63]

Inefficient intracellular delivery is a significant barrier to efficacy that is shared across virtually all types of nucleic acid therapeutics.[11,34,68,69,72,76] Nucleic acids do not passively diffuse across the plasma membrane, are cleared rapidly after administration, and are endocytosed with relatively low efficiency. Additionally, while several immunostimulatory nucleic acids (e.g. CpG DNA, poly(I:C)) act through receptors residing in endosomal membranes, a larger number must access cytosolic targets to exert their immunoregulatory effects. This includes more common classes of nucleic acid therapeutics that can be leveraged for immunotherapy, such as siRNA, miRNA, and mRNA, but also an emerging family of immunostimulatory agents that engage cytosolic pattern recognition receptors (PRRs), such as RIG-I, MDA-5, cGAS, and STING.[1,24,31] This pervasive challenge has led to the widespread development of synthetic nucleic acid carriers that enhance cellular uptake and promote endosomal escape of associated cargo.[4,36,66] Our group, and others, have recently utilized pH-responsive, endosomolytic polymer nanoparticles (NPs) to enhance the cytosolic delivery and activity of siRNA and immunostimulatory 5′-triphosphate RNA.[19,24,31,46] These NPs are assembled using amphiphilic diblock copolymers that self-assemble into micelles with a cationic dimethylaminoethyl methacrylate (DMAEMA) corona for electrostatic complexation of nucleic acids, and a pH-responsive, endosomolytic core comprising DMAEMA, butyl methacrylate (BMA), and propylacrylic acid (PAA) (Fig. 1b).[18,19] While highly efficient at cytosolic delivery, the cationic corona has restricted the use of such NPs to local delivery applications, including tissue regeneration, vaccine delivery, and intratumoral cancer immunotherapy.[7,31,73,77]

While systemic administration of nucleic acid therapeutics is necessary for many applications, directed, local delivery circumvents critical systemic delivery barriers and ensures sufficiently high doses reach target tissues, while also reducing systemic side effects.[52,66] Indeed, local delivery is commonly used, and often preferred, for many immunotherapeutics, the most salient example being vaccines, which are delivered intradermally or intramuscularly.[53,83] Additionally, image-guided, direct injection into lymph nodes (intranodal), considered the "command centers" of an immune response, is used clinically for treatment of allergy.[67] Finally, intratumoral injection of immunotherapeutics, including several different nucleic acids, has become increasingly prevalent in recent clin-

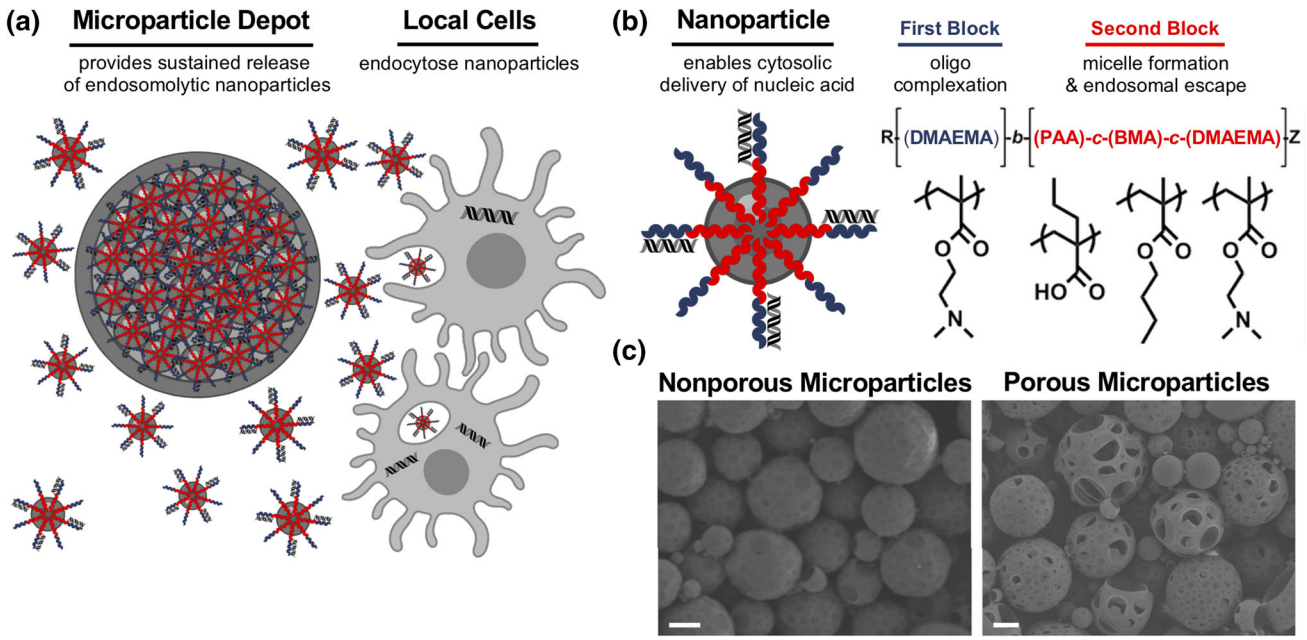

FIGURE 1. PLGA microparticle depots for controlled release of endosomolytic nanoparticles. (a) PLGA MP depots mediate local nanoparticle release and subsequent intracellular delivery of nucleic acid to local cell populations. (b) Structure and composition of the endosomolytic diblock copolymers used for cytosolic nucleic acid delivery. (c) Representative scanning electron microscopy (SEM) images of nonporous microparticles (left) and porous microparticles (right). Scale: 3 μm.

ical trials among substantial preclinical evidence that local immunotherapy can generate systemic immunity capable of eliminating distal, untreated tumors (e.g. abscopal effect).[48,71] However, for nearly all of these applications, multiple, repeated injections are necessary to stimulate desired immune responses and attendant therapeutic activitiy.[9,39,80] This requirement for multiple injections can pose a significant practical challenge for both physicians and patients and, in some cases, may not be feasible. Additionally, the timing, dose, and localization of immunomodulators plays a critical role in determining the magnitude and phenotype of the resultant immune response.[5,10,65,81,82] Yet, locally administered biomacromolecules, including nucleic acids, typically rapidly clear from the injection site, which not only limits local bioavailability but can also result in systemic distribution with an increased risk of toxicity.[37,39,80] These challenges have motivated the development of delivery technologies for controlled and sustained release of nucleic acid immunotherapeutics.[2,3,32,55,58,75] These drug delivery depots can be either injectable or implantable scaffolds or microparticles, and are typically composed of biodegradable materials that release cargo in a controlled and sustained manner.[64] Depots can also be engineered to exhibit a wide variety of drug release profiles by altering their chemical and physical properties.[14]

The NP system used here has been previously used in sustained and controllable release scaffolds aimed toward wound healing applications.[50,54,73] Here, we describe an intratumorally-injectable nanoparticle-in-microparticle strategy for controlled, localized delivery of cytosolically-active nucleic acid therapeutics. Poly(lactic-*co*-glycolic) (PLGA) microparticle (MP) depots were designed for sustained release of endosomolytic NPs that can mediate the cytosolic delivery of various nucleic acids, exemplified here by intratumoral delivery of siRNA. Through enhanced retention, controlled and sustained release, and prolonged functionality of encapsulated NPs, this approach offers a simple and potentially universally applicable strategy for achieving enhanced spatial and temporal control of nucleic acid delivery for applications in immunotherapy.

MATERIALS AND METHODS

Materials

All chemicals were supplied by Sigma Aldrich unless otherwise specified.

Synthesis of Endosomolytic Polymers

The amphiphilic diblock copolymer, poly(dimethylaminoethyl methacrylate)-*block*-[(propylacrylic acid)$_{0.3}$-*co*-(dimethylaminoethyl methacrylate)$_{0.3}$-*co*-(butyl methacrylate)$_{0.4}$] (p[DMAEMA]-*bl*-[PAA$_{0.3}$-*co*-DMAEMA$_{0.3}$-*co*-BMA$_{0.4}$]; D-PDB) was synthesized *via* reversible addition-fragmentation chain transfer

(RAFT) polymerizations following a protocol adapted from Convertine *et al.*[19] Briefly, 4-cyano-4-(ethylsulfanylthiocarbonyl)sulfanylpentanoic acid (ECT; Boron Molecular) was used as a chain transfer agent (CTA), and 2,2′-azobis(4-methoxy-2,4-dimethyl valeronitrile) (V-70; Wako Chemicals) was used as an initiator for RAFT polymerization. Mass measurements were performed using an analytical mass balance (XSE205DU DualRange; Mettler Toledo). Gravity filtration was employed in columns packed with aluminum oxide to remove inhibitors from monomer solutions. For the polymerization of the first block, DMAEMA, CTA, and initiator were dissolved in dioxane at a molar ratio of 100:1:0.05 at 40 wt% monomer, purged with nitrogen gas for 30 min on ice, and reacted at 30 °C for 18 h. The resultant polymer was then purified by precipitation (6x) in cold pentane followed by dialysis (3.5 kDa MWCO) in deionized water. Poly(-DMAEMA) was then frozen at − 80 °C and then lyophilized for 3 days to obtain a dry powder.

For the polymerization of the second block, poly(-DMAEMA) was used as a macroCTA (mCTA) and was added to DMAEMA, PAA, and BMA (30:30:40 mol%). PAA was synthesized as previously described using diethyl propylmalonate as the precursor.[25] Using N,N-dimethylacetamide (DMAC) as the reaction solvent, initiator was added to mCTA and monomers at a molar ratio of 450:1:0.4 representing total monomer, mCTA, and initiator, respectively at 40 wt% mCTA and monomer. The reaction vessel was purged with nitrogen gas for 30 min on ice followed by reaction for 24 h at 30 °C in an oil bath. The resultant polymer was then purified by precipitation (6×) in pentane:ether (80:20) followed by dialysis in acetone (4 exchanges) and subsequent dialysis in deionized water. D-PDB was then frozen at − 80 °C and then lyophilized for 3 days. All lyophilized polymer was stored at − 20 °C until used.

The experimental degree of polymerization, polymer composition, and theoretical molecular weight were obtained by ^{1}H nuclear magnetic resonance (NMR) Spectroscopy ($CDCl_3$ with TMS, Bruker AV 400). Experimental molecular weight and polydispersity were determined *via* gel permeation chromatography (GPC) using HPLC-grade dimethylformamide (DMF) containing 0.1% LiBr as a mobile phase with inline light scattering (Wyatt Technology) and refractive index (Agilent) detectors. The ASTRA V Software (Wyatt Technology) was used for all GPC calculations. Hydrodynamic size of the polymer micelles at physiological pH 7.4 was measured *via* digital light scattering (DLS) using a Zetasizer Nano ZS Instrument (Malvern, USA). D-PDB used herein had a 1st block molecular weight of 10.3 kDa, a 2nd block molecular weight of 31.0 kDa, and a polydispersity index (PDI) of 1.24. The 2nd block composition was determined to be 28:33:39 for PAA, DMAEMA, and BMA, respectively. Additionally, the hydrodynamic diameter of the D-PDB micelles was ~ 100 nm by an intensity particle size distribution.

Formulation of Polymer Nanoparticles and Nucleic Acid Complexes for In Vitro Experiments

Micellar nanoparticles (NPs) were formulated according to a protocol adapted from Wilson *et al.*[77] Lyophilized D-PDB was dissolved in ethanol to 50 mg/mL and rapidly diluted in 100 mM phosphate buffer (pH 7.0) to a concentration of 10 mg/mL to induce self-assembly into micelles. Polymer micelles were subsequently diluted in phosphate buffer saline (PBS; pH 7.4, 155 mM NaCl, 1.05 mM KH_2PO_3, 4 mM Na_2HPO_4, Gibco) to a concentration to 1 mg/mL. The micelles were then added to nucleic acid solutions at concentrations corresponding to a charge ratio (i.e. N/P ratio: molar charge from the polymer's tertiary amines relative to the molar charge of phosphate from the nucleic acid backbone) of 4:1. Note that the N:P ratio is based on the poly(DMAEMA) first block and assuming 50% protonation of DMAEMA groups at pH 7.4. D-PDB micelles and nucleic acid were incubated at room temperature for 20 min to ensure complete electrostatic complexation.

Formulation of Polymer Nanoparticles and Nucleic Acid Complexes for In Vivo Experiments

D-PDB micelles were formulated as described above, followed by sterile filtration (0.2 μm polyethersulfone sterile filter) and subsequent concentration to 30–60 mg/mL in PBS *via* centrifugal filtration (Amicon® Ultra 0.5 mL Centrifugal Filter Units; Ultracel®—3 K, Regenerated Cellulose 3000 NMWL, Millipore) following manufacturer's instructions. The final concentrated solution was collected, and an aliquot was used to determine the resultant polymer concentration using UV–Vis spectroscopy (Synergy H1 Multi-Mode Microplate Reader, Biotek) based on an absorbance-wavelength of 310 nm corresponding to ECT. The solution was added to nucleic acids at concentrations corresponding to a charge ratio (i.e. N/P ratio) of 4:1 as described above.

Cell Culture

All cell handling procedures were performed in accordance with published technical data sheets. Murine mammary epithelial 4T1-LUC tumor cells stably co-express destabilized copepod green fluorescent protein (cop-GFP) and firefly luciferase were

generated using psuedotyped lentiviral particles. Briefly, a transfection mixture consisting of pGreen-Fire1-CMV (System Biosciences, Cat. No. TR011PA-1), psPAX2 (Addgene Plasmid #12260), and pCMV-VSV-G (Addgene Plasmid #8454) in water at a quantity of 10, 10, and 1 μg, respectively, was added to a final volume of 558 μL in Opti-MEM media (Gibco, Cat. No. 31985062) in a polypropylene tube, followed by the addition of 42 μL FuGENE 6 (Promega, Cat. No. E2691). The tube was gently flicked to mix the plasmids before and after the addition of FuGENE 6. The transfection mixture was added dropwise to a T-75 tissue culture flask at approximately 50% confluency of HEK-293-T cells in 11 mL Dulbecco's modified eagle medium (DMEM, Gibco) supplemented to 10% heat-inactivated fetal bovine serum (HI-FBS) without antibiotics. Cells were incubated at 37 °C for 18 h, and then the media on the HEK-293-T cells was exchanged for DMEM supplemented with 10% HI-FBS and 1% penicillin/streptomycin (P/S). At 24 and 48 h after this media change, the viral supernatant was removed, clarified by centrifugation (1000×g, 5 min, room temperature) and syringe filtered (0.45 μm, nylon). To transduce 4T1 cells, viral supernatant was mixed 1:1 with fresh DMEM supplemented with 10% HI-FBS without antibiotics and applied to cells for 24 h. Cells were selected with 5 μg/mL puromycin for 2 weeks then sorted into approximately equal populations of low, medium, and high expressing cop-GFP cells using fluorescence activated cell sorting of GFP (BD FACSARIA IIIu, BD Biosciences) in the Vanderbilt Flow Cytometry Shared Resource Facility. The high expressing cop-GFP 4T1-LUC cells were used for all luminescent experiments herein. 4T1 and 4T1-LUC cells were maintained in DMEM supplemented with 2 mM L-glutamine, 4.5 g/L glucose, 10% HI-FBS, and 1% P/S. Cells were kept in a humidified environment at 37 °C with 5% CO_2. Puromycin was added to 4T1-LUC cells after every cell passage at a concentration of 1 μg/mL for the continual selection of cells.

Preparation of PLGA Microparticles Encapsulating Micellar Nanoparticles

PLGA MPs encapsulating pH-responsive NPs were formed using a water-in-oil-in-water ($W_1/O/W_2$) double emulsion synthesis method previously reported.[15,27,47,51,56] A fluorescently labelled double-stranded DNA (5′-[6FAM]ATAGGCGTATTA-TACGCGATTAACG-3′, negative control sequence) was used as representative cargo to determine the ideal conditions for the loading of NPs into PLGA MPs. Briefly, 100 mg of poly(D,L-lactide-*co*-glycolide) (PLGA, Resomer® RG 503, 50:50, ester-terminated, MW 24,000–38,000 Da) was dissolved in 750 μL of dichloromethane (DCM) for 30 min under continuous shaking at room temperature. 200 μL of NP solution (i.e. polyplexes prepared with D-PBD and various amounts of nucleic acid strands ranging in concentration from 1.9 nmol to 11.4 nmol) was added dropwise to the PLGA solution at a primary aqueous phase (W_1) to oil phase (O) volume ratio of 0.27. The primary emulsion (W_1/O) was prepared by sonicating the two phases for 30 s at 40% amplitude on ice using a Sonic Dismembrator (Fisher Scientific^{TM} Model 120). The secondary emulsion ($W_1/O/W_2$) was formulated by homogenizing the primary emulsion into 15 mL of 1% polyvinyl alcohol solution (PVA) for 30 s at 20,000 rpm on ice using a T18 digital ULTRA-TURRAX®, equipped with a S18N-10G dispersing tool (IKA). The double emulsion was then transferred to a round bottom flask and rotary evaporated for 1 h at 400 torr to allow complete evaporation of DCM. MPs were collected by centrifugation (10,000×g, 10 min, 4 °C) and washed 3 times with sterile water. PLGA MPs were then frozen at − 80 °C for 5 h and then lyophilized for 3 days. The effervescent salt, ammonium bicarbonate was employed as a porogen to create porous MPs. 20 wt% NH_4HCO_3 was incorporated into the W_1 aqueous phase along with the NPs and then emulsified with the oil phase as described. All PLGA MPs were stored at − 20 °C until used.

The hydrodynamic diameter of the PLGA MPs was measured by laser-diffraction size analysis using a Mastersizer 2000 (Malvern, USA). Approximately, 10–20 mg of PLGA MPs were dissolved in deionized water and used for analysis. Measurements detected within the acceptable range, between 10 and 15% obscuration, were deemed to be reproducible data points. Surface morphology and porosity of the PLGA MPs were analyzed using a Zeiss Merlin scanning electron microscope (SEM; Carl Zeiss Microscopy, LLC, ZEISS Group, Thornwood, NY) equipped with a GEMINI II column. SEM samples were prepared by reconstituting PLGA MPs in deionized water at a concentration of 2 mg/mL and then placing 20 μL of the solution on a strip of carbon tape (Ted Pella Inc.) adhered onto an aluminum SEM stub (Ø12.7 mm, Ted Pella Inc). After drying overnight, samples were sputter coated with gold–palladium for 120 s and immediately imaged *via* SEM.

Evaluation of Loading and Encapsulation Efficiency

To determine the nucleic acid loading and encapsulation efficiency, nucleic acids were extracted from PLGA MPs. In brief, 7.5 mg of PLGA MPs were dissolved in 400 μL DCM and continuously mixed for 45 min at room temperature. 400 μL of TE buffer supplemented with 100 mM NaCl was added to this

mixture and vortexed vigorously for 5 min. The suspension was then centrifuged (15,000×*g*, 10 min, 4 °C). The aqueous layer was collected into a fresh tube, and the extraction was performed again. The two extracted layers were combined, incubated with 1% sodium dodecyl sulfate (SDS) for 10 min at room temperature to disassemble the any electrostatically associated nucleic acids, and nucleic acid concentration was determined *via* fluorescence spectroscopy (excitation/emission wavelengths of 495/525 nm for 6FAM-DNA or 650/685 nm for Alexa Fluor® 647 (A647)-siRNA). Nucleic acid loading and encapsulation efficiencies were determined based on the ratio of encapsulated nucleic acid to PLGA MPs (μg/mg) and percentage relative to the theoretical maximum loading (%), respectively.

In Vitro Release of Nanoparticles from PLGA Microparticles

To investigate the *in vitro* release profiles of NPs from porous and nonporous MPs, 20 mg of PLGA MPs was suspended 1 mL sterile PBS (pH 7.4, 0.02% sodium azide) in microcentrifuge tubes and maintained at 37 °C with constant rotation. At pre-determined time intervals, tubes were centrifuged (15,000 rpm, 10 min, 4 °C), and 900 μL of supernatant was removed for analysis, replaced by the same volume of fresh buffer, and frozen and lyophilized for further analysis. Each lyophilized sample was reconstituted in 220 μL TE buffer supplemented with 100 mM NaCl, pipetted into a UV-Star® microplate (100 μL/well), and quantified by a fluorescence plate reader (Synergy H1 Hybrid Multi-Mode Reader, BioTek) as described above. All samples were run in technical duplicates.

In Vivo Controlled Release of Nanoparticles from PLGA Microparticles

Female BALB/c mice were obtained from The Jackson Laboratory (Bar Harbor, ME) and maintained at the animal facilities of Vanderbilt University under conventional conditions. The mice were anesthetized with isoflurane gas and maintained at 37 °C while their flanks or abdomens were depilated and sterilized for subcutaneous or intratumoral administration. NPs were prepared with A647-DNA (negative control sequence, IDT DNA) and loaded into PLGA MPs with or without porogen for subcutaneous and intratumoral *in vivo* release studies. 6–8 week old mice were anesthetized with isoflurane gas and given a single subcutaneous injection of porous MP ($n = 5$), nonporous MP ($n = 5$), or NP ($n = 3$). For the murine tumor studies, 10^6 4T1-LUC cells were inoculated (50 μL injection volume) into the inguinal mammary fatpads of 6–8 week old mice anesthetized with isoflurane gas. Tumor volume was calculated using the equation: Volume = (Length × Width^2)/2. When tumor volumes reached 50–100 mm^3, mice were anesthetized with isoflurane gas and administered a single intratumoral injection of porous MPs ($n = 3$), nonporous MPs ($n = 3$), or NPs ($n = 3$). All treatments were administered at a 10 μg dose of nucleic acid in a 100 μL injection volume. Using constant image capture settings on an IVIS Spectrum (PerkinElmer), mice were imaged at predetermined time intervals to quantify A647 fluorescence. Relative release of NPs was determined by measuring the total fluorescent efficiency (cm^2) of A647 overtime and normalizing to the respective initial (day 0) values.

In Vitro Evaluation of Luciferase Knockdown

NPs were prepared with the siRNA oligos, siLUC (anti-luciferase sequence, 5′-CAAUUGCACUGAUAAUGAACUCCTC[3AlexF647N]-3′; IDT DNA) or siNC (negative control sequence, 5′-[5AlexF647-N]AUACGCGUAUUAUACGCGAUUAACGAC-3′; IDT DNA) and encapsulated into porous MPs as described above. 4T1-LUC cells were seeded in five black 24-well plates (a separate plate for each day of imaging) with clear tissue culture treated bottoms (Sensoplate REF:662892; Greiner Bio-One) at 2000 cells per well (500 μL seeding volume). NPs were complexed with either siLUC (siLUC/NP) or siNC (siNC/NP) and embedded in porous MPs (siLUC/MP and siNC/MP). Cells were treated 24 h later with free NPs or porous MPs at a final concentration of 50 nM nucleic acid per well. The supernatant in the free NP-treated wells was removed from all plates at 24 h to mimic the NP clearance observed *in vivo*. Every 24 h over the course of 5 days, Pierce D-luciferin (ThermoFisher Scientific) was administered to all the wells within the plate for the corresponding day to a final D-luciferin concentration of 0.15 mg/mL. 5 min after the addition of D-luciferin, plates were imaged for bioluminescent signal using an IVIS Lumina III (PerkinElmer). Images were captured at 24, 48, 72, 96, 120 h post-treatment, and luciferase knockdown was quantified for each day based on the percent decrease in bioluminescent signal (i.e. Total Flux, photons/second) relative to each respective negative control siRNA.

In Vivo Evaluation of Luciferase Knockdown

Female BALB/c mice were obtained from The Jackson Laboratory (Bar Harbor, ME) and maintained at the animal facilities of Vanderbilt University under conventional conditions. Orthotopic 4T1-LUC tumors were generated as described above. siLUC/NPs

and siNC/NPs were prepared as described above and loaded into porous MPs (siLUC/MP and siNC/MP). When tumor volumes reached 50–100 mm^3, mice were anesthetized with isoflurane gas and administered a single intratumoral injection of free NPs or porous MPs ($n = 10$ for all treatment groups). All treatments were administered at a 10 μg oligonucleotide dose (0.5 mg/kg) in a 100 μL injection volume. Using constant image capture settings on an IVIS Lumina III (PerkinElmer), mice were analyzed at predetermined time intervals for fluorescence and bioluminescence. Bioluminescence within the mice was measured 10 min after dorsal subcutaneous injection of 300 μL Pierce D-luciferin (15 mg/mL). After 14 days mice were euthanized and tumor samples were isolated postmortem for histological analysis.

Statistical Analysis

All data analysis was performed on Graphpad Prism (Version 7.0c). One-way analysis of variance (ANOVA) coupled with Tukey's post-test was used to compare statistical significance among multiple groups (> 2). Differences between two groups were analyzed by unpaired t tests. *In vivo* experiments were performed with at least three biological replicates, with $^{****}p < 0.0001$, $^{***}p < 0.001$, $^{**}p < 0.01$, $^{*}p < 0.05$ being considered statistically significant.

RESULTS AND DISCUSSION

Design and In Vitro Characterization of PLGA Microparticle Depots

To generate depots for controlled release of cytosolically-active nucleic acids, we encapsulated endosomolytic polymer NPs complexed with nucleic acid (either double-stranded DNA or siRNA) within MPs of PLGA, a biocompatible, hydrolytically-degradable, and commonly used biomaterial for local and sustained therapeutic drug delivery.[17,21–23,29,35,40,41,44,45,74] PLGA MPs were synthesized using DCM as a volatile organic solvent and PVA as a surfactant in a $W_1/O/W_2$ double emulsion as previously described.[15,27,47,56] Sonication and homogenization were employed after the primary and secondary emulsions, respectively. NPs were incorporated into the W_1 aqueous phase, resulting in a drug loading of approximately 1.8 ± 0.05 μg nucleic acid per mg PLGA and an encapsulation efficiency of about $75 \pm 2\%$. To generate porous MPs with a faster release profile, the effervescent salt ammonium bicarbonate was added to the W_1 aqueous phase. Following

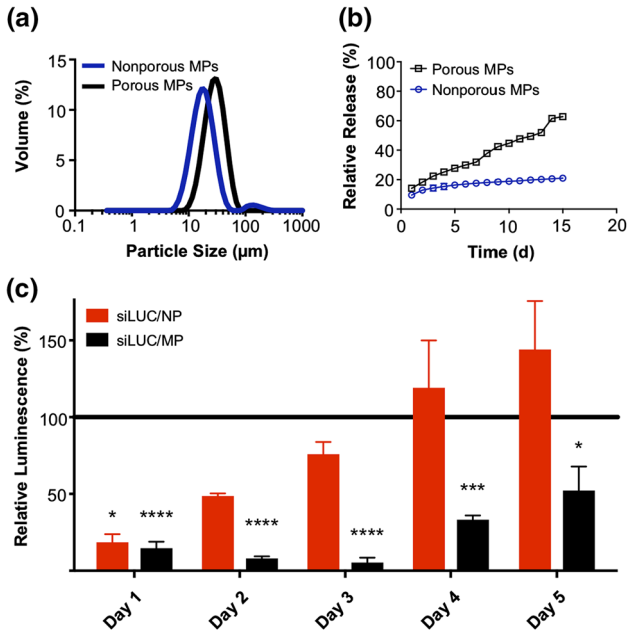

FIGURE 2. ***In vitro*** **characterization of PLGA microparticle depots. (a) Particle size distribution of nonporous and porous MPs determined by laser diffraction particle sizing. (b)** ***In vitro*** **release profiles of NPs from porous and nonporous MP depots over a 15 day period. (c) Longitudinal analysis of luciferase silencing in 4T1-LUC breast cancer cells treated with a single administration of either free NPs or porous MPs. The NP treatments were removed after 24 h, while MPs were left in coculture with the cells throughout the experiment to mimic biological residence. Luminescent signal for each treatment group was normalized to that of an analogous treatment containing scrambled negative control RNA substituted for luciferase siRNA.**

PLGA MP synthesis, SEM imaging was performed to characterize MP morphology, which confirmed that ammonium bicarbonate was an effective porogen for NP-loaded PLGA MPs (Fig. 1c). Laser diffraction size analysis was used to quantitatively characterize the particle size distribution (Fig. 2a). Nonporous MPs and porous MPs had an average diameter of 21.21 μm and 28.33 μm, respectively. An *in vitro* release assay was performed to characterize the release profiles of NPs from PLGA MP depots with varying porosity (Fig. 2b). As expected, the addition of pores and the associated increase in surface area within PLGA MPs resulted in faster release of the NP cargo, likely reflecting the shorter diffusion distance for release. While cationic excipients, such as polyethyleneimine or polyamines, have been incorporated into PLGA to increase nucleic acid loading and intracellular delivery,[6,59,61,78] this represents the first demonstration of a PLGA MP depot used for sustained release of endosomolytic nanoparticles that enhance cytosolic nucleic acid delivery.

In Vitro RNAi Luciferase Silencing

An *in vitro* RNAi protein knockdown assay was performed to demonstrate that PLGA MP depots could sustain the release and biological activity of nucleic acid-loaded NPs (Fig. 2c). As a model nucleic acid cargo, siRNA specific for luciferase (siLUC) or a scrambled negative control siRNA (siNC) were complexed with D-PDB micelles (siRNA/NP) and loaded into porous MPs (siRNA/MP). 4T1-LUC breast cancer cells, engineered to constitutively express luciferase, were treated with free NP or porous MPs each complexed to either siLUC or siNC at 50 nM siRNA per well. Free NPs were removed after 24 h to approximate a transient residence time at an injected site, whereas cells were incubated with MP depots for an additional 4 days. Bioluminescence imaging was used to quantify luciferase expression each day, following an administration of D-luciferin. While comparable silencing was observed between free siLUC/NP and siLUC/MP after 1 day (~ 75% knockdown), continuous incubation with depots resulted in significantly greater knockdown on days 2–5. The luciferase expression of the cells treated for 24 h with siLUC/NP returned to near baseline intensity within 3 days. Due to the short doubling time of 4T1 cells, cultures approached confluence within 5 days, which therefore precluded evaluation of knockdown at later timepoints. Nonetheless, these data demonstrate the capacity of PLGA MP depots to sustain the release and silencing activity of encapsulated siRNA/NP complexes.

Cytotoxicity is a well-established challenge of all polycationic nucleic acid delivery platforms that can indeed limit their utility in local delivery applications. However, this may be advantageous or detrimental depending on the intended application of the system; for example, in an intratumoral setting, some toxicity can galvanize cancer cell antigen release and may therefore be beneficial toward priming an anti-cancer immune response. Notably, we observed similar expression of bioluminescence in both the NP and MP negative control groups, suggesting that there is no difference in cell viability between the various treatments and that the PLGA used to entrap the NPs does not contribute to cellular toxicity, which is consistent with its high cytocompatibility.

In Vivo Nanoparticle Release from PLGA Microparticle Depots

To monitor NP release and retention *in vivo*, NPs were electrostatically complexed with a fluorescently-labeled double-stranded DNA (dsDNA/NP) and then loaded into PLGA MP depots (dsDNA/MP). Fluorescent dsDNA was used as representative cargo as it is a cost-effective analog to other nucleic acid sequences of similar length such as fluorescent siRNA. Free dsDNA/NP, nonporous dsDNA/MP, and porous dsDNA/MP were administered subcutaneously (s.c.) at a dose of 10 μg DNA (0.5 mg/kg) into BALB/c mice, and fluorescence was monitored with an *in vivo* imaging system (IVIS) to track the retention of dsDNA at the injection site (Figs. 3a and 3c). Free dsDNA/NP rapidly cleared the injection site, with > 50% clearance within 24 h and undetectable levels present by 5 days. By contrast, both MP depots enhanced retention and sustained release of dsDNA/NP, with porous depots demonstrating faster release than analogous nonporous depots, particularly within the first week of administration. Gradual release from both depots was observed over the following month with significant fluorescence still evident at day 56.

We also evaluated NP retention in the context of intratumoral (i.t.) delivery, which is increasing in use both preclinically and clinically as an administration route for cancer immunotherapeutics, including several nucleic acid drugs.[8,12,28] Here, we administered free dsDNA/NP, nonporous dsDNA/MP, and porous dsDNA/MP into 50 mm^3 4T1 tumors growing in the inguinal mammary fat pad, fluorescence was monitored within the tumor over time with intravital fluorescence imaging *via* IVIS. Similar to the release profiles observed with s.c. administration, MP depots enabled sustained release of dsDNA/NP over a 2-week period, the longest possible time-frame based on the endpoint tumor volume (~ 1500 mm^3). Again, the porous MP depots exhibited faster release with ~ 75% of cargo cleared within 2 weeks, whereas minimal release from nonporous MPs was observed (Figs. 3a and 3b). Notably, despite their cationic surface charge, free dsDNA/NP drained quickly with > 60% of nucleic acid cleared from the tumor site within 24 h. This rapid clearance may in part explain the need for multiple injections when using these or similar NPs for localized intratumoral delivery of siRNA or 5′ppp-RNA ligands of RIG-I.[24,31] Moreover, these data add to a large body of evidence indicating that the fate of most intratumorally administered nanoparticles and/or macromolecular therapeutics is a short and often suboptimal intratumoral half-life followed by ultimate systemic clearance. This also further motivates the design of implantable or injectable depots for intratumoral administration[16,60] or the incorporation of ligand to tether agents to local cells and/or extracellular matrix.[30,38]

In Vivo RNAi Luciferase Silencing

Based on their capacity to release ~ 50% of NP cargo into tumors within 1 week, we evaluated the ability of porous MP depots to sustain activity of a

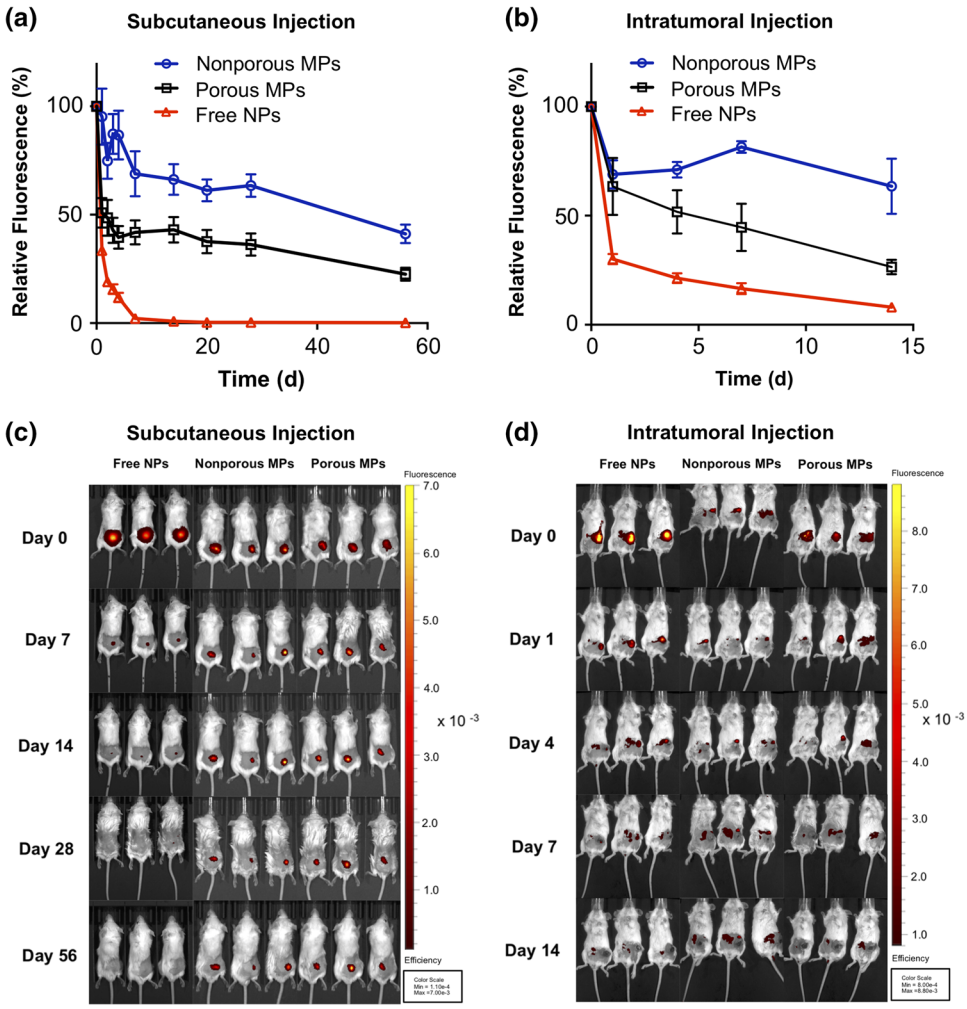

FIGURE 3. ***In vivo*** **retention and release of nanoparticles from PLGA microparticles.** ***In vivo*** **analysis of injection site localization of free NPs, nonporous MP depots, and porous MP depots in BALB/c mice. (a) Relative fluorescence of Alexa Fluor® 647(A647)-labelled dsDNA cargo injected subcutaneously and monitored over 56 days. (b) Relative fluorescence of A647-labelled dsDNA cargo, releasing from an intratumoral injection site over 14 days. The fluorescent efficiency of each mouse was captured by IVIS imaging and was normalized to the respective initial (day 0) fluorescence. (c) Representative IVIS images of mice bearing subcutaneously administered particles containing fluorescent dsDNA (Red). (d) Representative IVIS images of the mice treated intratumorally with particles containing fluorescent dsDNA (Red).**

nucleic acid therapeutic, here, siRNA targeting luciferase. Inspired by several ongoing clinical trials exploring intratumoral immunotherapy,[8,12,28,48] intratumoral injections were employed for protein knockdown studies to demonstrate the utility of PLGA MP depots in a cancer setting. While subcutaneous injections are undoubtedly easier for physicians to perform, recent advances in surgical intervention have made intratumoral injections more practical, as almost every site in the human body can be biopsied and therefore injected.[49] Thus, both administration routes explored within the retention studies have potential for clinical translation. To evaluate luciferase knockdown, mice with 4T1-LUC tumors growing in the inguinal mammary fat pad were intratumorally administered a single 10 μg siRNA dose (0.5 mg/kg) of siLUC/NP either free or loaded into depots (siLUC/MP); siNC/NP and siNC/MP were used as negative controls. IVIS imaging of both luminescence and fluorescence demonstrated a qualitatively high degree of co-localization between siLUC/NP and tumor cells (Fig. 4b), and MPs could also be identified within cyrosections of resected tumors (Fig. 4a). Using longitudinal IVIS imaging, we also quantified bioluminescence to determine the degree of luciferase knockdown from the anti-luciferase siRNA cargo 1–4 days post-intratumoral injection (Fig. 4c). We found that porous MP depots loaded with siLUC/NP resulted in ~ 50% reduction in luminescent signal relative to analogous depots loaded with siNC/NP control complexes. By contrast, at a 10 μg siRNA dose, no luciferase knockdown was observed using free siLUC/NP, potentially reflecting the rela-

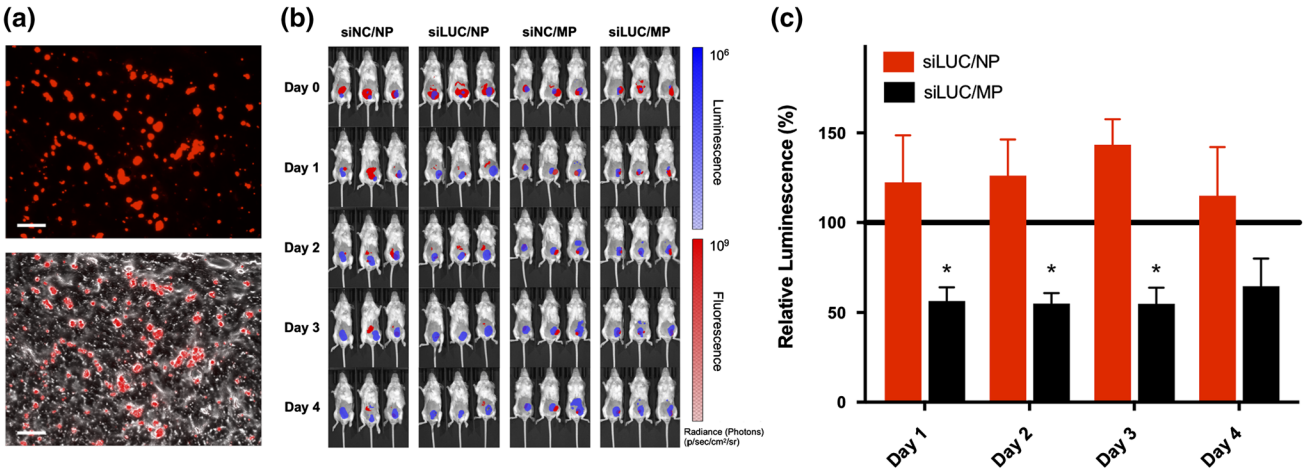

FIGURE 4. ***In vivo*** **activity of PLGA microparticle depots for siRNA delivery.** ***In vivo*** **activity of free NP and porous MPs delivering Alexa Fluor® 647 siRNA cargo was investigated in an orthotopic 4T1-LUC breast cancer model. (a) Fluorescent (top) and overlaid fluorescent and bright field (bottom) images of cyrosections of tumor tissue following intratumoral injection of porous MPs. Scale: 75 μm. (b) Representative IVIS images of mice bearing luciferase-expressing 4T1-LUC cells (Blue), treated intratumorally with fluorescent RNA (Red). (c) Longitudinal analysis of luciferase silencing in a 4T1-LUC breast cancer tumor model treated with a single intratumoral injection of either free NPs or porous MPs. Luminescent signal for each treatment group was normalized to that of an analogous treatment containing scrambled negative control RNA substituted for luciferase siRNA.**

tively short half-life of NPs within the tumor after local administration. Collectively, these data demonstrate that increasing intratumoral residence time of nucleic acid therapeutics *via* sustained release can enhance and prolong biological activity.

In these studies, we utilized PLGA MPs as a depot for siRNA/NP owing to their favorable biocompatibility and tunable biodegradability. However, inefficient loading of hydrophilic cargo during the $W_1/O/W_2$ emulsion synthesis is a known limitation of PLGA depots, which we found to be the case as well for the loading of NPs (~ 1.8 μg oligonucleotide per mg PLGA). This necessitates delivery of a relatively high volume of MPs to obtain relevant doses of NPs in the context of RNAi, which may restrict the applications of this approach. While we achieved ~ 50% luciferase silencing over 3 days using a single dose of MPs, further enhancements may be achieved using doses higher than those employed herein, which were restrained by the volume of MPs that could be physically injected into 4T1 tumors. Therefore, for cancer therapy applications, PLGA MP depots for NP release may be better suited for localized delivery into tumor resection cavities that can be filled with a larger volume of MPs. To establish proof-of-concept, we used siRNA as a well-established model nucleic acid cargo throughout our investigations, but in principle this approach can be used for local and sustained delivery of any cytosolically-active nucleic acid, including immunostimulatory agonists such as 5′ppp-RNA RIG-I ligands[31] or immunostimulatory DNA ligands of cGAS.[1] However, exploration of these promising immunotherapeutics is at a stage of relative infancy, and therefore much remains to be elucidated regarding dose and treatment regimens that result in optimal efficacy. Nonetheless, PLGA MP depots for release of endosomolytic NPs offer a promising strategy for enhancing the cytosolic delivery of such nucleic acids and locally sustaining their bioavailability and immunostimulatory activity *in vivo*.

CONCLUSION

Localized delivery of cytosolically-active nucleic acids offers a promising approach for spatiotemporal modulation of immune responses with broad potential applicability in the treatment of many diseases. However, efficacy in this setting is limited by inefficient cytosolic delivery as well as rapid clearance from the administration site. To address these challenges, we developed a nano-in-microparticle delivery platform using PLGA MPs as a depot for the controlled release of endosomolytic NPs that promote cytosolic delivery of electrostatically complexed nucleic acid cargo. Using siRNA as a model therapeutic, we demonstrated that the rate of release of siRNA/NP complexes both *in vitro* and *in vivo* could be increased using ammonium bicarbonate as a porogen during the fabrication process. Importantly, we found that release of siRNA/NP complexes from PLGA MP depots resulted in sustained protein silencing *in vitro* as well as in an orthotopic murine breast cancer model *via* intratumoral administration. The observed 50% protein knockdown in breast cancer tumors may indeed be sufficient for delivery of an immunomodulatory agent

where only a portion of cells within a tumor need to be stimulated in order to produce a more immunogenic tumor microenvironment. Collectively, these studies demonstrate that controlled release of endosomolytic nanoparticles from porous MP depots may offer an enabling strategy for controlled and localized delivery of nucleic acid therapeutics that target cytosolic immunoregulatory machinery. While this technology holds promise for local administration, improved performance could be achieved with a higher degree of drug loading and more tightly controlled kinetics of drug release that might enable sustained silencing and/or enhanced cytosolic delivery of siRNA or innate immune agonists. Additionally, co-administering chemotherapy or radiotherapy to ablate the majority of the tumor cells and allow for decreased tumor burden at the site of injection would likely synergize well with this platform.

ACKNOWLEDGMENTS

We gratefully acknowledge Dr. Bob Weinberg and Dr. Didier Trono for gifts of plasmids *via* Addgene.org. We thank Dr. Steven Goodbred Jr. and his laboratory for use of the Mastersizer 2000 (Malvern, USA). We thank Kyle Becker for his assistance with the orthotopic tumor inoculations. We thank the core facilities of Vanderbilt, including the Vanderbilt Institute of Nanoscale Sciences and Engineering (VINSE) for the use of both the Zetasizer Nano ZS Instrument (Malvern, USA) and the Zeiss Merlin SEM (Carl Zeiss Microscopy, LLC, ZEISS Group, Thornwood, NY), the Vanderbilt Translational Pathology Shared Resource (supported in part by the NCI/NIH Cancer Center Support Grant 5P30 CA684850-19) for cryosectioning of tumor samples, and Vanderbilt University Medical Center Flow Cytometry Shared Resource (supported by the Vanderbilt Ingram Cancer Center P30 CA68485) and the Vanderbilt Digestive Disease Research Center (DK058404) for cell sorting. This research was supported by grants from Alex's Lemonade Stand Foundation 'A' Award SID924 (JTW) and Pediatric Oncology Student Training (POST) Award cosponsored by Love Your Mellon (KMG), the American Cancer Society Institutional Research Grant IRG-58-009-56 (JTW), the Congressionally-Directed Medical Research Program W81XWH-161-0063 (JTW) and W81XWH-161-0063 (RSC), the National Institutes of Health R01CA224241 (CLD) and R01EB019409 (CLD), and the National Science Foundation Graduate Research Fellowship Program 0909667 and 1445197 (KVK).

CONFLICT OF INTEREST

The authors declare no conflicts of interest.

ETHICAL APPROVAL

All animal experiments were approved by the Vanderbilt University Institutional Animal Care and Use Committee (IACUC), and all surgical and experimental procedures were performed in accordance with the regulations and guidelines of the Vanderbilt University IACUC. Female BALB/cJ mice (6–8 weeks old; The Jackson Laboratory, Bar Harbor, ME) were maintained at the animal facilities of Vanderbilt University under specific pathogen-free conditions. Tumor volume, total mass, and animal well-being were monitored every other day.

REFERENCES

[1]Ahn, J., T. Xia, A. Rabasa Capote, D. Betancourt, and G. N. Barber. Extrinsic phagocyte-dependent STING signaling dictates the immunogenicity of dying cells. *Cancer Cell* 33(5):862–873e5, 2018.

[2]Ali, O. A., N. Huebsch, L. Cao, G. Dranoff, and D. J. Mooney. Infection-mimicking materials to program dendritic cells in situ. *Nat. Mater.* 8(2):151–158, 2009.

[3]Ali, O. A., C. Verbeke, C. Johnson, R. W. Sands, S. A. Lewin, D. White, E. Doherty, G. Dranoff, and D. J. Mooney. Identification of immune factors regulating antitumor immunity using polymeric vaccines with multiple adjuvants. *Cancer Res.* 74(6):1670–1681, 2014.

[4]Aliabadi, H. M. Natural polymers in nucleic acid delivery. In: Polymers and Nanomaterials for Gene Therapy, edited by R. Narain. Cambridge: Woodhead Publishing, 2016, pp. 55–80.

[5]Aliru, M. L., J. E. Schoenhals, B. P. Venkatesulu, C. C. Anderson, H. B. Barsoumian, A. I. Younes, K. M. Ls, M. Soeung, K. E. Aziz, J. W. Welsh, and S. Krishnan. Radiation therapy and immunotherapy: what is the optimal timing or sequencing? *Immunotherapy* 10(4):299–316, 2018.

[6]Amar-Lewis, E., A. Azagury, R. Chintakunta, R. Goldbart, T. Traitel, J. Prestwood, D. Landesman-Milo, D. Peer, and J. Kost. Quaternized starch-based carrier for siRNA delivery: from cellular uptake to gene silencing. *J. Control. Release* 185:109–120, 2014.

[7]Arany, S., D. S. Benoit, S. Dewhurst, and C. E. Ovitt. Nanoparticle-mediated gene silencing confers radioprotection to salivary glands *in vivo*. *Mol. Ther.* 21(6):1182–1194, 2013.

[8]Aznar, M. A., N. Tinari, A. J. Rullan, A. R. Sanchez-Paulete, M. E. Rodriguez-Ruiz, and I. Melero. Intratumoral delivery of immunotherapy-act locally, think globally. *J. Immunol.* 198(1):31–39, 2017.

[9]Bartlett, D. W., and M. E. Davis. Insights into the kinetics of siRNA-mediated gene silencing from live-cell and live-animal bioluminescent imaging. *Nucleic Acids Res.* 34(1):322–333, 2006.

[10]Beyranvand Nejad, E., M. J. Welters, R. Arens, and S. H. van der Burg. The importance of correctly timing cancer immunotherapy. *Expert Opin. Biol. Ther.* 17(1):87–103, 2017.
[11]Bobbin, M. L., and J. J. Rossi. RNA Interference (RNAi)-Based Therapeutics: delivering on the Promise? *Annu. Rev. Pharmacol. Toxicol.* 56:103–122, 2016.
[12]Brody, J. D., W. Z. Ai, D. K. Czerwinski, J. A. Torchia, M. Levy, R. H. Advani, Y. H. Kim, R. T. Hoppe, S. J. Knox, L. K. Shin, I. Wapnir, R. J. Tibshirani, and R. Levy. In situ vaccination with a TLR9 agonist induces systemic lymphoma regression: a phase I/II study. *J. Clin. Oncol.* 28(28):4324–4332, 2010.
[13]Broz, P., and D. M. Monack. Newly described pattern recognition receptors team up against intracellular pathogens. *Nat. Rev. Immunol.* 13(8):551–565, 2013.
[14]Brudno, Y., and D. J. Mooney. On-demand drug delivery from local depots. *J. Control. Release* 219:8–17, 2015.
[15]Chang, E., A. J. McClellan, W. J. Farley, D. Q. Li, S. C. Pflugfelder, and C. S. De Paiva. Biodegradable PLGA-based drug delivery systems for modulating ocular surface disease under experimental murine dry eye. *J. Clin. Exp. Ophthalmol.* 2(11):191, 2011.
[16]Chen, Q., C. Wang, X. Zhang, G. Chen, Q. Hu, H. Li, J. Wang, D. Wen, Y. Zhang, Y. Lu, G. Yang, C. Jiang, J. Wang, G. Dotti, and Z. Gu. In situ sprayed bioresponsive immunotherapeutic gel for post-surgical cancer treatment. *Nat. Nanotechnol.* 14(1):89–97, 2019.
[17]Cohen, H., R. J. Levy, J. Gao, I. Fishbein, V. Kousaev, S. Sosnowski, S. Slomkowski, and G. Golomb. Sustained delivery and expression of DNA encapsulated in polymeric nanoparticles. *Gene Ther.* 7(22):1896–1905, 2000.
[18]Convertine, A. J., D. S. Benoit, C. L. Duvall, A. S. Hoffman, and P. S. Stayton. Development of a novel endosomolytic diblock copolymer for siRNA delivery. *J. Control. Release* 133(3):221–229, 2009.
[19]Convertine, A. J., C. Diab, M. Prieve, A. Paschal, A. S. Hoffman, P. H. Johnson, and P. S. Stayton. pH-Responsive polymeric micelle carriers for siRNA drugs. *Biomacromolecules* 11(11):2904–2910, 2010.
[20]Cooper, C., and D. Mackie. Hepatitis B surface antigen-1018 ISS adjuvant-containing vaccine: a review of HEPLISAV safety and efficacy. *Expert Rev. Vaccines* 10(4):417–427, 2011.
[21]Cun, D., C. Foged, M. Yang, S. Frokjaer, and H. M. Nielsen. Preparation and characterization of poly(D,L-lactide-*co*-glycolide) nanoparticles for siRNA delivery. *Int. J. Pharm.* 390(1):70–75, 2010.
[22]Cun, D., D. K. Jensen, M. J. Maltesen, M. Bunker, P. Whiteside, D. Scurr, C. Foged, and H. M. Nielsen. High loading efficiency and sustained release of siRNA encapsulated in PLGA nanoparticles: quality by design optimization and characterization. *Eur. J. Pharm. Biopharm.* 77(1):26–35, 2011.
[23]Danhier, F., E. Ansorena, J. M. Silva, R. Coco, A. Le Breton, and V. Preat. PLGA-based nanoparticles: an overview of biomedical applications. *J. Control. Release* 161(2):505–522, 2012.
[24]Elion, D. L., M. E. Jacobson, D. J. Hicks, B. Rahman, V. Sanchez, P. I. Gonzales-Ericsson, O. Fedorova, A. M. Pyle, J. T. Wilson, and R. S. Cook. Therapeutically active RIG-I agonist induces immunogenic tumor cell killing in breast cancers. *Cancer Res.* 78(21):6183–6195, 2018.
[25]Ferritto, M. S., and D. A. Tirrell. Photoregulation of the binding of an azobenzene-modified poly(methacrylic acid) to phosphatidylcholine bilayer membranes. *Biomaterials* 11(9):645–651, 1990.
[26]Fire, A., S. Xu, M. K. Montgomery, S. A. Kostas, S. E. Driver, and C. C. Mello. Potent and specific genetic interference by double-stranded RNA in *Caenorhabditis elegans*. *Nature* 391(6669):806–811, 1998.
[27]Frauke Pistel, K., A. Breitenbach, R. Zange-Volland, and T. Kissel. Brush-like branched biodegradable polyesters, part III. Protein release from microspheres of poly(vinyl alcohol)-graft-poly(D,L-lactic-*co*-glycolic acid). *J. Control. Release* 73(1):7–20, 2001.
[28]Hammerich, L., A. Binder, and J. D. Brody. In situ vaccination: cancer immunotherapy both personalized and off-the-shelf. *Mol Oncol* 9(10):1966–1981, 2015.
[29]Han, F. Y., K. J. Thurecht, A. K. Whittaker, and M. T. Smith. Bioerodable PLGA-based microparticles for producing sustained-release drug formulations and strategies for improving drug loading. *Front Pharmacol.* 7:185, 2016.
[30]Ishihara, J., K. Fukunaga, A. Ishihara, H. M. Larsson, L. Potin, P. Hosseinchi, G. Galliverti, M. A. Swartz, and J. A. Hubbell. Matrix-binding checkpoint immunotherapies enhance antitumor efficacy and reduce adverse events. *Sci. Transl. Med.* 9(415):eaan0401, 2017.
[31]Jacobson, M. E., L. Wang-Bishop, K. W. Becker, and J. T. Wilson. Delivery of 5′-triphosphate RNA with endosomolytic nanoparticles potently activates RIG-I to improve cancer immunotherapy. *Biomater. Sci.* 7(2):547–559, 2019.
[32]Jewell, C. M., S. C. B. López, and D. J. Irvine. In situ engineering of the lymph node microenvironment via intranodal injection of adjuvant-releasing polymer particles. *Proc. Natl. Acad. Sci. USA* 108(38):15745–15750, 2011.
[33]Jiang, W., F. G. Zhu, L. Bhagat, D. Yu, J. X. Tang, E. R. Kandimalla, N. La Monica, and S. Agrawal. A toll-like receptor 7, 8, and 9 antagonist inhibits Th1 and Th17 responses and inflammasome activation in a model of IL-23-induced psoriasis. *J. Invest. Dermatol.* 133(7):1777–1784, 2013.
[34]Johannes, L., and M. Lucchino. Current challenges in delivery and cytosolic translocation of therapeutic RNAs. *Nucleic Acid Ther.* 28(3):178–193, 2018.
[35]Khan, A., M. Benboubetra, P. Z. Sayyed, K. W. Ng, S. Fox, G. Beck, I. F. Benter, and S. Akhtar. Sustained polymeric delivery of gene silencing antisense ODNs, siRNA, DNAzymes and ribozymes: *in vitro* and *in vivo* studies. *J. Drug Target.* 12(6):393–404, 2004.
[36]Krhac Levacic, A., S. Morys, and E. Wagner. Solid-phase supported design of carriers for therapeutic nucleic acid delivery. *Biosci. Rep.* 37(5):BSR20160617, 2017.
[37]Kwong, B., S. A. Gai, J. Elkhader, K. D. Wittrup, and D. J. Irvine. Localized immunotherapy via liposome-anchored Anti-CD137 + IL-2 prevents lethal toxicity and elicits local and systemic antitumor immunity. *Can. Res.* 73(5):1547–1558, 2013.
[38]Kwong, B., H. Liu, and D. J. Irvine. Induction of potent anti-tumor responses while eliminating systemic side effects via liposome-anchored combinatorial immunotherapy. *Biomaterials* 32(22):5134–5147, 2011.
[39]Langer, R. Drug delivery and targeting. *Nature* 392(6679 Suppl):5–10, 1998.
[40]Langer, R., and D. A. Tirrell. Designing materials for biology and medicine. *Nature* 428(6982):487–492, 2004.
[41]Luby, T. M., G. Cole, L. Baker, J. S. Kornher, U. Ramstedt, and M. L. Hedley. Repeated immunization with plasmid DNA formulated in poly(lactide-co-glycolide)

microparticles is well tolerated and stimulates durable T cell responses to the tumor-associated antigen cytochrome P450 1B1. *Clin. Immunol.* 112(1):45–53, 2004.
[42]Lurescia, S., D. Fioretti, and M. Rinaldi. Targeting cytosolic nucleic acid-sensing pathways for cancer immunotherapies. *Front. Immunol.* 9:711, 2018.
[43]Lurescia, S., D. Fioretti, and M. Rinaldi. Nucleic acid sensing machinery: targeting innate immune system for cancer therapy. *Recent Pat. Anticancer Drug Discov.* 13(1):2–17, 2018.
[44]Luten, J., C. F. van Nostrum, S. C. De Smedt, and W. E. Hennink. Biodegradable polymers as non-viral carriers for plasmid DNA delivery. *J. Control. Release* 126(2):97–110, 2008.
[45]Makadia, H. K., and S. J. Siegel. Poly lactic-*co*-glycolic acid (PLGA) as biodegradable controlled drug delivery carrier. *Polymers (Basel)* 3(3):1377–1397, 2011.
[46]Malcolm, D. W., M. A. T. Freeberg, Y. Wang, K. R. Sims, H. A. Awad, and D. S. W. Benoit. Diblock copolymer hydrophobicity facilitates efficient gene silencing and cytocompatible nanoparticle-mediated siRNA delivery to musculoskeletal cell types. *Biomacromolecules* 18(11):3753–3765, 2017.
[47]Mao, S., J. Xu, C. Cai, O. Germershaus, A. Schaper, and T. Kissel. Effect of WOW process parameters on morphology and burst release of FITC-dextran loaded PLGA microspheres. *Int. J. Pharm.* 334(1–2):137–148, 2007.
[48]Marabelle, A., H. Kohrt, C. Caux, and R. Levy. Intratumoral immunization: a new paradigm for cancer therapy. *Clin. Cancer Res.* 20(7):1747–1756, 2014.
[49]Marabelle, A., L. Tselikas, T. de Baere, and R. Houot. Intratumoral immunotherapy: using the tumor as the remedy. *Ann. Oncol.* 28(suppl 12):xii33–xii43, 2017.
[50]Martin, J. R., C. E. Nelson, M. K. Gupta, F. Yu, S. M. Sarett, K. M. Hocking, A. C. Pollins, L. B. Nanney, J. M. Davidson, S. A. Guelcher, and C. L. Duvall. Local delivery of PHD2 siRNA from ROS-degradable scaffolds to promote diabetic wound healing. *Adv. Healthc. Mater.* 5(21):2751–2757, 2016.
[51]McGinity, J. W., and P. B. O'Donnell. Preparation of microspheres by the solvent evaporation technique. *Adv. Drug Deliv. Rev.* 28(1):25–42, 1997.
[52]Milling, L., Y. Zhang, and D. J. Irvine. Delivering safer immunotherapies for cancer. *Adv. Drug Deliv. Rev.* 114:79–101, 2017.
[53]National Center for Immunization and Respiratory Diseases. General recommendations on immunization: recommendations of the Advisory Committee on Immunization Practices (ACIP). *MMWR Recomm. Rep.* 60(2):1–64, 2011.
[54]Nelson, C. E., M. K. Gupta, E. J. Adolph, J. M. Shannon, S. A. Guelcher, and C. L. Duvall. Sustained local delivery of siRNA from an injectable scaffold. *Biomaterials* 33(4):1154–1161, 2012.
[55]Nishikawa, M., Y. Mizuno, K. Mohri, N. Matsuoka, S. Rattanakiat, Y. Takahashi, H. Funabashi, D. Luo, and Y. Takakura. Biodegradable CpG DNA hydrogels for sustained delivery of doxorubicin and immunostimulatory signals in tumor-bearing mice. *Biomaterials* 32(2):488–494, 2011.
[56]Ogawa, Y., M. Yamamoto, H. Okada, T. Yashiki, and T. Shimamoto. A new technique to efficiently entrap leuprolide acetate into microcapsules of polylactic acid or *co*poly(lactic/glycolic) acid. *Chem. Pharm. Bull. (Tokyo)* 36(3):1095–1103, 1988.
[57]Ozcan, G., B. Ozpolat, R. L. Coleman, A. K. Sood, and G. Lopez-Berestein. Preclinical and clinical development of siRNA-based therapeutics. *Adv. Drug Deliv. Rev.* 87:108–119, 2015.
[58]Pannier, A. K., and L. D. Shea. Controlled release systems for DNA delivery. *Mol. Ther.* 10(1):19–26, 2004.
[59]Pantazis, P., K. Dimas, J. H. Wyche, S. Anant, C. W. Houchen, J. Panyam, and R. P. Ramanujam. Preparation of siRNA-encapsulated PLGA nanoparticles for sustained release of siRNA and evaluation of encapsulation efficiency. *Methods Mol. Biol.* 906:311–319, 2012.
[60]Park, C. G., C. A. Hartl, D. Schmid, E. M. Carmona, H. J. Kim, and M. S. Goldberg. Extended release of perioperative immunotherapy prevents tumor recurrence and eliminates metastases. *Sci. Transl. Med.* 10(433):eear1916, 2018.
[61]Patil, Y., and J. Panyam. Polymeric nanoparticles for siRNA delivery and gene silencing. *Int. J. Pharm.* 367(1–2):195–203, 2009.
[62]Poeck, H., R. Besch, C. Maihoefer, M. Renn, D. Tormo, S. S. Morskaya, S. Kirschnek, E. Gaffal, J. Landsberg, J. Hellmuth, A. Schmidt, D. Anz, M. Bscheider, T. Schwerd, C. Berking, C. Bourquin, U. Kalinke, E. Kremmer, H. Kato, S. Akira, R. Meyers, G. Häcker, M. Neuenhahn, D. Busch, J. Ruland, S. Rothenfusser, M. Prinz, V. Hornung, S. Endres, T. Tüting, and G. Hartmann. 5′-Triphosphate-siRNA: turning gene silencing and RIG-I activation against melanoma. *Nat. Med.* 14(11):1256–1263, 2008.
[63]Radovic-Moreno, A. F., N. Chernyak, C. C. Mader, S. Nallagatla, R. S. Kang, L. Hao, D. A. Walker, T. L. Halo, T. J. Merkel, C. H. Rische, S. Anantatmula, M. Burkhart, C. A. Mirkin, and S. M. Gryaznov. Immunomodulatory spherical nucleic acids. *Proc. Natl. Acad. Sci. USA* 112(13):3892–3897, 2015.
[64]Rathbone, M. J., J. Hadgraft, and M. S. Roberts. Modified-release drug delivery technology. London: Taylor & Francis, 2002.
[65]Rothschilds, A. M., and K. D. Wittrup. What, why, where, and when: bringing timing to immuno-oncology. *Trends Immunol.* 40(1):12–21, 2019.
[66]Sarett, S. M., C. E. Nelson, and C. L. Duvall. Technologies for controlled, local delivery of siRNA. *J. Control. Release* 218:94–113, 2015.
[67]Senti, G., A. U. Freiburghaus, D. Larenas-Linnemann, H. J. Hoffmann, A. M. Patterson, L. Klimek, D. Di Bona, O. Pfaar, L. Ahlbeck, M. Akdis, D. Weinfeld, F. A. Contreras-Verduzco, A. Pedroza-Melendez, S. H. Skaarup, S. M. Lee, L. O. Cardell, J. M. Schmid, U. Westin, R. Dollner, and T. M. Kundig. Intralymphatic immunotherapy: update and unmet needs. *Int. Arch. Allergy Immunol.* 178(2):141–149, 2019.
[68]Sioud, M. RNA interference: mechanisms, technical challenges, and therapeutic opportunities. *Methods Mol. Biol.* 1218:1–15, 2015.
[69]Smith, S. A., L. I. Selby, A. P. R. Johnston, and G. K. Such. The endosomal escape of nanoparticles: towards more efficient cellular delivery. *Bioconjug. Chem.* 30(2):263–272, 2018.
[70]van den Boorn, J. G., W. Barchet, and G. Hartmann. Nucleic acid adjuvants: toward an educated vaccine. *Adv. Immunol.* 114:1–32, 2012.
[71]van den Boorn, J. G., and G. Hartmann. Turning tumors into vaccines: co-opting the innate immune system. *Immunity* 39(1):27–37, 2013.

[72]Wang, L. L., and J. A. Burdick. Engineered hydrogels for local and sustained delivery of RNA-interference therapies. *Adv. Healthc. Mater.* 6(1):1601041, 2017.
[73]Wang, Y., D. W. Malcolm, and D. S. W. Benoit. Controlled and sustained delivery of siRNA/NPs from hydrogels expedites bone fracture healing. *Biomaterials* 139:127–138, 2017.
[74]Wang, D., D. R. Robinson, G. S. Kwon, and J. Samuel. Encapsulation of plasmid DNA in biodegradable poly(D,L-lactic-*co*-glycolic acid) microspheres as a novel approach for immunogene delivery. *J. Control. Release* 57(1):9–18, 1999.
[75]Wang, C., W. Sun, G. Wright, A. Z. Wang, and Z. Gu. Inflammation-triggered cancer immunotherapy by programmed delivery of CpG and anti-PD1 antibody. *Adv. Mater.* 28(40):8912–8920, 2016.
[76]Whitehead, K. A., R. Langer, and D. G. Anderson. Knocking down barriers: advances in siRNA delivery. *Nat. Rev. Drug Discov.* 8(2):129–138, 2009.
[77]Wilson, J. T., S. Keller, M. J. Manganiello, C. Cheng, C.-C. Lee, C. Opara, A. Convertine, and P. S. Stayton. pH-Responsive nanoparticle vaccines for dual-delivery of antigens and immunostimulatory oligonucleotides. *ACS Nano.* 7(5):3912–3925, 2013.
[78]Woodrow, K. A., Y. Cu, C. J. Booth, J. K. Saucier-Sawyer, M. J. Wood, and W. M. Saltzman. Intravaginal gene silencing using biodegradable polymer nanoparticles densely loaded with small-interfering RNA. *Nat. Mater.* 8(6):526–533, 2009.
[79]Wu, S. Y., G. Lopez-Berestein, G. A. Calin, and A. K. Sood. RNAi therapies: drugging the undruggable. *Sci. Transl. Med.* 6(240):240, 2014.
[80]Wu-Pong, S., and Y. Rojanasakul. Biopharmaceutical Drug Design and Development (2nd ed.). Totowa: Humana Press, p. 375, 2008.
[81]Yan, J., Z.-Y. Wang, H.-Z. Yang, H.-Z. Liu, S. Mi, X.-X. Lv, X.-M. Fu, H.-M. Yan, X.-W. Zhang, Q.-M. Zhan, and Z.-W. Hu. Timing is critical for an effective anti-metastatic immunotherapy: the decisive role of IFNγ/STAT1-mediated activation of autophagy. *PLoS ONE* 6(9):e24705, 2011.
[82]Young, K. H., J. R. Baird, T. Savage, B. Cottam, D. Friedman, S. Bambina, D. J. Messenheimer, B. Fox, P. Newell, K. S. Bahjat, M. J. Gough, and M. R. Crittenden. Optimizing timing of immunotherapy improves control of tumors by hypofractionated radiation therapy. *PLoS ONE* 11(6):e0157164, 2016.
[83]Zhang, L., W. Wang, and S. Wang. Effect of vaccine administration modality on immunogenicity and efficacy. *Expert Rev. Vaccines* 14(11):1509–1523, 2015.
[84]Zhu, F. G., W. Jiang, L. Bhagat, D. Wang, D. Yu, J. X. Tang, E. R. Kandimalla, N. La Monica, and S. Agrawal. A novel antagonist of Toll-like receptors 7, 8 and 9 suppresses lupus disease-associated parameters in NZBW/F1 mice. *Autoimmunity* 46(7):419–428, 2013.
[85]Zhu, X., F. Nishimura, K. Sasaki, M. Fujita, J. E. Dusak, J. Eguchi, W. Fellows-Mayle, W. J. Storkus, P. R. Walker, A. M. Salazar, and H. Okada. Toll like receptor-3 ligand poly-ICLC promotes the efficacy of peripheral vaccinations with tumor antigen-derived peptide epitopes in murine CNS tumor models. *J. Transl. Med.* 5:10, 2007.

Published OnlineFirst September 17, 2018; DOI: 10.1158/0008-5472.CAN-18-0730

Tumor Biology and Immunology

Cancer Research

Therapeutically Active RIG-I Agonist Induces Immunogenic Tumor Cell Killing in Breast Cancers

David L. Elion[1], Max E. Jacobson[2], Donna J. Hicks[3], Bushra Rahman[3], Violeta Sanchez[4], Paula I. Gonzales-Ericsson[4], Olga Fedorova[5,6], Anna M. Pyle[5,6,7], John T. Wilson[1,2,3,8], and Rebecca S. Cook[1,3,4,8]

Abstract

Cancer immunotherapies that remove checkpoint restraints on adaptive immunity are gaining clinical momentum but have not achieved widespread success in breast cancers, a tumor type considered poorly immunogenic and which harbors a decreased presence of tumor-infiltrating lymphocytes. Approaches that activate innate immunity in breast cancer cells and the tumor microenvironment are of increasing interest, based on their ability to induce immunogenic tumor cell death, type I IFNs, and lymphocyte-recruiting chemokines. In agreement with reports in other cancers, we observe loss, downregulation, or mutation of the innate viral nucleotide sensor retinoic acid-inducible gene I (RIG-I/*DDX58*) in only 1% of clinical breast cancers, suggesting potentially widespread applicability for therapeutic RIG-I agonists that activate innate immunity. This was tested using an engineered RIG-I agonist in a breast cancer cell panel representing each of three major clinical breast cancer subtypes. Treatment with RIG-I agonist resulted in upregulation and mitochondrial localization of RIG-I and activation of proinflammatory transcription factors STAT1 and NF-κB. RIG-I agonist triggered the extrinsic apoptosis pathway and pyroptosis, a highly immunogenic form of cell death in breast cancer cells. RIG-I agonist also induced expression of lymphocyte-recruiting chemokines and type I IFN, confirming that cell death and cytokine modulation occur in a tumor cell–intrinsic manner. Importantly, RIG-I activation in breast tumors increased tumor lymphocytes and decreased tumor growth and metastasis. Overall, these findings demonstrate successful therapeutic delivery of a synthetic RIG-I agonist to induce tumor cell killing and to modulate the tumor microenvironment *in vivo*.

Significance: These findings describe the first in vivo delivery of RIG-I mimetics to tumors, demonstrating a potent immunogenic and therapeutic effect in the context of otherwise poorly immunogenic breast cancers. *Cancer Res; 78(21); 6183–95. ©2018 AACR.*

Introduction

Breast cancer is the most frequently diagnosed cancer in women (1). Despite advances in early detection and treatment, breast cancer remains the second leading cause of cancer-related deaths for women. With an eye toward new treatment strategies, recent attention has focused on immune-checkpoint inhibitors (ICI), antibodies that block regulatory receptors that dampen adaptive immunity (e.g., PD-1, PD-L1, CTLA-4). ICI-mediated inhibition of checkpoint receptors releases regulatory restraints on adaptive immunity, permitting a proinflammatory lymphocytic response against tumor neoantigens, and resulting in robust and durable antitumor immune responses (2). ICI treatments have seen remarkable success in cases of melanoma and lung cancer (2–4). However, ICI response rates reported in breast cancer clinical trials have thus far been disappointing, achieving success in only a fraction of patients (5–7). The relatively diminished response to ICIs in breast cancer is not completely understood, but may relate to fewer tumor-infiltrating lymphocytes (TIL; refs. 8, 9), a decreased mutational burden (10, 11), limited or absent expression of antigen presentation machinery on tumor cells (12), or enhanced expression of counterregulatory factors in breast cancers as compared with what is seen in other cancer types (13). A fraction of the highly aggressive triple-negative breast cancer (TNBC) subtypes, which on average harbor a greater number of TILs and a greater mutational burden than the other clinical breast cancer subtypes, have shown greater response to ICI over those breast cancer subtypes expressing estrogen receptor (ER^+) or harboring *HER2* gene amplification

[1]Cancer Biology Graduate Program, Vanderbilt University School of Medicine, Nashville, Tennessee. [2]Department of Chemical and Biomolecular Engineering, Vanderbilt University School of Engineering, Nashville, Tennessee. [3]Vanderbilt Ingram Cancer Center, Vanderbilt University Medical Center, Nashville, Tennessee. [4]Department of Cell and Developmental Biology, Vanderbilt University School of Medicine, Nashville, Tennessee. [5]Department of Molecular, Cellular, and Developmental Biology, Yale University, New Haven, Connecticut. [6]Howard Hughes Medical Institute, Chevy Chase, Maryland. [7]Department of Chemistry, Yale University, New Haven, Connecticut. [8]Department of Biomedical Engineering, Vanderbilt University School of Engineering, Nashville, Tennessee.

Note: Supplementary data for this article are available at Cancer Research Online (http://cancerres.aacrjournals.org/).

Corresponding Author: Rebecca S. Cook, Vanderbilt University, 2220 Pierce Avenue, Room 759, Nashville, TN 37232. Phone: 615-936-3813; Fax: 615-636-3148; E-mail: Rebecca.cook@vanderbilt.edu

doi: 10.1158/0008-5472.CAN-18-0730

Published OnlineFirst September 17, 2018; DOI: 10.1158/0008-5472.CAN-18-0730

($HER2^+$). Further, decreased TILs within the aggressive TNBC subtype predict poor outcome and decreased response to ICI. Interestingly, certain chemotherapeutic regimens increase TILs in breast cancers, which often correlates with improved response to treatment. Therefore, a new treatment paradigm may be needed in breast cancers to promote *de novo* inflammation to instigate antitumor immunity, or to enable efficacy of existing ICIs. It is possible that treatment strategies that increase TILs improve antigen presentation or increase inflammatory cytokines in the tumor microenvironment might improve immunogenicity of all breast cancer subtypes.

Pattern recognition receptors (PRR) of the innate immune system, which recognize conserved pathogen-associated molecular patterns (PAMP; e.g., viral nucleotide motifs), are gaining interest as a potential treatment strategy (14, 15). PRR activation by their viral nucleotide ligand induces proinflammatory transcription factors, including NF-κB, signal transduction and transcription, and interferon regulatory factors (IRF), which drive production of IFNs and other proinflammatory cytokines that orchestrate antimicrobial innate immune responses and stimulate adaptive immunity (14, 16). Certain PRRs are expressed in nearly every cell in the human body, including cancer cells, suggesting that some PRRs might be leveraged therapeutically as part of a cancer treatment strategy. This idea is being explored extensively in regard to the PRR known as stimulator of interferon genes (STING; refs. 17, 18). Synthetic STING ligands potently induce type I IFNs and support antitumor immunity across a variety of cancers, including breast, CLL, colon, and squamous cell carcinoma (19–23). However, there is increasing evidence that STING signaling is defective in many cancers, including breast some breast cancers, due to mutations, promoter methylation, and decreased expression of genes in the STING pathway (24, 25).

Retinoic acid-inducible gene I (RIG-I) is another PRR, playing a key role in recognizing RNA viruses. In contrast to the frequent STING pathway alterations seen in breast cancers, alterations in the RIG-I gene *DDX58* have been infrequently reported, and *DDX58* promoter methylation was not significantly higher in breast tumor versus normal breast tissue (24). RIG-I recognizes double-stranded viral RNAs (dsRNA) containing two or three 5′-phosphates (26–29). RIG-I activation by its ligand causes RIG-I translocation to mitochondria, where it interacts with its binding partner Mitochondrial antiviral signaling (MAVS) to activate signaling pathways that produce proinflammatory cytokines (30). Importantly, RIG-I activation also promotes the elimination of virally infected cells through apoptotic pathways (31–33). These attributes make RIG-I mimetics an attractive therapeutic approach in immune oncology.

Therapeutic efficacy of RIG-I mimetics has been seen in several cancer cell lines originating from a variety of tissues, although the impact of RIG-I activation in breast cancers is relatively understudied as compared with other cancers. Further, the use of RIG-I agonists as a cancer treatment requires a specific and potent RIG-I ligand that is functional *in vivo*, which has only recently been reported in a study using a minimal 5′-triphophosphorylated stem-loop RNA (SLR) sequence for intravenous delivery to mice (28). The stem-loop structure enhances structural stability of the complex, a key determinant of RIG-I ligand potency. Delivery of SLR sequences to mice *in vivo* activated in RIG-I signaling, IFN induction, and expression of genes required for potent antiviral immunity. However, the efficacy of RIG-I ligands, including SLRs, in animal models of cancer has not yet been tested.

We tested the hypothesis that RIG-I–mediated activation of innate immune responses might be therapeutically efficacious in breast cancers, while increasing the inflammatory phenotype of breast cancers. We demonstrate here that RIG-I activation in breast cancer cells resulted in tumor cell–intrinsic tumor cell death due in part to activation of pyroptosis and induced expression of inflammatory cytokines, leukocyte-recruiting chemokines, and increased expression of major histocompatibility (MHC)-I components. Delivery of synthetic RIG-I ligands to breast tumors *in vivo* recapitulated these results, recruiting leukocytes to the tumor microenvironment and decreasing tumor growth and metastasis.

Materials and Methods

Generation of SLR20

Oligoribonucleotides sequence OH-SLR20 (5′-GGACGUACGUUUCGACGUACGUCC) was synthesized on an automated MerMade synthesizer (BioAutomation) using standard phosphoramidite chemistry. The hydroxylated oligonucleotide was deprotected and gel purified as previously described (34). Triphosphorylated oligoribonucleotide SLR20 (5′ppp-GGACGUACGUUUCGACGUACGUCC) was synthesized as described (35), deprotected, and gel purified. The triphosphorylation state and purity were confirmed using mass spectrometry. The oligonucleotides were resuspended in RNA storage buffer (10 mmol/L MOPS pH 7, 1 mmol/L EDTA) and snap cooled to ensure hairpin formation, as previously described (28).

Cell line authentication

The human cell lines MCF-7, BT474, and murine cell line 4T1 were purchased from ATCC in 2015. All cells were maintained at low passage in DMEM with 10% fetal bovine serum and 1% antibiotics and antimyotics. Cell identity was verified by ATCC using genotyping with a Multiplex STR assay. All cell lines were screened monthly for *Mycoplasma*. Cells were used within 20 passages for each experiment.

Cell culture

SLR20 and OH-SLR20 were delivered to cells in serum-free Opti-MEM media at a final concentration of 0.25 μmol/L using lipofectamine 2000 (Invitrogen). Where indicated, cells were treated with staurosporine (Cell Signaling Technology) at a final concentration of 1 μmol/L in serum-free Opti-MEM. Cells expressing shRNA against RIG-I were generated by transduction with pLKO lentiviral particles (Sigma-Aldrich) harboring shRNA sequences against human or mouse RIG-I (*DDX58*) and selected with puromycin (2 μg/mL). Cells were treated with inhibitors for caspase-9 (Z-LEHD-FMK, BD Pharmingen), caspase-10 (Z-AEVD-FMK, Cayman Chemical), and caspase-1 (Ac-YVAD-CHO, Cayman Chemical) at a final concentration of 5 μmol/L.

Western analysis

Whole-cell lysate was harvested by homogenization of cells in ice-cold lysis buffer [50 mmol/L Tris pH 7.4, 100 mmol/L NaF, 120 mmol/L NaCl, 0.5% nonidet P-40, 100 μmol/L Na_3VO_4, 1 × protease inhibitor cocktail (Roche), 0.5 μM MG132 (Selleck Chem)]. Mitochondrial and cell membrane extracts were harvested from cells using the Cell Fractionation Kit (Cell

Published OnlineFirst September 17, 2018; DOI: 10.1158/0008-5472.CAN-18-0730

Signaling Technologies) according to the manufacturer's instructions. Lysates (20 μg protein measured by BCA assay) were resolved on 4% to 12% polyacrylamide gels (Novex) and transferred to nitrocellulose membranes (iBlot), blocked in 3% gelatin in TBS-T (Tris-buffered saline, 0.1% Tween-20), incubated in primary antibodies from Cell Signaling Technologies: (RIG-I (D14G6, 1:1,000), MAVS (3993, 1:1,000), SOD2 (D3 × 8F, 1:1,000), p65 (D14E12, 1:1,000), P-p65 Y701 (D4A7, 1:1,000), STAT1 (D1K9Y, 1:1,000), P-STAT1 S536 (93H1, 1:1,000), PARP (9542, 1:1,000), caspase-1 (2225, 1:1,000), cleaved caspase-1 (D57A2, 1:1,000), gasdermin D (96458, 1:1,000), Rab11 (7100, 1:1,000); β-actin (Sigma-Aldrich, AC-15, 1:10,000); and E-cadherin (BD Transduction Laboratories, 610182, 1:1,000). Secondary antibodies were from PerkinElmer [goat anti-rabbit (1:5,000) and goat anti-mouse (1:10,000)]. Western blots were developed with ECL substrate (Thermo Fisher Scientific).

Cytofluorescence

Live cells were incubated in MitoTracker Red (Invitrogen) for 45 minutes to stain mitochondria then 100% methanol fixed, blocked in TBS-T 3% gelatin and stained with rabbit anti–RIG-I (1:100, Cell Signaling Technology) and goat anti-rabbit Alexa Fluor 488 (1:1,000, Invitrogen). For apoptotic analysis, live cells were stained with Annexin V, AlexaFluor-488 conjugate (1:500, Invitrogen) for 4 hours before imaging. For pyroptotic studies, live cells were stained in propidium iodide (PI; Sigma-Aldrich, 1:1,000) for 1 hour before imaging.

Generation of nanoparticles for intratumoral delivery

Amphiphilic diblock copolymer composed of a 10.3 kDa dimethylaminoethyl methacrylate (DMAEMA) first block and a 31.0 kDa, 35% DMAEMA, 39% butyl methacrylate (BMA), and 26% propylacrylic acid (PAA) second block were synthesized as previously described (36). Dry amphiphilic diblock polymer was dissolved into ethanol at 50 mg/mL, rapidly diluted into phosphate buffer (pH 7.0, 100 mmol/L) to 10 mg/mL, concentrated, and buffer was exchanged into PBS (Gibco) using 3 kDa molecular weight cutoff centrifugal filtration columns (Ambion, Millipore) and sterile filtered. Polymer concentration was measured by absorbance at 310 nm (Synergy H1 microplate reader, BioTek). Concentrated polymer solution was rapidly mixed with SLR20 (or OH-SLR20) at a charge ratio of 5:1 (N:P) for 30 minutes and diluted into PBS (pH 7.4, Gibco) to 20 μg of SLR and 400 μg of polymer in 50 μL total volume.

Animal studies

All studies were performed in accordance with Association for Assessment and Accreditation of Laboratory Animal Care International (AAALAC) guidelines and were approved by the Institutional Animal Care and Use Committee at Vanderbilt University. All mice were housed in pathogen-free conditions. Left inguinal mammary fat pads of wild-type (WT) female Balb/c mice or athymic (*nu/nu*) Balb/c mice (Jackson Labs) were injected with 10^6 4T1 cells. Mice were randomized into treatment groups when tumors reached 50 to 100 mm^3. Intratumoral injection of nanoparticle in 50 μL of saline (or saline without nanoparticle) was performed at 48-hour intervals for a total of 3 treatments, or at 72- to 96-hour intervals for a total of 4 treatments. Intraperitoneal injection of InVivoMab αPD-L1 (B7-H1) and control IgG2b κ from Bio X Cell were delivered at 25 mg/kg in sterile saline twice weekly for 10 days. Mice were monitored daily, and tumor volume was measured with calipers twice weekly for up to 25 days.

Histologic analyses

Lungs and tumors were formalin-fixed and paraffin-embedded, and sections (5 μm) were stained with hematoxylin and eosin. *In situ* TUNEL analysis was performed on paraffin-embedded sections using the ApopTag kit (Millipore). IHC was performed using the following antibodies: RIG-I (Invitrogen, PA5-20276, 1:400), P-STAT1 (Cell Signaling Technology, 9167, 1:100), Ki67 (Biocare Medical, CFM325B, 1:100), CD45 (Abcam, ab10558, 1:5,000), F4/80 (Bio-Rad, MCA497GA, 1:100), CD4 (eBioscience, 14-0195-82, 1:1,000), CD8 (eBioscience, 14-0195-82, 1:100), TRAIL (GeneTex, 6TX11700, 1:800). Immunodetection was performed using the Vectastain kit (Vector Laboratories) according to the manufacturer's instructions.

RNA isolation and expression analyses

Total RNA was extracted using NucleoSpin RNA (Machery-Nagel), reverse transcribed (iScript cDNA Synthesis; Bio-Rad), and using for qPCR with iTaq Universal SYBR Green (Bio-Rad) on a Bio-Rad CFX96 thermocycler. Gene expression is normalized to *36B4*. The following primers were obtained from Integrated DNA Technologies: *IFNB1* [forward 5′-TGCTCTC-CTGTTGTGCTTCTCC; reverse 5′-GTTCATCCTGTCCTTGAGGC-AGT]; *Ifnb1* [forward 5′-CAGCTCCAAGAAAGGACGAAC; reverse 5′-GGCAGTGTAACTCTTCTGCAT]; *HLA-A* [forward 5′-GCGGCTACTACAACCAGAGC; reverse 5′-GATGTAATCCTTG-CCGTCGT]; *TNF* [forward 5′-CCTCTCTCTAATCAGCCCTCTG; reverse 5′-GAGGACCTGGGAGTAGATGAG]; *Tnf* [forward 5′-CCCTCACACTCAGATCATCTTCT; reverse 5′-GCTACGACGT-GGGCTACAG]; *TNFSF10* [forward 5′-TGCGTGCTGATCGT-GATCTTC; reverse 5′-GCTCGTTGGTAAAGTACACGTA]; *Tnfsf10* [forward 5′-ATGGTGATTTGCATAGTGCTCC; reverse 5′-GCA-AGCAGGGTCTGTTCAAGA]. Other genes were analyzed via PCR array (RT^2 Profiler Array, Qiagen).

Cytokine array

Cells (1×10^6) were seeded. After 24 hours, cells were transfected with SLR20 or OH-SLR20 as described above. Cell culture media were removed 32 hours after transfection, filtered with a 0.2 micron strainer, and immediately added to blocked membranes from Human Cytokine Antibody Array C1000 (RayBiotech), and processed according to the manufacturer's instructions. Chemiluminescent cytokine arrays were imaged digitally using Amersham Imager 600 (GE Healthcare).

Statistical analysis

Experimental groups were compared with controls using Student unpaired, two-tailed *t* test. Multiple groups were compared across a single condition using one-way analysis of variance (ANOVA). $P < 0.05$ was used to define significant differences from the null hypothesis. qPCR array data sets were compared using multiple *t* tests with an FDR cutoff of 0.05.

Ethics statement

Animals were housed under pathogen-free conditions, and experiments were performed in accordance with AAALAC

Published OnlineFirst September 17, 2018; DOI: 10.1158/0008-5472.CAN-18-0730

guidelines and with Vanderbilt University Institutional Animal Care and Use Committee approval.

Results

Breast cancer cell autonomous RIG-I signaling is activated by a synthetic RIG-I mimetic

To assess the potential applicability of a RIG-I agonist in breast cancer, we examined RIG-I/*DDX58* expression in a clinical invasive breast cancer data set curated by The Cancer Genome Atlas (TCGA; ref. 37). We found genomic *DDX58* deletion in only 1 of 817 tumors and mRNA downregulation in only 8 of 817 tumors (Fig. 1A), suggesting that loss of RIG-I expression is a rare event. Similar results were produced upon the analysis of 2509 breast tumors from the METABRIC invasive breast cancer data set (Supplementary Fig. S1A; ref. 38). Whole-exome sequencing data identified 3 nonrecurrent missense mutations within *DDX58*, and no recurrent, truncating, or in-frame mutations (Supplementary Fig. S1B), suggesting that RIG-I/*DDX58* is rarely lost or mutated in breast cancers.

Western analysis confirmed RIG-I expression in two human breast cancer cell lines, MCF7 (ER^+), and BT474 (HER2 amplified; Fig. 1B), but not in HER2-amplified, ER^+ MDA-MB-361 cells (Supplementary Fig. S2A). To determine if RIG-I signaling pathways are functional in breast cancer cells, we used a previously described synthetic minimal RIG-I agonist composed of a double-stranded, triphosphorylated 20-base pair stem-loop RNA, which was then modified with a 5′ triphosphate sequence (SLR20; ref. 39). Previous studies demonstrated that SLRs containing the 5′ ppp motif, but not those lacking the motif, activate type I IFN production via RIG-I/MAVS signaling. We transfected SLR20 (and the nonphosphorylated, but otherwise identical sequence, OH-SLR20) into MCF7 cells and measured RIG-I expression and distribution by immunofluorescence. RIG-I expression was robustly increased in cells transfected with the RIG-I ligand SLR20 as compared with the control ligand OH-SLR20 (Fig. 1C). Counterstaining of mitochondria demonstrated mitochondrial localization of RIG-I in many cells following SLR20 treatment. Further, analysis of mitochondrial cell fractions by Western analysis confirmed mitochondrial RIG-I localization in MCF7 and BT474 cells transfected with SLR20, but not OH-SLR20 (Fig. 1D). Western analysis confirmed RIG-I upregulation following transfection with SLR20 in MCF7, BT474, and mouse 4T1 cells, a mammary tumor line used as a model of aggressive, metastatic, and poorly immunogenic TNBC (Fig. 1E). Importantly, SLR20 increased phosphorylation of the proinflammatory transcription factors p65 (an NF-κB subunit) and STAT1 in MCF7, BT474, and 4T1 cells. Importantly, SLR20 did not affect P-p65 in MDA-MB-361 cells, which lack RIG-I expression (Supplementary Fig. S2B). These data support use of these breast cancer cell lines, and the SLR20 agonist, to model the therapeutic impact of RIG-I signaling in breast cancer.

A nanoparticle-based approach for RIG-I activation *in vivo* decreases breast tumor growth and metastasis

A recent study examining SLR delivery *in vivo* confirmed rapid induction of type I IFNs following delivery of a 10-bp SLR sequence (SLR10; ref. 28). However, the impact of RIG-I activation in the complex breast tumor microenvironment has not been explored. We used a nanoparticle-based platform previously optimized for oligonucleotide delivery *in vivo* for intratumoral (i.t.) treatment of breast tumors with SLR20 (Fig. 2A). These pH-responsive nanoparticles (NP) were composed of amphiphilic diblock copolymers formulated with a hydrophobic core-forming block that is endosomolytic and drives micellar assembly, and a polycationic corona for electrostatic complexation with oligonucleotide (i.e., SLR20), as described previously (36). This formulation has been shown to maximize cytoplasmic delivery of oligonucleotides, an ideal scenario for cytoplasmic RIG-I activation by SLR20. NPs were delivered i.t. to 4T1 mammary tumors grown in WT Balb/c female mice when tumors reached 50 to 100 mm^3. As an additional control, a third group of tumor-bearing mice were treated by i.t. injection of saline, the vehicle in which NPs were delivered. A total of 3 treatments were administered (days 0, 2, and 4; Fig. 2B). IHC of tumors collected at day 5 (24 hours after final treatment) revealed RIG-I protein upregulation in 4T1 tumors treated with SLR20 NPs over saline-treated or OH-SLR20 NP-treated tumors (Fig. 2C–D and Supplementary Fig. S2C). Further, tumors treated with SLR20 NPs, but not OH-SLR20 NPs, exhibited a 3-fold increase in phosphorylation of STAT1 (Fig. 2C and D), confirming RIG-I signaling in SLR20-treated tumors *in vivo*.

We used a slightly modified treatment scheme to assess the therapeutic impact of SLR20-NP on tumor growth. Tumors were treated on days 0, 3, 6, and 9 with i.t. delivery of SLR20 NPs, at which point treatment stopped and tumor volume was monitored through day 25 (Fig. 2E). Tumors treated with SLR20 NPs did not increase in volume during the treatment window (days 0–9), while tumors treated with saline or with OH-SLR20 NPs increased nearly 4-fold (Fig. 2F). Once treatment was complete, tumors treated with SLR20 resumed volumetric increase, but still grew at a diminished rate as compared with tumors treated with OH-SLR20 NPs or with saline. Lungs harvested from mice on day 25 revealed a decreased number of lung metastases in the SLR20-treated mice as compared with control groups (Fig. 2G). Treatment extended through treatment day 25 (Supplementary Fig. S3A) resulted in sustained tumor growth inhibition in response to SLR20 (Supplementary Fig. S3B).

RIG-I signaling induces breast cancer cell death through tumor cell–intrinsic pathways

We investigated potential mechanisms responsible for decreased tumor growth and metastasis following treatment with SLR20 NPs, first measuring Ki67-positive cells by IHC as a marker of cell proliferation (Fig. 3A; Supplementary Fig. S4A). Assessing 4T1 tumors collected on treatment day 5, we found a decreased percentage of $Ki67^+$ tumor cells in samples treated with SLR20 NPs as compared with samples treated with OH-SLR20-NPs or with saline (Fig. 3B). Conversely, tumor cell death, measured by terminal dUTP nick-end labeling (TUNEL) analysis (Fig. 3A), was increased 5-fold in samples treated with SLR20 NPs (Fig. 3B). RIG-I signaling is capable of inducing programmed cell death in many cell types, including some cancer cell types (40), although this possibility remains unclear in breast cancers. Therefore, we transfected MCF7, BT474, and 4T1 cells in culture with SLR20, assessing cells 12 hours after transfection for PARP cleavage, a molecular marker of cell death. Cleaved PARP was increased in cells transfected with SLR20 versus OH-SLR20 (Fig. 3C). Annexin V-FITC staining was used to enumerate apoptotic cells, revealing increased

Published OnlineFirst September 17, 2018; DOI: 10.1158/0008-5472.CAN-18-0730

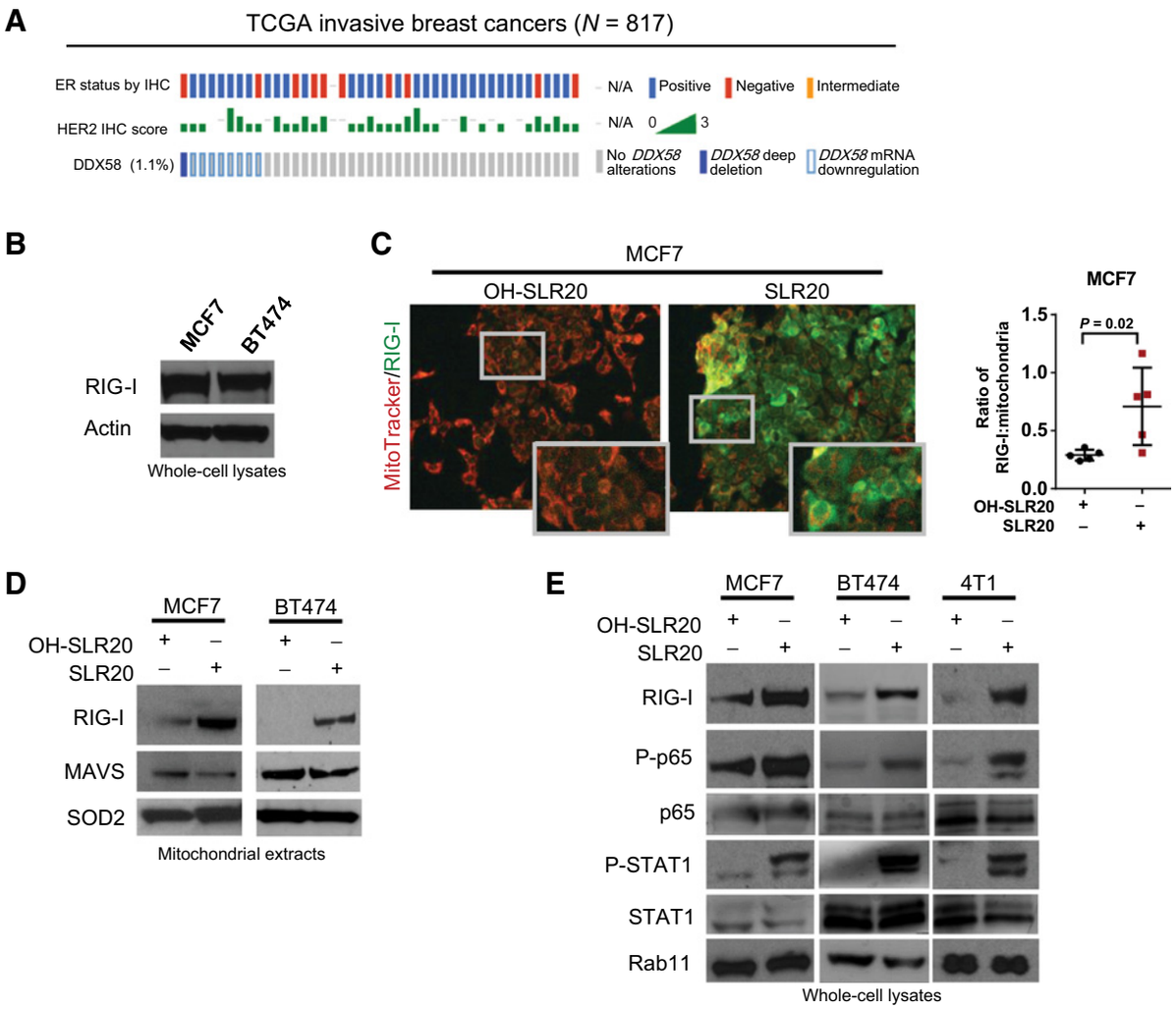

Figure 1.

RIG-I/DDX58 is expressed in breast cancers and is activated by the RIG-I agonist SLR20. **A,** TCGA-curated clinical data set of invasive breast cancers ($N = 817$; ref. 37) was assessed for samples harboring genomic *DDX58* loss (solid blue) and/or *DDX58* mRNA downregulation (defined as <−1 SD from the mean *DDX58* expression among the entire data set and shown in blue outline). Reported scores for IHC analysis of ER and HER2 corresponding to each clinical specimen are shown. **B,** Whole-cell lysates were assessed by Western analysis using the antibodies indicated to the left of each blot. **C,** Sixteen hours after transfection with OH-SLR20 and SLR20, cells were fixed, assessed by immunofluorescence to detect RIG-I (green fluorescence), and counterstained with MitoTracker Red (red fluorescence). Left, representative images are shown. The inset shows a high-power magnification of the boxed area within each respective panel. Right, the ratio of RIG-I staining to MitoTracker is shown. MitoTracker staining was quantified as the number of red fluorescent pixels per 40× field using ImageJ. RIG-I immunofluorescent staining was quantified as the number of green fluorescent pixels per 40× field. Each point represents the average value of three random fields per sample, $N = 5$ samples. Midlines and error bars show average ± SD. *P* value was calculated using Student unpaired *t* test. **D,** Mitochondrial fractions of cells were assessed by Western analysis 18 hours after transfection, using the antibodies shown on the left of each panel. Representative images are shown. $N = 3$. **E,** Whole-cell lysates collected 12 hours after transfection were assessed by Western analysis using the antibodies shown on the left of each panel. Representative images are shown. $N = 3$.

Annexin V^+ cells following SLR20 treatment in MCF7, BT474, and 4T1 cells (Fig. 3D), but not in MDA-MB-361 cells, which lack RIG-I expression (Supplementary Fig. S4B). Importantly, knockdown of RIG-I in MCF7, BT474, and 4T1 cells using shRNA sequences against RIG-I (Fig. 3E) abrogated the increased Annexin V staining in response to SLR20 (Fig. 3F), while SLR20 remained capable of inducing Annexin V staining in cells expressing nontargeting shRNA sequences. These findings demonstrate that SLR20 activates RIG-I signaling in breast cancer cells, inducing cell death in a tumor cell–intrinsic manner.

RIG-I signaling in breast cancer cells induces intrinsic apoptosis and pyroptosis

Because RIG-I signaling is reported to induce apoptosis through several distinct pathways, including intrinsic apoptosis, extrinsic apoptosis, and pyroptosis pathways across a variety of cell types (33), it is unclear by which pathway RIG-I

Published OnlineFirst September 17, 2018; DOI: 10.1158/0008-5472.CAN-18-0730

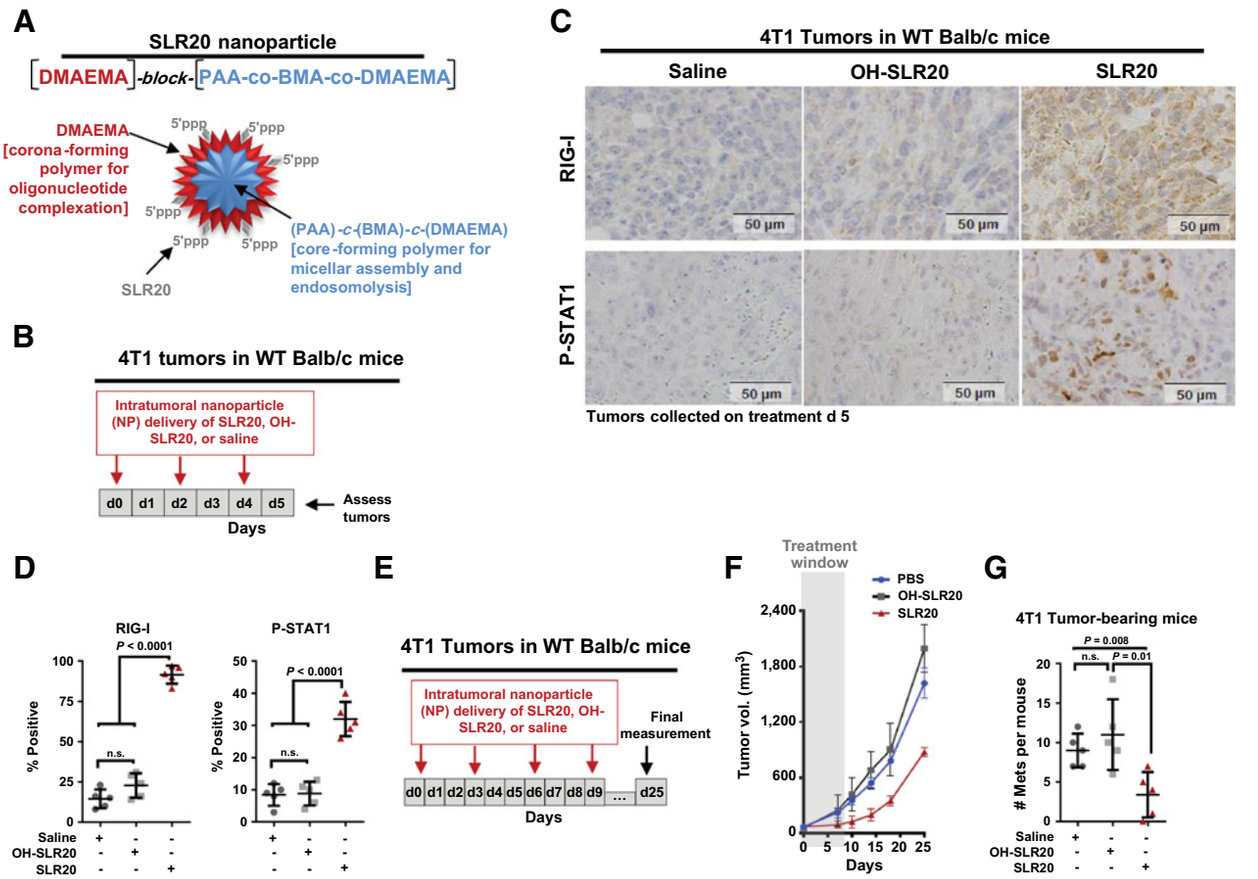

Figure 2.

RIG-I agonist SLR20 induces RIG-I signaling and impairs tumor progression *in vivo*. **A,** Schematic representation of nanoparticle formulation used to treat tumor-bearing mice *in vivo*. **B,** Schematic of treatment strategy for intratumoral nanoparticle delivery of SLR20 (or OH-SLR20) to WT Balb/c mice harboring 4T1 mammary tumors. Saline was delivered intratumorally as a control. **C** and **D,** IHC was used to measure RIG-I and P-STAT1 in tumors harvested at day 14. **B**, Representative images are shown. $N = 5$. **C**, IHC staining for RIG-I and P-STAT1 was quantitated. Each point represents the average of three random fields per sample, $N = 5$. Midlines show average (±SD). *P* values were calculated using Student *t* test. **E,** Schematic of treatment strategy for intratumoral nanoparticle delivery of SLR20 (or OH-SLR20) to WT Balb/c mice harboring 4T1 mammary tumors. Saline was delivered intratumorally as a control. Tumors were measured throughout treatment (days 0–9) and for 16 days after treatment ceased (days 10–25). Tumors were collected on day 25 (16 days after the final treatment). **F,** Tumor volume was measured beginning at treatment day 1. $N = 10$ per group through day 5. $N = 5$ per group from days 6 to 25. **G,** Lungs harvested at day 25 were assessed histologically for metastatic lesions. Each point represents the number of metastases per individual mouse. Midlines represent the average (± SD); Student *t* test. n.s., nonsignificant.

induces cell death in breast cancers. We investigated this using an apoptosis expression array, assessing expression changes in 84 genes associated with the intrinsic and extrinsic apoptosis pathways. RNA harvested from BT474 cells collected 16 hours after transfection harbored changes in 18 of the 84 genes assessed. Genes arranged in order of expression fold change revealed that genes regulating intrinsic apoptosis (e.g., *BAD, BAX, CASP9*) were downregulated, while expression of genes regulating the extrinsic apoptosis pathway (*TNFSF10, FAS, CASP10, CASP8*) were upregulated (Fig. 4A), suggesting that the extrinsic apoptosis pathway might be activated in response to RIG-I signaling in breast cancer cells. We confirmed that SLR20 induced expression of the extrinsic apoptotic factor *TNFSF10* in MCF7, BT474, and 4T1 cells (Fig. 4B). Additionally, 4T1 tumors treated *in vivo* with SLR20 NPs were assessed by IHC for expression of the *Tnfsf10* gene product, TRAIL. Although TRAIL was expressed at only low levels in 4T1 tumors treated with saline or with OH-SLR20 NPs (Fig. 4C), TRAIL protein levels were markedly upregulated in samples treated with SLR20 NPs.

These data suggest that RIG-I might activate the extrinsic apoptosis pathway in breast cancer cells but do not rule out that RIG-I signaling might also induce breast cancer cells to undergo pyroptosis, an inflammatory type of programmed cell death that requires activation of caspase-1 and oligomerization of gasdermin D on the cell membrane (41). Western analysis of MCF7 and BT474 cells transfected with SLR20 revealed potent activation of caspase-1 (Fig. 4D) and localization of gasdermin D to cell membranes (Fig. 4E). These findings were confirmed in 4T1 cells (Supplementary Fig. S4C). Upregulation of *CASP1* and *CASP4* (encoding another mediator of pyroptosis, caspase-4) was seen in BT474 cells transfected with SLR20 (Fig. 4F).

Published OnlineFirst September 17, 2018; DOI: 10.1158/0008-5472.CAN-18-0730

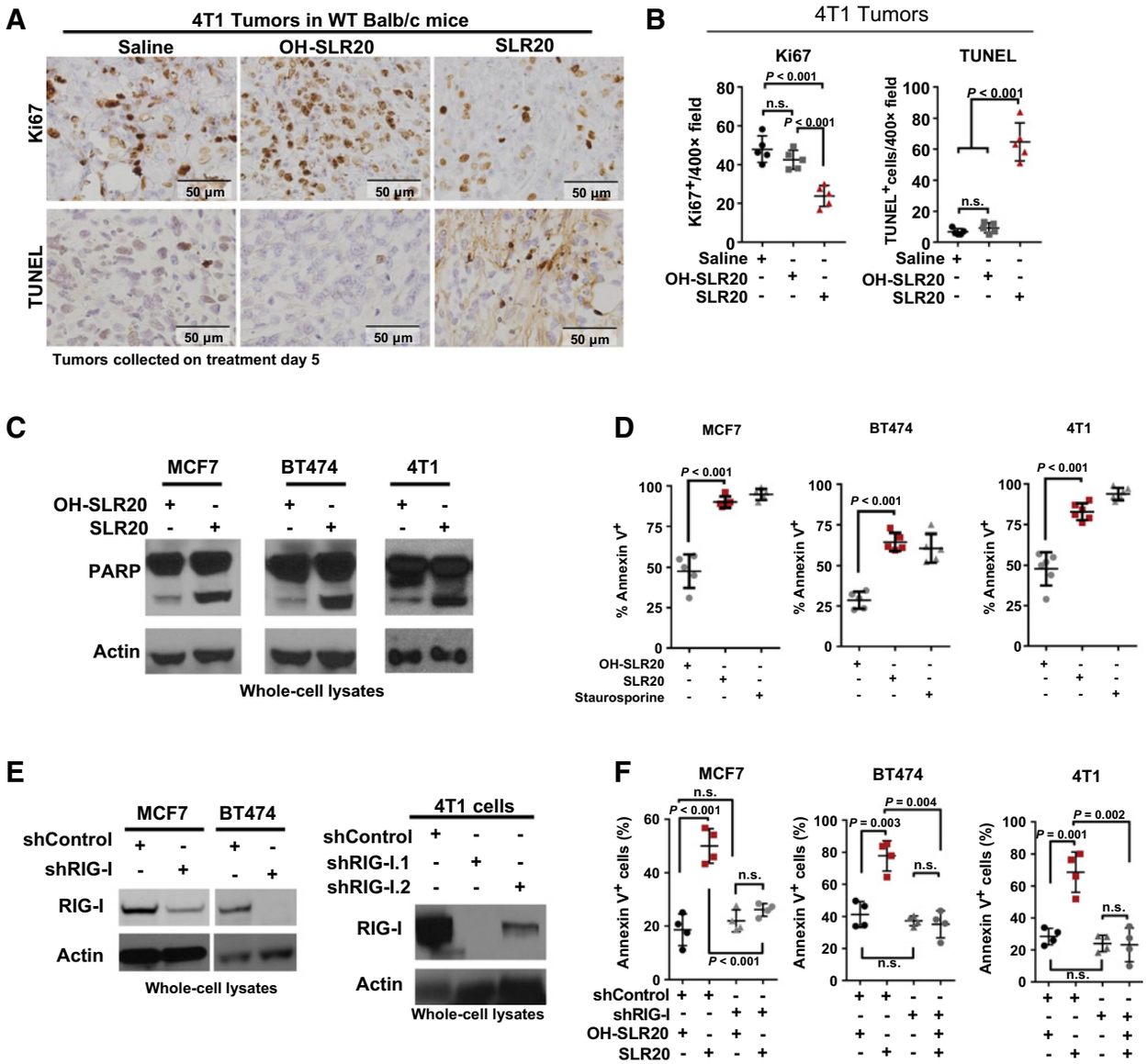

Figure 3.

RIG-I agonist SLR20 induces tumor cell apoptosis. **A** and **B,** histologic analysis of tumor sections using IHC against Ki67 and TUNEL analysis. **B,** Representative images are shown. $N = 5$. **C,** The number of Ki67$^+$ cells and TUNEL$^+$ cells per 400× field was quantitated. Each point represents the average of three random fields per sample, $N = 5$. Midlines show average (± SD). *P* values were calculated using Student *t* test. **C,** Western analysis of whole-cell lysates harvested 12 hours after transfection, using antibodies indicated on the left of each panel. **D,** Cells were transfected, and after 18 hours, cells were stained with Annexin V-AlexaFluor488 for 4 hours. AlexaFluor488$^+$ cells were imaged by fluorescence microscopy. The number of Annexin V$^+$ cells per well was counted. Each point shown represents the average of two experimental replicates, $N = 5$. Midlines represent the average (± SD). *P* values were calculated using Student *t* test. Staurosporine treatment (1 μmol/L) was performed in parallel as a positive control for induction of apoptosis/Annexin V staining. **E,** Western analysis of whole-cell lysates using antibodies shown on left of each panel. **F,** Cells were transfected and stained with Annexin V-FITC as shown in **D**. n.s., nonsignificant.

Importantly, *Casp1* levels were increased in 4T1 tumors treated *in vivo* with SLR20 NPs, but not in tumors treated with OH-SLR20 NPs (Fig. 4G), suggesting the RIG-I–mediated activation of pyroptotic signaling pathway may be maintained even within the complex tumor microenvironment.

Next, we used a selective inhibitor of caspase-10, AEVD-FMK, to block the extrinsic apoptotic pathway, resulting in a moderate, but significant, diminution of Annexin V$^+$ cells following treatment with SLR20 (Fig. 4H). In contrast, the caspase-9 inhibitor Z-LEHD-FMK, which blocks activation of the intrinsic apoptotic pathway, had little impact on Annexin V staining in cells transfected with SLR20. We also tested an inhibitor of caspase-1, Z-YVAD-FMK, to block the pyroptosis pathway in SLR20-transfected cells, resulting in partial inhibition of

Published OnlineFirst September 17, 2018; DOI: 10.1158/0008-5472.CAN-18-0730

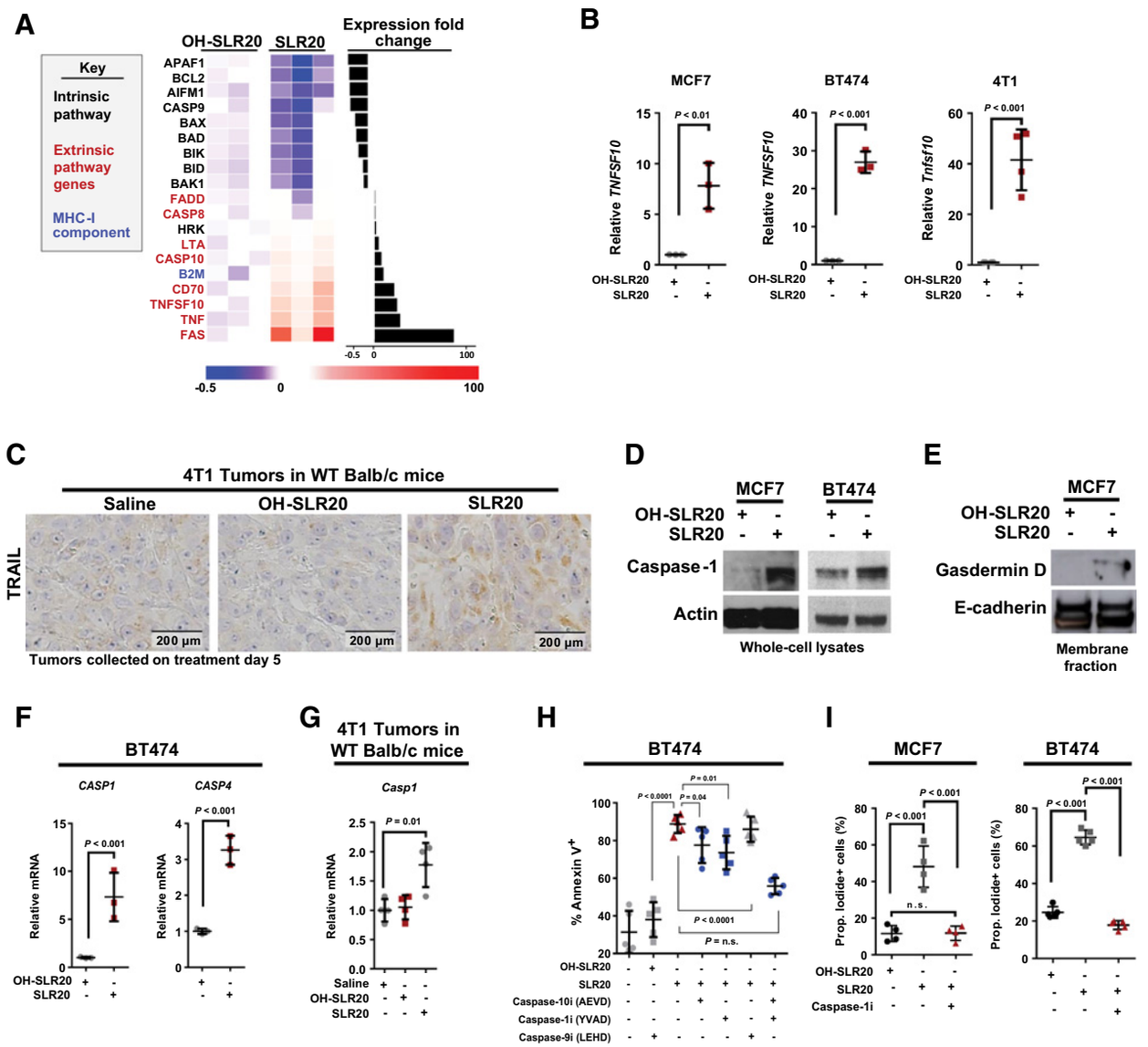

Figure 4.

RIG-I signaling in breast cancer cells induces extrinsic apoptosis and pyroptosis. **A,** BT474 cells were transfected with SLR20 or OH-SLR20. After 12 hours, RNA was collected and assessed for expression of genes within the intrinsic and extrinsic apoptosis pathway (RT2 Profiler Apoptosis Array). Relative gene-expression values were calculated using the ddCT method, correcting for expression of *ACTB* and *GAPDH*, and are shown as expression relative to the average value for each gene in OH-SLR20-transfected cells, as shown in the heat map**.** Genes (listed at left) were ranked in order of expression fold change, as shown on the right. **B,** Cells were transfected, and after 12 hours, total RNA was assessed by RT-qPCR to measure expression of the indicated genes involved in pyroptosis. Each point represents the average of three experimental replicates, $N = 3$. Midlines are average ± SD. Student *t* test. **C,** IHC analysis to detect TRAIL in 4T1 tumors harvested on treatment day 5. **D** and **E,** Western analysis of whole-cell lysates (**D**) or membrane fractions (**E**) harvested 16 hours after transfection using the antibodies shown on left of each panel. **F,** Cells were transfected, and after 12 hours, total RNA was assessed by RT-qPCR to measure expression of the indicated genes involved in pyroptosis. Each point represents the average of three experimental replicates, $N = 3$. Midlines are average ±SD. Student *t* test. **G,** RNA harvested from 4T1 tumors collected on treatment day 5 was assessed by RT-qPCR for *Casp1* gene expression as described in **C**. **H** and **I,** Cells were transfected and immediately treated with caspase-specific inhibitors (each used at 10 µmol/L). After 18 hours, cells were stained with Annexin V-AlexFluor488 for 4 hours (**H**) or PI for 10 minutes (**I**). AlexaFluor488$^+$ and PI$^+$ cells were imaged by fluorescence microscopy. The number of fluorescent cells per well was counted. Each point shown represents the average of two experimental replicates, $N = 5$ (**H**) and $N = 4$–5 (**I**). Midlines represent the average (±SD). *P* values use Student *t* test.

Annexin V staining. These results were confirmed in MCF7 cells (Supplementary Fig. S4D). Interestingly, the combination of the caspase-10 inhibitor with the caspase-1 inhibitor produced a greater reduction in Annexin V staining in BT474 cells as compared with either inhibitor used alone (Fig. 4H), consistent with the idea that these two inhibitors operate through distinct

Published OnlineFirst September 17, 2018; DOI: 10.1158/0008-5472.CAN-18-0730

pathways in BT474 cells, and suggesting that RIG-I signaling in breast cancer cells may use both the intrinsic apoptosis pathway and pyroptosis to potently induce programmed cell death. Because pyroptosis produces pores in the plasma membrane (41), making them permeable to PI, we stained MCF7 and BT474 cells with PI at 12 hours after transfection with OH-SLR20 or SLR20, finding a robust increase in PI^+ staining when cells were transfected with SLR20 (Fig. 4I). However, PI staining was completely abolished in MCF7 and BT474 cells pretreated with the caspase-1 inhibitor, confirming that pyroptosis is induced by SLR20 in breast cancer cells.

RIG-I signaling increases breast tumor-infiltrating leukocytes

In contrast to the intrinsic apoptosis pathway, which is considered an immunologically silent form of programmed cell death, pyroptosis is thought to be an immunogenic form of cell death that may recruit inflammatory leukocytes to the site of a viral infection through cytokine modulation, while increasing immunogenicity of the infected cell through increased expression of the major histocompatibility complex (MHC)-I, the antigen presentation machinery expressed on most nucleated cells. Consistent with this idea, both MCF7 and BT474 breast cancer cells transfected with SLR20 showed upregulation of *HLAB* (Fig. 5A), encoding a key MHC-I component. The gene *B2M*, encoding another key MHC-I component, β2 microglobulin, was similarly upregulated in BT474 cells (Fig. 4A).

We assessed leukocyte recruitment to 4T1 mammary tumors grown in immune-competent Balb/c mice following treatment with SLR20 NPs. IHC analysis for CD45, a pan-leukocyte marker, revealed substantially increased $CD45^+$ cells in tumors treated with SLR20 NPs versus saline or OH-SLR20 NPs (Fig. 5B and Supplementary Fig. S5). Further, IHC analysis using antibodies against F4/80 (a mature macrophage marker), CD4 (a marker of helper T lymphocytes), and CD8, a marker of cytotoxic T lymphocytes (CTL), natural killer T cells (NK-T) and inflammatory dendritic cell (DC) populations, were each increased in tumors treated with SLR20 NPs as compared with saline OH-SLR20 NP-treated tumors (Fig. 5B and C). These data suggest that RIG-I activation results in active recruitment of leukocytes to the TME, consistent with a more immunogenic tumor microenvironment. Consistent with this notion, we found that SLR20 delivery to 4T1 tumors grown in immunocompromised athymic Balb/c (*nu/nu*) mice displayed more rapid resurgence of tumor growth once the SLR20 treatment was discontinued (Supplementary Fig. S6). This use of the RIG-I ligand to generate a more immunogenic tumor microenvironment was tested more directly using SLR20 in combination with the ICI, αPD-L1. Tumor-bearing WT Balb/c mice were randomized into groups to receive treatment with SLR20, OH-SLR20, or saline and were randomized further into groups receiving αPD-L1 or an isotype-matched control IgG (Fig. 5D). Tumors were treated twice weekly through treatment day 10 and monitored through treatment day 18. We found that tumors treated with SLR20 alone grew at a slower rate than tumors treated with OH-SLR20 or with saline (Fig. 5E). Tumor growth was inhibited by treatment with αPD-L1 alone. However, the combination of SLR20 with αPD-L1 decreased tumor growth to a greater extent than either agent alone, and to a greater extent than αPD-L1 in combination with the control OH-SLR20 NP. These findings are consistent with the idea that SLR20 increases the immunogenicity of the tumor microenvironment in this model of breast cancer.

Cytokine and chemokine modulation by RIG-I signaling in breast cancer cells

Like many PRRs, RIG-I induces expression of inflammatory cytokines required for lymphocyte recruitment (42). Therefore, we measured expression of *IFNB1* in MCF7, BT474, and 4T1 cells following transfection with SLR20, revealing *IFNB1* upregulation (Fig. 6A). Notably, *Ifnb1* upregulation was also seen in 4T1 tumors treated *in vivo* with SLR20 NPs (Fig. 6B). SLR20-mediated upregulation of *IFN1B* was impaired in MCF7 and BT474 cells expressing RIG-I-directed shRNA sequences (Fig. 6C; Supplementary Fig. S7). This suggests that RIG-I signaling in breast cancer cells might be capable of activating *in trans* the antigen presenting cells, such as macrophages, within the tumor microenvironment. We tested this hypothesis by harvesting cultured media from 4T1 cells transfected with SLR20 or OH-SLR20, and adding the cultured media to macrophage-derived Raw264.7 cells. After 30 minutes of exposure to cultured media harvested from 4T1 cells treated with SLR20, we found phosphorylation of the proinflammatory transcription factor STAT1 (Supplementary Fig. S8A). Induction of *TNF* gene expression following transfection with SLR20 also was seen in MCF7, BT474, and 4T1 (Fig. 6D), but not in cells expressing RIG-I shRNA sequences (Supplementary Fig. S8B). To confirm that these gene-expression changes were seen at the protein level, we assessed cultured media harvested from MCF7 cells 48 hours after transfection with SLR20 by cytokine array analysis. Although this array did not carry IFNβ, we observed increased protein levels of TNFα and TNFβ in the cultured media harvested from SLR20 transfected MCF7 cells (Fig. 6E). Additionally, MCF7 cells transfected with SLR20 harbored increased protein expression of several IFNβ-inducible chemokines known to recruit T lymphocytes, including chemokine (C-C) motif ligand (CCL)-3, CCL5, CCL13, C-X-C motif chemokine ligand 11 (CXCL11), lymphotactin/C-motif ligand (XCL1) and interleukin (IL)-8.

Discussion

Although RIG-I–dependent anticancer immunity has been reported in several cancers, including pancreatic cancer, hepatocellular carcinoma (40), leukemias (43), and melanomas (31), little is known regarding RIG-I signaling in breast cancers. We used a synthetic agonist to activate the innate immune effector RIG-I in breast cancer cells in culture and *in vivo*, resulting in decreased tumor growth, decreased metastasis, increased TILs, and induction of tumor cell death via pyroptosis, an immunogenic form of cell death. These results suggest that RIG-I signaling remains intact in breast cancer cells and can be exploited to increase tumor cell death and, perhaps, tumor immunogenicity. Similar results have been reported from preclinical tumor models and clinical trials in cancers assessing the STING-mediated DNA/viral-sensing pathway (19, 20, 23), although STING signaling reportedly may be defective in a variety of cancers (24, 25). Nonetheless, these findings suggest that the developing field of RIG-I mimetics and the wider field of innate anticancer immunity may yield novel treatment strategies for breast cancers, which historically have not benefited to the same extent as other cancers from recent breakthroughs in immuno-oncology.

Published OnlineFirst September 17, 2018; DOI: 10.1158/0008-5472.CAN-18-0730

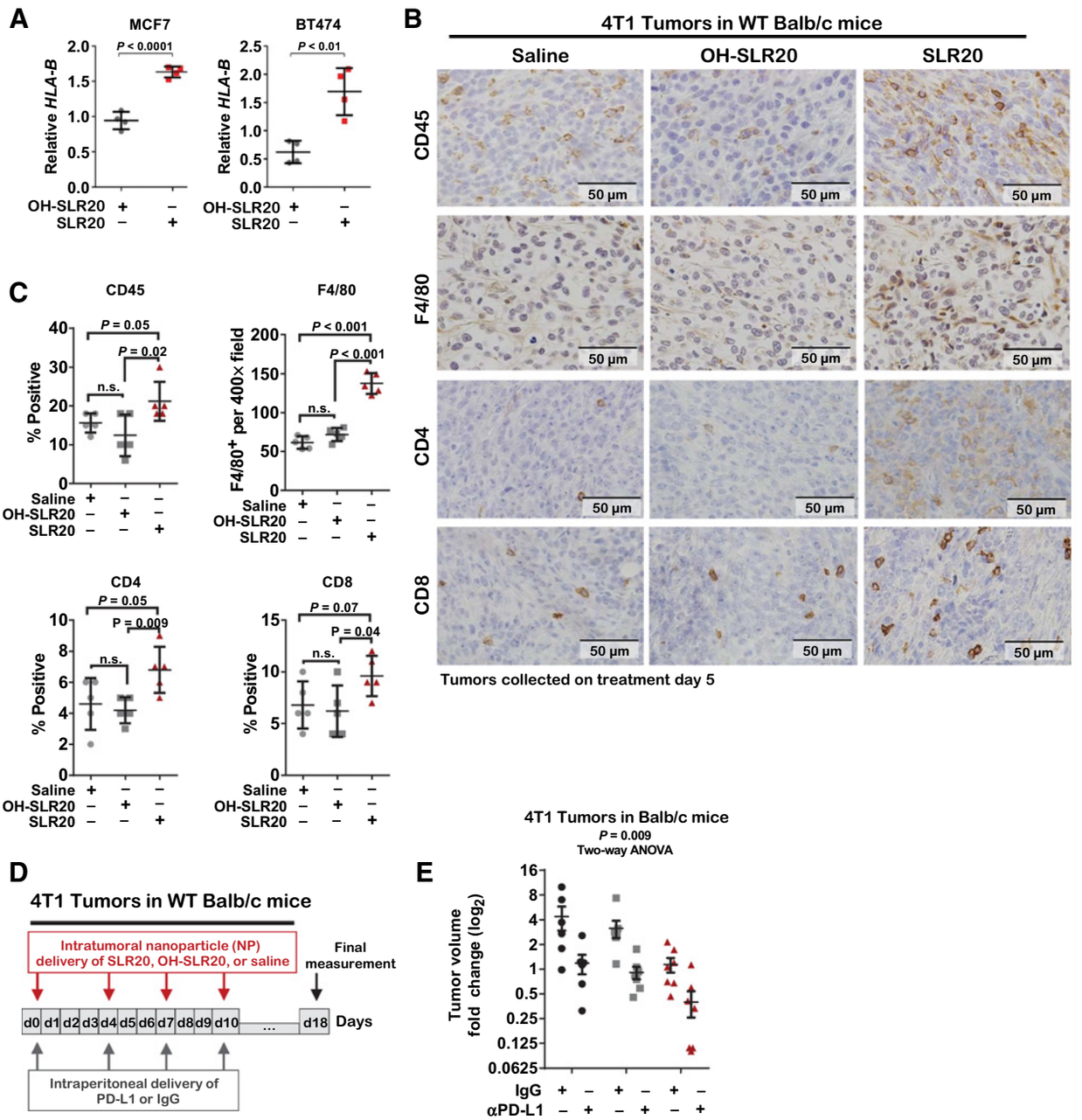

Figure 5.

RIG-I signaling induces immunogenic cell death and increases tumor leukocyte infiltration. **A,** Cells were transfected, and after 12 hours, total RNA was assessed by RT-qPCR to measure expression of the MHC Class II gene *HLAB*. Each point represents the average of three experimental replicates, $N = 3$. Midlines are average ± SD. Student *t* test. **B** and **C,** histologic analysis of tumor sections using IHC against F4/80analysis. **B,** Representative images are shown. $N = 5$. **C**, The number of $CD45^+$, $F4/80^+$, $CD4^+$, and $CD8^+$ cells per 400× field was quantitated. Each point represents the average of three random fields per sample, $N = 5$. Midlines show average (±SD). *P* values were calculated using Student *t* test. **D,** Schematic of treatment strategy for intraperitoneal delivery of αPD-L1 or IgG, and intratumoral nanoparticle delivery of SLR20 (or OH-SLR20, or saline) to WT Balb/c mice harboring 4T1 mammary tumors. Tumors were measured throughout treatment (days 1–10) and for 8 days after treatment ceased (days 11–18). **E,** Tumor volume was measured beginning at treatment day 1. $N = 7$ to 8 per group. n.s., nonsignificant.

The data shown herein are the first (to our knowledge) showing that RIG-I signaling provides a therapeutic benefit in breast cancer cells, *per se*, and in a mouse model of breast cancer *in vivo*. Interestingly, a previous report identified RIG-I/*DDX58* as belonging to an antimetastatic gene signature in breast cancer cells (44); however, the significance of this interesting finding remains unclear. Our findings here are consistent with a previous report using poly(I:C), a

Published OnlineFirst September 17, 2018; DOI: 10.1158/0008-5472.CAN-18-0730

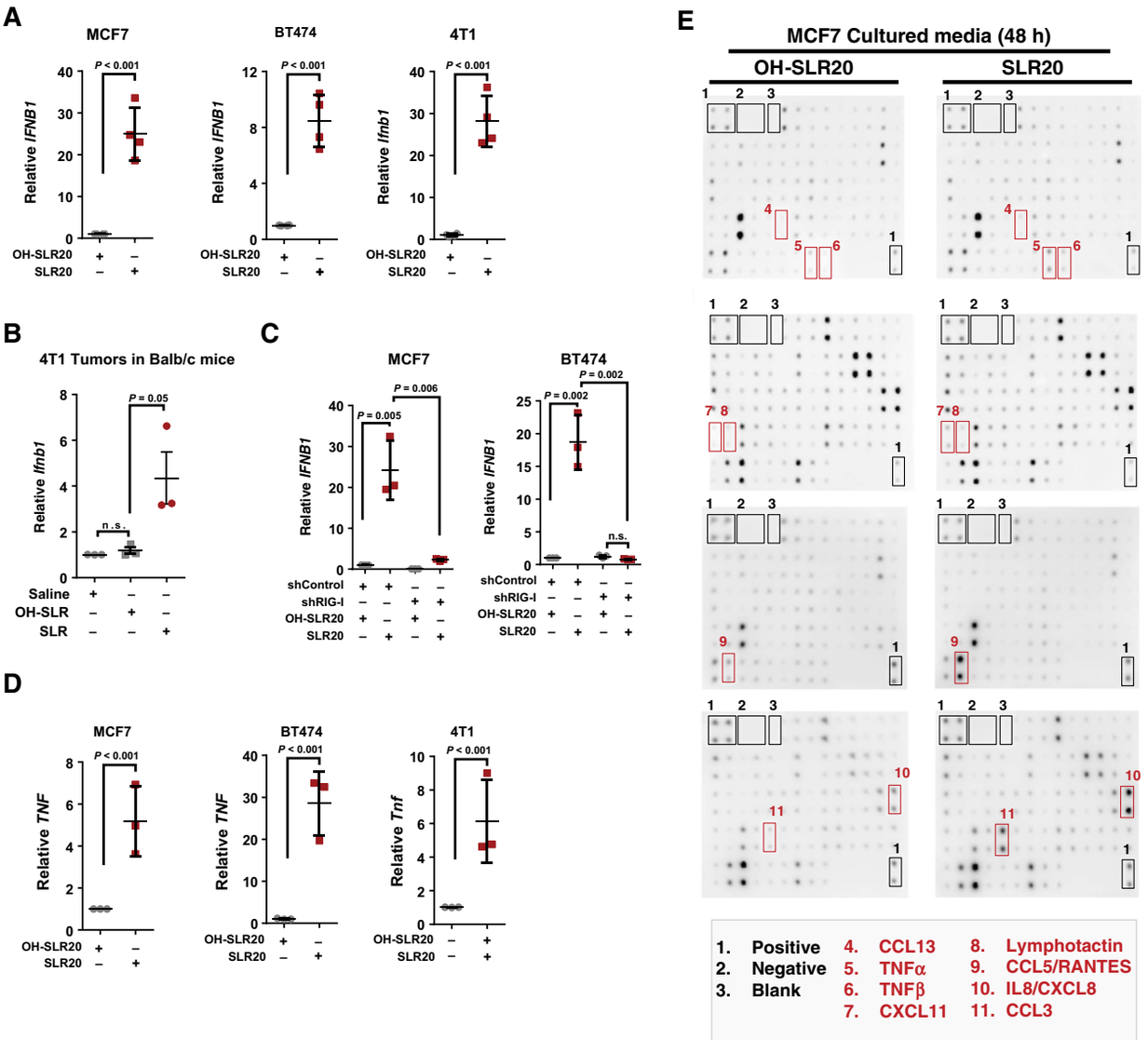

Figure 6.

RIG-I signaling induces expression of proinflammatory cytokines from breast cancer cells. **A–D,** Cells were transfected, and after 12 hours, total RNA was assessed by RT-qPCR to measure expression of the indicated genes. Each point represents the average of three experimental replicates, $N = 3$. Midlines are average ± SD. Student *t* test. **E,** Cytokine array assessing cultured media harvested from MCF7 cells 48 hours after transfection. Representative images are shown.

double-stranded RNA that binds to a RIG-I like receptor known as MDA5, as well as Toll-like receptor 3 (TLR3), to demonstrate that viral-sensing RNA helicases can activate proinflammatory signaling pathways that can be exploited therapeutically in breast cancers (45). We have built upon these important early studies by investigating models of each of the three major clinical subtypes of breast cancer, including poorly immunogenic ER^+ breast cancers, and highly aggressive TNBCs (1). We have also studied the impact of RIG-I signaling in the context of an immune-competent mouse model, finding that RIG-I signaling not only induces tumor cell death and cytokine modulation, but also increases tumor infiltration by leukocytes, a significant finding given that increased TILs predict a better outcome for patients with breast cancer and correlates with increased response to ICIs (5, 8, 9).

Although proinflammatory cytokines, such as those induced by RIG-I signaling, support antitumor immunity, these are likely to have multifaceted effects on antitumor immunity, depending on their expression dose and duration. For example, type I IFNs promote DC maturation and T-cell priming during an antitumor immune response, but prolonged IFN exposure induces regulatory factors that restrain inflammation and antitumor immunity, such as PD-L1, IDO-1, and others. This has been shown in the context of therapeutic STING signaling in tumors, causing sustained induction of type I

Published OnlineFirst September 17, 2018; DOI: 10.1158/0008-5472.CAN-18-0730

IFNs, which ultimately recruited immune-suppressive myeloid-derived suppressor cells (MDSC) to the tumor microenvironment (46). Further, studies demonstrating that RIG-I may respond to endogenous "unshielded" long noncoding RNAs (lnRNA) or genomically incorporated retroviral sequences, derived from neighboring tumor-associated fibroblasts and delivered to tumor cells through exosomal transport, may actually increase tumor cell growth, treatment resistance and malignant progression (47), despite production of inflammatory cytokines. These observations support further investigation into the longer-term consequences of RIG-I signaling in tumors. Future studies also need to consider the potential risk for unrestrained inflammation, because RIG-I is expressed in virtually all cell types, and RIG-I activation induces feed-forward signaling to amplify RIG-I and IFN-responsive genes. Recently described conditional RIG-I agonists, in which the 5′-triphosphorylated terminus of the RNA duplex remains shielded until release by predetermined molecular cues, may help enrich delivery of RIG-I agonist to the target tissue (48).

In summary, we demonstrate that RIG-I signaling induces immunogenic tumor cell death and upregulates expression of MHC-I components, proinflammatory cytokines, and chemokines in ER^+ breast cancer cells, $HER2^+$ breast cancer cells, and TNBC cells, resulting in inhibition of tumor growth and increased TILs *in vivo*. These findings suggest that RIG-I activation using a synthetic agonist activates innate immunity in breast cancer cells increases immunogenicity of breast cancers and may be a feasible treatment approach for treatment of breast cancers, including those with lower mutational burden that are considered poor candidates for immunotherapy.

Disclosure of Potential Conflicts of Interest

No potential conflicts of interest were disclosed.

Authors' Contributions

Conception and design: D.L. Elion, J.T. Wilson, R.S. Cook

Development of methodology: D.L. Elion, M.E. Jacobson, V. Sanchez, J.T. Wilson, R.S. Cook

Acquisition of data (provided animals, acquired and managed patients, provided facilities, etc.): D.L. Elion, E. Jacobson, D.J. Hicks, P.I. Gonzalez-Ericsson, O. Fedorova

Analysis and interpretation of data (e.g., statistical analysis, biostatistics, computational analysis): D.L. Elion, B. Rahman, R.S. Cook

Writing, review, and/or revision of the manuscript: D.L. Elion, A.M. Pyle, J.T. Wilson, R.S. Cook

Administrative, technical, or material support (i.e., reporting or organizing data, constructing databases): D.L. Elion, D.J. Hicks, B. Rahman, P.I. Gonzalez-Ericsson

Study supervision: D.L. Elion, D.J. Hicks, J.T. Wilson, R.S. Cook

Acknowledgments

We would like to acknowledge the shared resources at Vanderbilt University, Vanderbilt University Medical Center, and the Vanderbilt-Ingram Cancer Center that contributed to the studies reported herein, including the VICC Breast SPORE pathology service under the direction of Dr. Melinda Sanders, the VUMC Translational Pathology Shared Resource under the direction of Dr. Kellye Boyd, the Vanderbilt Digital Histology Shared Resource (DHSR) under the direction of Joseph Roland for access to a slide scanner and assistance with histology quantification. This work was supported by Specialized Program of Research Excellence (SPORE) grant NIH P50 CA098131 (VICC; to R.S. Cook, D.J. Hicks, V. Sanchez, and P.I. Gonzalez-Ericsson), Cancer Center Support grant NIH P30 CA68485 (VICC; to R.S. Cook, D.J. Hicks, V. Sanchez, and P.I. Gonzalez-Ericsson), CTSA UL1TR000445 (R. S. Cook) from the National Center for Advancing Translational Sciences, W81XWH-161-0063 (J.T. Wilson and R.S. Cook) from the Congressionally Directed Medical Research Program, and CBET-1554623 (J.T. Wilson) from the National Science Foundation.

The costs of publication of this article were defrayed in part by the payment of page charges. This article must therefore be hereby marked *advertisement* in accordance with 18 U.S.C. Section 1734 solely to indicate this fact.

Received March 13, 2018; revised June 29, 2018; accepted September 4, 2018; published first September 17, 2018.

References

1. Miller KD, Siegel RL, Lin CC, Mariotto AB, Kramer JL, Rowland JH, et al. Cancer treatment and survivorship statistics, 2016. CA Cancer J Clin 2016;66:271–289.
2. Pardoll DM. The blockade of immune checkpoints in cancer immunotherapy. Nat Rev Cancer 2012;12:252–264.
3. Hodi FS, O'Day SJ, McDermott DF, Weber RW, Sosman JA, Haanen JB, et al. Improved survival with ipilimumab in patients with metastatic melanoma. N Engl J Med 2010;363:711–723.
4. Ellis PM, Vella ET, Ung YC. Immune checkpoint inhibitors for patients with advanced non-small-cell lung cancer: a systematic review. Clin Lung Cancer 2017;18:444–459 e441.
5. Cimino-Mathews A, Foote JB, Emens LA. Immune targeting in breast cancer. Oncology (Williston Park) 2015;29:375–385.
6. Emens LA, Kok M, Ojalvo LS. Targeting the programmed cell death-1 pathway in breast and ovarian cancer. Curr Opin Obstet Gynecol 2016;28:142–147.
7. Nanda R, Chow LQ, Dees EC, Berger R, Gupta S, Geva R, et al. Pembrolizumab in patients with advanced triple-negative breast cancer: phase Ib KEYNOTE-012 Study. J Clin Oncol 2016;34:2460–2467.
8. Garcia-Teijido P, Cabal ML, Fernandez IP, Perez YF. Tumor-Infiltrating Lymphocytes in triple negative breast cancer: the future of immune targeting. Clin Med Insights Oncol 2016;10:31–39.
9. Luen SJ, Savas P, Fox SB, Salgado R, Loi S. Tumour-infiltrating lymphocytes and the emerging role of immunotherapy in breast cancer. Pathology 2017;49:141–155.
10. Luen S, Virassamy B, Savas P, Salgado R, Loi S. The genomic landscape of breast cancer and its interaction with host immunity. Breast 2016;29:241–250.
11. Marincola FM, Jaffee EM, Hicklin DJ, Ferrone S. Escape of human solid tumors from T-cell recognition: molecular mechanisms and functional significance. Adv Immunol 2000;74:181–273.
12. Garrido F, Algarra I. MHC antigens and tumor escape from immune surveillance. Adv Cancer Res 2001;83:117–158.
13. Gatalica Z, Snyder C, Maney T, Ghazalpour A, Holterman DA, Xiao N, et al. Programmed cell death 1 (PD-1) and its ligand (PD-L1) in common cancers and their correlation with molecular cancer type. Cancer Epidemiol Biomarkers Prev 2014;23:2965–2970.
14. Takeuchi O, Akira S. Pattern recognition receptors and inflammation. Cell 2010;140:805–820.
15. Shalapour S, Karin M. Immunity, inflammation, and cancer: an eternal fight between good and evil. J Clin Invest 2015;125:3347–3355.
16. Okamoto M, Tsukamoto H, Kouwaki T, Seya T, Oshiumi H. Recognition of Viral RNA by pattern recognition receptors in the induction of innate immunity and excessive inflammation during respiratory viral infections. Viral Immunol 2017;30:408–420.
17. Ishikawa H, Barber GN. STING is an endoplasmic reticulum adaptor that facilitates innate immune signalling. Nature 2008;455:674–678.
18. Ishikawa H, Ma Z, Barber GN. STING regulates intracellular DNA-mediated, type I interferon-dependent innate immunity. Nature 2009;461:788–792.

19. Chandra D, Quispe-Tintaya W, Jahangir A, Asafu-Adjei D, Ramos I, Sintim HO, et al. STING ligand c-di-GMP improves cancer vaccination against metastatic breast cancer. Cancer Immunol Res 2014;2:901–910.
20. Li T, Cheng H, Yuan H, Xu Q, Shu C, Zhang Y, et al. Antitumor Activity of cGAMP via Stimulation of cGAS-cGAMP-STING-IRF3 mediated innate immune response. Sci Rep 2016;6:19049.
21. Tang CH, Zundell JA, Ranatunga S, Lin C, Nefedova Y, Del Valle JR, et al. Agonist-Mediated Activation of STING induces apoptosis in malignant B cells. Cancer Res 2016;76:2137–2152.
22. Demaria O, De Gassart A, Coso S, Gestermann N, Di Domizio J, Flatz L, et al. STING activation of tumor endothelial cells initiates spontaneous and therapeutic antitumor immunity. Proc Natl Acad Sci U S A 2015;112:15408–15413.
23. Fu J, Kanne DB, Leong M, Glickman LH, McWhirter SM, Lemmens E, et al. STING agonist formulated cancer vaccines can cure established tumors resistant to PD-1 blockade. Sci Transl Med 2015;7:283ra252.
24. Konno H, Yamauchi S, Berglund A, Putney RM, Mule JJ, Barber GN. Suppression of STING signaling through epigenetic silencing and missense mutation impedes DNA damage mediated cytokine production. Oncogene 2018;37:2037–51.
25. Xia T, Konno H, Ahn J, Barber GN. Deregulation of STING signaling in colorectal carcinoma constrains DNA damage responses and correlates with tumorigenesis. Cell Rep 2016;14:282–297.
26. Goubau D, Schlee M, Deddouche S, Pruijssers AJ, Zillinger T, Goldeck M, et al. Antiviral immunity via RIG-I-mediated recognition of RNA bearing 5'-diphosphates. Nature 2014;514:372–375.
27. Hornung V, Ellegast J, Kim S, Brzozka K, Jung A, Kato H, et al. 5'-Triphosphate RNA is the ligand for RIG-I. Science 2006;314:994–997.
28. Linehan MM, Dickey TH, Molinari ES, Fitzgerald ME, Potapova O, Iwasaki A, et al. A minimal RNA ligand for potent RIG-I activation in living mice. Sci Adv 2018;4:e1701854.
29. Schlee M, Roth A, Hornung V, Hagmann CA, Wimmenauer V, Barchet W, et al. Recognition of 5' triphosphate by RIG-I helicase requires short blunt double-stranded RNA as contained in panhandle of negative-strand virus. Immunity 2009;31:25–34.
30. Seth RB, Sun L, Ea CK, Chen ZJ. Identification and characterization of MAVS, a mitochondrial antiviral signaling protein that activates NF-kappaB and IRF 3. Cell 2005;122:669–682.
31. Besch R, Poeck H, Hohenauer T, Senft D, Hacker G, Berking C, et al. Proapoptotic signaling induced by RIG-I and MDA-5 results in type I interferon-independent apoptosis in human melanoma cells. J Clin Invest 2009;119:2399–2411.
32. Liu LW, Nishikawa T, Kaneda Y. An RNA molecule derived from sendai virus DI particles induces antitumor immunity and cancer cell-selective apoptosis. Mol Ther 2016;24:135–145.
33. Rintahaka J, Wiik D, Kovanen PE, Alenius H, Matikainen S. Cytosolic antiviral RNA recognition pathway activates caspases 1 and 3. J Immunol 2008;180:1749–1757.
34. Wincott F, DiRenzo A, Shaffer C, Grimm S, Tracz D, Workman C, et al. Synthesis, deprotection, analysis and purification of RNA and ribozymes. Nucleic Acids Res 1995;23:2677–2684.
35. Zlatev I, Lackey JG, Zhang L, Dell A, McRae K, Shaikh S, et al. Automated parallel synthesis of 5'-triphosphate oligonucleotides and preparation of chemically modified 5'-triphosphate small interfering RNA. Bioorg Med Chem 2013;21:722–732.
36. Wilson JT, Keller S, Manganiello MJ, Cheng C, Lee CC, Opara C, et al. pH-Responsive nanoparticle vaccines for dual-delivery of antigens and immunostimulatory oligonucleotides. ACS Nano 2013;7:3912–3925.
37. Ciriello G, Gatza ML, Beck AH, Wilkerson MD, Rhie SK, Pastore A, et al. Comprehensive molecular portraits of invasive lobular breast cancer. Cell 2015;163:506–519.
38. Curtis C, Shah SP, Chin SF, Turashvili G, Rueda OM, Dunning MJ, et al. The genomic and transcriptomic architecture of 2,000 breast tumours reveals novel subgroups. Nature 2012;486:346–352.
39. Kohlway A, Luo D, Rawling DC, Ding SC, Pyle AM. Defining the functional determinants for RNA surveillance by RIG-I. EMBO Rep 2013;14:772–779.
40. Hou J, Zhou Y, Zheng Y, Fan J, Zhou W, Ng IO, et al. Hepatic RIG-I predicts survival and interferon-alpha therapeutic response in hepatocellular carcinoma. Cancer Cell 2014;25:49–63.
41. Galluzzi L, Vitale I, Aaronson SA, Abrams JM, Adam D, Agostinis P, et al. Molecular mechanisms of cell death: recommendations of the Nomenclature Committee on Cell Death 2018. Cell Death Differ 2018;25:486–541.
42. Duewell P, Steger A, Lohr H, Bourhis H, Hoelz H, Kirchleitner SV, et al. RIG-I-like helicases induce immunogenic cell death of pancreatic cancer cells and sensitize tumors toward killing by CD8(+) T cells. Cell Death Differ 2014;21:1825–1837.
43. Li D, Gale RP, Liu Y, Lei B, Wang Y, Diao D, et al. 5'-Triphosphate siRNA targeting MDR1 reverses multi-drug resistance and activates RIG-I-induced immune-stimulatory and apoptotic effects against human myeloid leukaemia cells. Leuk Res 2017;58:23–30.
44. Wallden B, Emond M, Swift ME, Disis ML, Swisshelm K. Antimetastatic gene expression profiles mediated by retinoic acid receptor beta 2 in MDA-MB-435 breast cancer cells. BMC Cancer 2005;5:140.
45. Venkatesh A, Nandigam H, Muccioli M, Singh M, Loftus T, Lewis D, et al. Regulation of inflammatory factors by double-stranded RNA receptors in breast cancer cells. Immunobiology 2018;223:466–76.
46. Liang H, Deng L, Hou Y, Meng X, Huang X, Rao E, et al. Host STING-dependent MDSC mobilization drives extrinsic radiation resistance. Nat Commun 2017;8:1736.
47. Nabet BY, Qiu Y, Shabason JE, Wu TJ, Yoon T, Kim BC, et al. Exosome RNA unshielding couples stromal activation to pattern recognition receptor signaling in cancer. Cell 2017;170:352–366 e313.
48. Palmer CR, Jacobson ME, Fedorova O, Pyle AM, Wilson JT. Environmentally triggerable retinoic acid-inducible gene I agonists using synthetic polymer overhangs. Bioconjug Chem 2018;29:742–7.

Published OnlineFirst September 17, 2018; DOI: 10.1158/0008-5472.CAN-18-0730

Cancer Research
The Journal of Cancer Research (1916–1930) | The American Journal of Cancer (1931–1940)

AACR American Association for Cancer Research

Therapeutically Active RIG-I Agonist Induces Immunogenic Tumor Cell Killing in Breast Cancers

David L. Elion, Max E. Jacobson, Donna J. Hicks, et al.

Cancer Res 2018;78:6183-6195. Published OnlineFirst September 17, 2018.

Editorial

Activation of RIG-I signaling to increase the pro-inflammatory phenotype of a tumor

David L. Elion and Rebecca S. Cook

Immune checkpoint inhibitors (ICIs) are achieving remarkable successes in several cancers, including melanoma, colon, and lung cancers. However, these same successes for ICIs are not yet being realized in estrogen receptor positive (ER+) breast cancer, the most common breast cancer subtype. Compared to triple-negative breast cancer (TNBC), ER+ breast cancers exhibit lower overall response rates to ICI treatments, including anti-programmed cell death (PD)-1, and anti-PD-ligand 1 (PD-L1) [1]. Accumulating evidence suggests that TNBCs harbor more tumor infiltrating lymphocytes (TILs), a higher mutational burden, and higher tumor cell PD-L1 expression as compared to ER+ breast cancers, characteristics that may prime TNBCs for ICI response [2]. If so, then it is possible that treatment strategies aimed at increasing TILs in the tumor microenvironment (TME) of ER+ breast cancers might increase ICI responsiveness [3]. This hypothesis underlies intense research efforts to identify treatment strategies that would increase TILs in ER+ breast cancers, potentially enabling effective and durable ICI responses.

Numerous reports demonstrate that most cells in the body, including tumor cells as well as cells of the TME, express receptors that recognize and respond to viral nucleotide motifs, referred to as pattern recognition receptors (PRRs) [4]. PRRs are an important element of innate immunity. Once activated, PRRs initiate signaling pathways that generate a pro-inflammatory microenvironment that becomes replete with lymphocytes. Therapeutic approaches that use non-infectious methods to activate PRR signaling within the TME is gaining momentum as a strategy for priming tumors for ICI sensitivity, with much excitement surrounding agonists of the PRR known as STING [4]. We recently investigated the PRR known as retinoic acid-inducible gene (RIG)-I in models of ER+ breast cancers, testing the possibility that, when appropriately delivered and modulated, RIG-I mimetics might have robust therapeutic as a cancer treatment, as is currently being explored for STING agonists. We found that RIG-I signaling resulted in potent TIL recruitment to the TME, and primed otherwise insensitive tumors for sensitivity to PD-L1 treatment [4, 5].

RIG-I is a cytosolic RNA helicase, recognizing RNA motifs specific to certain viruses. Years of RIG-I research has culminated in the discovery of synthetic non-infectious RIG-I mimetics, comprised of minimal stem-loop RNA (SLR) sequences harboring a 5'-triphosphate motif, capable of potent RIG-I activation in cultured tumor cells and in mice *in vivo* [6]. Delivery of SLR sequences to cultured ER+ breast cancer cells activated RIG-I signaling, and induced immunogenic programs of breast cancer cell death, including pyroptosis and extrinsic apoptosis [5], demonstrating that RIG-I signaling has important therapeutic consequences that occur in a breast cancer cell intrinsic manner. Interestingly, we also found that RIG-I activation using SLR sequences induced expression of pro-inflammatory and T-cell recruiting cytokines by ER+ breast cancer cells. Further, RIG-I signaling in response to SLR sequences increased expression of Major Histocompatibility (MHC)-I proteins by ER+ breast cancer cells, and increased breast cancer cell expression of PD-L1. Together, these observations support the hypothesis that therapeutic RIG-I activation might recruit TILs and prime the TME for ICI response.

The effective delivery of SLR sequences to the TME *in vivo* was enabled by recent advances in nanoparticle (NP)-mediated delivery of RNA interference (RNAi) technologies. We focused on a previously described NP design strategy used with siRNAs, based on its proven *in vivo* protection of siRNA sequences, longer circulating half-life, increased uptake of siRNA by tumor cells, and enhanced endosomal release of siRNA cargo into the cytoplasm of tumor cells [7]. Adapting this NP design for use with SLR sequences, we found that NP-SLR delivery activated RIG-I signaling in tumor cells *in vivo* [5]. Similar to what was seen in cultured breast cancer cells, we found that RIG-I activation in tumor cells *in vivo* resulted in increased expression of pro-inflammatory cytokines. Importantly, we found increased $CD4^+$ and $CD8^+$ TILs and heightened ICI sensitivity in tumors treated with NP-SLR, consistent with the larger hypothesis that activation of innate immunity in ER+ breast cancers may prime these tumors for response to ICI.

These findings support clinical translation of RIG-I agonists, which is currently underway (NCT03065023) using the RIG-I agonist from Merck, MK-4621, in advanced and recurrent tumors. Another clinical trial recently opened (NCT03739138) to identify the therapeutic effects of MK-4621 with anti-PD-1 (Pembrolizumab) in patients with advanced and recurrent tumors. These trials are supported by our data demonstrating that RIG-I agonists increase ICI response in breast cancers through at least two mechanisms, tumor

intrinsic apoptosis and enhanced immunogenicity of the TME. It is anticipated that, although RIG-I agonists are only in earliest phases of exploration as cancer treatment strategy, the field will move forward at a rapid pace, based on the vast potential for its success in immune-oncology.

Rebecca S. Cook: Cancer Biology Graduate Program, Vanderbilt University School of Medicine, Nashville, TN, USA; Department of Cell and Developmental Biology, Vanderbilt University School of Medicine, Nashville, TN, USA; Department of Biomedical Engineering, Vanderbilt University School of Engineering, Nashville, TN, USA; Vanderbilt Ingram Cancer Center, Vanderbilt University Medical Center, Nashville, TN, USA

Correspondence to: *Rebecca S. Cook,*
email *Rebecca.cook@vanderbilt.edu*

Keywords: immunotherapy; RIG-I; intrinsic immunity; apoptosis; pyroptosis

Received: *January 24, 2019*

Published: *March 22, 2019*

REFERENCES

1. Wein L, et al. Br J Cancer. 2018; 119:4-11. https://doi.org/10.1038/s41416-018-0126-6.
2. Polk A, et al. Cancer Treat Rev. 2018; 63:122-34. https://doi.org/10.1016/j.ctrv.2017.12.008.
3. Fridman WH, et al. Nat Rev Clin Oncol. 2017; 14:717-34. https://doi.org/10.1038/nrclinonc.2017.101.
4. Vanpouille-Box C, et al. Cancer Cell. 2018; 34:361-78. https://doi.org/10.1016/j.ccell.2018.05.013.
5. Elion DL, et al. Cancer Res. 2018; 78:6183-95. https://doi.org/10.1158/0008-5472.CAN-18-0730.
6. Linehan MM, et al. Sci Adv. 2018; 4:e1701854. https://doi.org/10.1126/sciadv.1701854.
7. Wilson JT, et al. ACS Nano. 2013; 7:3912-25. https://doi.org/10.1021/nn305466z.

www.oncotarget.com Oncotarget, 2018, Vol. 9, (No. 48), pp: 29007-29017

Review

Harnessing RIG-I and intrinsic immunity in the tumor microenvironment for therapeutic cancer treatment

David L. Elion[1] and Rebecca S. Cook[2,3,4]

[1]Cancer Biology Program, Vanderbilt University School of Medicine, Nashville, TN 37232, USA

[2]Department of Cell and Developmental Biology, Vanderbilt University School of Medicine, Nashville, TN 37232, USA

[3]Department of Biomedical Engineering, Vanderbilt University School of Engineering, Nashville, TN 37232, USA

[4]Vanderbilt Ingram Cancer Center, Vanderbilt University Medical Center, Nashville, TN 37232, USA

Correspondence to: *Rebecca S. Cook,* ***email:*** *Rebecca.cook@vanderbilt.edu*

Keywords: *immunotherapy; RIG-I; innate immunity; pyroptosis; tumor microenvironment*

Received: *March 24, 2018* ***Accepted:*** *May 24, 2018* ***Published:*** *June 22, 2018*

ABSTRACT

Cancer immunotherapies that remove checkpoint restraints on adaptive immunity are gaining clinical momentum. Approaches aimed at intrinsic cellular immunity in the tumor microenvironment are less understood, but are of intense interest, based on their ability to induce tumor cell apoptosis while orchestrating innate and adaptive immune responses against tumor antigens. The intrinsic immune response is initiated by ancient, highly conserved intracellular proteins that detect viral infection. For example, the RIG-I-like receptors (RLRs), a family of related RNA helicases, detect viral oligonucleotide patterns of certain RNA viruses. RLR activation induces immunogenic cell death of virally infected cells, accompanied by increased inflammatory cytokine production, antigen presentation, and antigen-directed immunity against virus antigens. Approaches aimed at non-infectious RIG-I activation in cancers are being tested as a treatment option, with the goal of inducing immunogenic tumor cell death, stimulating production of pro-inflammatory cytokines, enhancing tumor neoantigen presentation, and potently increasing cytotoxic activity of tumor infiltrating lymphocytes. These studies are finding success in several pre-clinical models, and are entering early phases of clinical trial. Here, we review pre-clinical studies of RLR agonists, including the successes and challenges currently faced RLR agonists on the path to clinical translation.

INTRODUCTION

The immune system is capable of targeted tumor cell killing through the process of immunosurveillance. Although tumors often develop ways to escape immunosurveillance, the growing interest and understanding of molecular interactions that occur between the tumor and the immune system have resulted in treatment strategies aimed at harnessing the immune system to target cancers. Recent advances in tumor immunology have produced immune checkpoint inhibitors (ICIs), cancer treatments designed to relieve the checkpoint restraints on adaptive immunity [1]. ICIs have revolutionized treatments for many types of cancer [1–3]. Despite these successes, not all patients respond to ICI therapy, for reasons that are varied and incompletely understood. It is thought that ICIs may be less effective in tumors that are poorly immunogenic, as defined by low levels of tumor infiltrating lymphocytes (TILs), minimal cross-presentation of tumor neoantigens, and high levels of immune suppressive leukocytes such as regulatory T-cells (T_{Reg}s), tumor associated macrophages (TAMs) and myeloid derived suppressor cells (MDSCs) [4–7]. Innovative strategies to increase immunogenicity in

tumors are being explored through a variety of approaches. One emerging strategy is based on activation of innate immunity in the tumor microenvironment (TME) [8, 9]. Innate immunity is a powerful arm of the immune system responsible for rapid anti-microbial immunity, often inducing programmed cell death of an infected cell. Innate immunity functions beyond the infected cell as well, by modulating the expression of cytokines and chemokines that recruit T-lymphocytes to the affected tissue, enhance antigen presentation, and increase cross-priming to antigen-specific T-cells [8, 10]. This idea is being explored extensively in regards to the pattern recognition receptor (PRR) known as Stimulator of Interferon Genes (STING) [11, 12]. Synthetic STING ligands potently induce anti-tumor immunity in several cancers, including breast cancer, chronic lymphocytic leukemia, colon cancer, and squamous cell carcinoma [13–17]. However, there is increasing evidence that STING signaling might be defective in some cancers, due to mutations, promoter methylation, and decreased expression of STING pathway effectors [18, 19], thus limiting their potential efficacy in the tumor cell compartment of the TME. However, other cells of the TME, particularly cells of the immune compartment, may retain STING signaling even when the STING pathway is defective within the tumor cells, per se, allowing STING ligands to induce innate immunity within the TME under these circumstances [20].

Viral nucleic acid sensors, such as the RNA helicase known as retinoic acid-inducible gene I (RIG-I, encoded by the gene *DDX58*) [21], are expressed in most cells of the human body, including tumor cells [22]. When infected by an RNA virus, double-stranded RNA replication intermediates derived from the virus bind to RIG-I [23–26] and activate a RIG-I inflammasome leading to pyroptosis, a highly immunogenic mechanism of programmed cell death [27–29]. A hallmark of pyroptosis is the formation of pores in the plasma membrane [30], leading to hypotonic cell swelling and leakage of intracellular contents, including danger associated molecular patterns (DAMPs), into the microenvironment. RIG-I signaling simultaneously induces expression of pro-inflammatory cytokines [8, 10]. Together, DAMPs and pro-inflammatory cytokines stimulate a local acute inflammatory immune response aimed at removal of virus and virally-infected cells [31]. Interestingly, viral nucleotide motifs can be mimicked using synthetic, non-infectious oligonucleotides. These RIG-I agonists are capable of triggering RIG-I signaling, pyroptosis, and acute inflammation [26, 32–35]. In the cancer setting, RIG-I activation could thus provide a three-pronged attack: 1.) direct activation of tumor cell death; 2.) cytokine-mediated activation of innate immune effectors (e.g., macrophages, natural killer cells), and 3.) increased recruitment and cross priming of adaptive immune effectors (*e.g.*, CD8+ T-lymphocytes) through a cytokine-enriched microenvironment and enhanced activity of professional antigen presenting cells [APCs, *e.g.*, dendritic cells (DCs) or macrophages] (Figure 1). Synthetic RIG-I agonists are being explored as a therapeutic approach in a diverse range of cancers [27, 33, 34, 36]. Here, we review studies of RIG-I signaling in the tumor microenvironment, and preclinical studies investigating RIG-I agonists for cancer treatment.

Activation of RIG-I induces pro-inflammatory signaling in a cell-intrinsic manner

RIG-I was first identified as a cytosolic DExD/H box RNA helicase activated in response to certain RNA viruses [21]. RIG-I is activated upon recognition of its ligand, double-stranded RNA sequences modified with a 5'-triphosphate (5'-3pRNA) or 5'-diphosphate (5'-2pRNA) motif [24, 26, 27, 37]. RIG-I activation may occur in response to other RNA motifs, including blunt dsRNAs [38], monomeric RNA within defective human immunodeficiency virus (HIV)-1 particles [39], cytoplasmic long non-coding RNAs [40], small nuclear RNAs [41–44], or endogenous retroviral transcripts. In addition to the DexD/H box RNA helicase domain, RIG-I is characterized by an amino-terminal Caspase Activation and Recruitment Domain (CARD) domain, and a Carboxy-Terminal Domain (CTD) [45–47]. Once activated by its ligand, RIG-I undergoes an ATP-dependent conformational change, exposing its CARD domain for polyubiquitylation [48] by ubiquitin ligases such as TRIM25, Riplet and others [49–52]. Once polyubiquitylated, a mitochondrial signalosome, comprised of the proteins WHIP, PPP6C and TRIM14, recruits RIG-I to the mitochondrial surface where the CARD domain of RIG-I interacts with the CARD domain of Mitochondrial Anti-Viral Signaling (MAVS), a requisite RIG-I co-factor [49, 53–55].

Once engaged, MAVS signaling activates three kinases that serve as regulators of inflammation, Inhibitor of κB-Kinase (IKK)-γ, TANK-Binding Kinase (TBK)-1 and IKK-ε [56–58]. These kinases phosphorylate Interferon (IFN) Regulatory Factor (IRF)-1, IRF-3, IRF-7, and Nuclear Factor (NF)-κB [59–61], transcription factors that drive expression of a pro-inflammatory transcriptional program that includes type I IFNs and pro-inflammatory cytokines [45, 62]. Importantly, IFN-α, IFN-β, and other pro-inflammatory cytokines produced in response to RIG-I activation drive a feed-forward signaling loop that maintains high expression levels of RIG-I, IFNs and additional pro-inflammatory IFN-stimulated genes (ISGs), by maintaining phosphorylation and activation of the transcription factors IRF-3, IRF-7, and NF-κB, and by phosphorylation of the transcription factor Signal Transducer and Activator of Transcription (STAT)-1, which occurs in response to IFN-α/β receptor (IFNAR)-mediated activation of JAK-STAT signaling (Figure 2) [62]. This feed-forward signaling model amplifies

inflammatory cytokine production in the infected and neighboring cells, while recruiting leukocytes to the infected area, including pro-inflammatory lymphocytes. Since a 'T-cell inflamed' microenvironment is often associated with an improved prognosis for several cancers, and correlates with increased tumor sensitivity to ICIs, the pro-inflammatory phenotype induced by RIG-I activation may be an attractive treatment approach to increase tumor immunogenicity and clinical success of ICIs.

Two RIG-I-like receptors (RLRs) with structural similarity to RIG-I have been identified. One of these RLRs, Melanoma Differentiation Associated (MDA)-5, harbors an amino-terminal CARD domain, a DexD/H box motif, and a CTD domain [63, 64]. Like RIG-I, MDA-5 induces type I IFNs and other pro-inflammatory cytokines in response to viral nucleotides, albeit viral nucleotide motifs that are distinct from those that activate RIG-I. MDA-5 is activated by blunt-ended, long double-stranded RNA [*e.g.* polyinosinic-polycytidylic acid, or poly(I:C)], a ligand that also activated some Toll-Like Receptors (TLRs). In contrast to RIG-I and MDA-5, the other RLR known as Laboratory of Genetics and Physiology (LGP)-2 lacks the CARD domain shared by RIG-I and MDA-5, but is otherwise similar to the other RLRs [65]. Without the CARD domain, LGP-2 is unable to interact directly with MAVS to initiate a pro-inflammatory response. There are reports suggesting that LGP-2 activation interferes with RIG-I signaling, but that MDA-5 signaling may be enhanced by LGP2 [48, 66–69]. The implications of LGP2 expression and signaling in the context of cancer therapy, and how LGP2 might affect therapeutic responses to RIG-I agonists, are currently unclear.

RIG-I signaling potently activates programmed cell death

In the context of viral infection, RIG-I signaling is capable of inducing programmed cell death (PCD) as a mechanism to eliminate virally-infected cells. Cellular mechanisms by which RIG-I induces PCD include activation of the intrinsic apoptosis pathway, the extrinsic apoptosis pathway, and a type of programmed necrosis

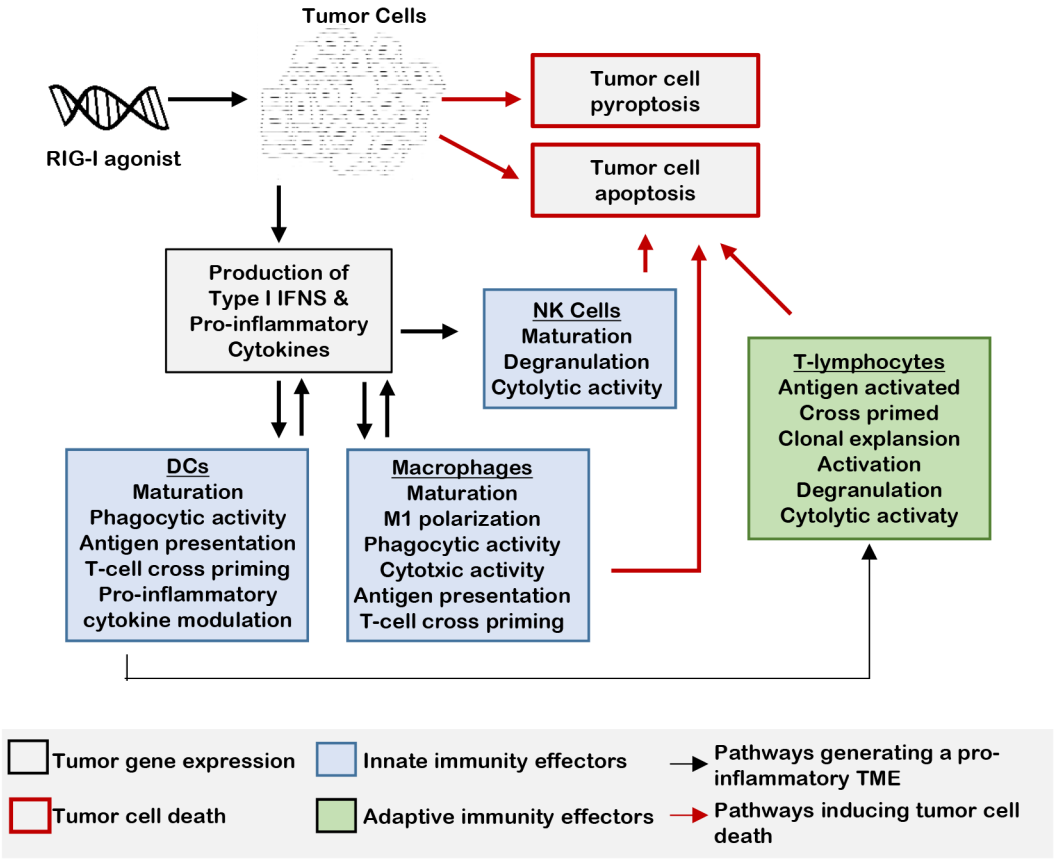

Figure 1: RLR activation signals innate immunity in the TME. When tumor cells are treated with an RIG-I mimetic, inflammatory cytokine and type I IFN expression is rapidly upregulated, inducing innate immune responses in the tumor microenvironment. The cytolytic activity of leukocytes, such NK cells and macrophages, is increased in response to this IFN-enriched microenvironment. Maturation and activation of macrophages and DCs result in enhanced antigen presentation to T-lymphocytes in tumor draining lymph nodes. T-regulatory cell differentiation is decreased by the pro-inflammatory microenvironment produced by RIG-I activation.

termed 'pyroptosis.' The molecular factors governing the mode of RIG-I mediated cell death may depend to some extent on cell type. For example, RLR activation in keratinocytes, melanoma cells, glioblastoma cells, and many leukemia cells cause mitochondrial outer membrane permeabilization (MOMP), cytochrome-C release from mitochondria, and activation of caspase-9 and Apaf-1, the irreversible molecular switch that governs the intrinsic apoptotic pathway [27]. However, RIG-I signaling in pancreatic and prostate cancer cells robustly induces expression of several factors that activate the extrinsic apoptotic pathway, including Fas, Fas Ligand, Tumor Necrosis Factor (TNF), TNF-related apoptosis-inducing ligand (TRAIL), and the TRAIL receptors Death

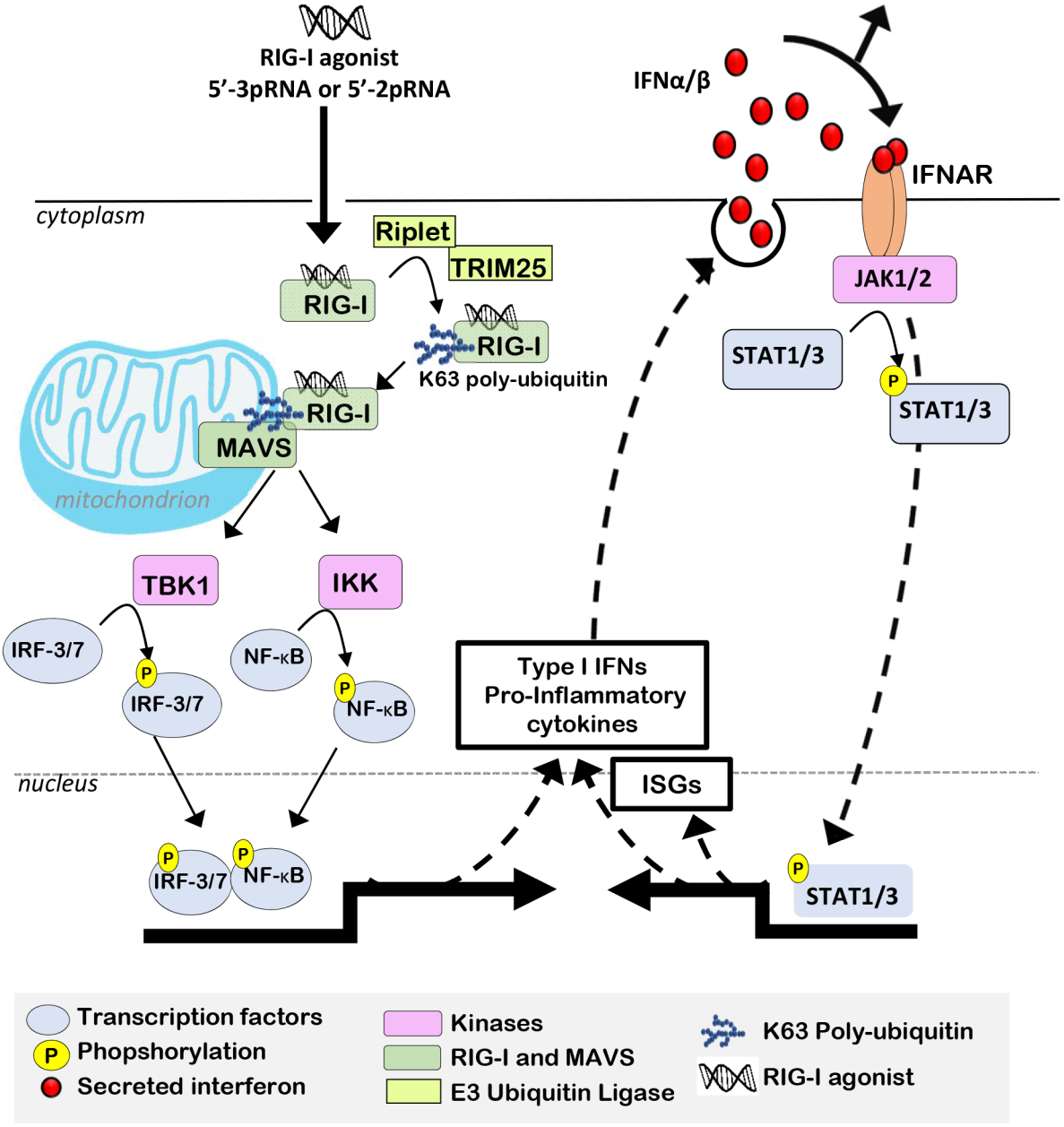

Figure 2: RIG-I activation induces Type I IFNs, which support pro-inflammatory transcriptional reprogramming. RIG-I binding to 5'-3pRNA or 5'-2pRNA induces a conformational change, allowing RIG-I CARD domains to be polyubiquitylated by E3 ligases (*e.g.*, Riplet or TRIM25). Polyubiquitylated RIG-I is recruited to mitochondria outer membranes, where it interacts with MAVS, which then activates IKK-ε, IKK-γ, and TBK1, kinases responsible for phosphorylation/activation of transcription factors (ATF-1, c-Jun, CBP, IRF-3, NF-κB). These transcription factors induce an expression profile that includes Type I I IFNs and additional pro-inflammatory cytokines. Type I IFNs bind to IFNAR, activating the intracellular tyrosine kinase JAK1/2, which in turn phosphorylates pro-inflammatory STAT transcription factors, thus driving expression of additional ISGs and amplifying the IFN-inducible positive feedback loop to support and maintain a pro-inflammatory microenvironment.

Receptor (DR)-4 and DR-5, causing caspase-8 activation and extrinsic apoptosis. The mechanism by which RIG-I signaling upregulates TRAIL, FAS and other extrinsic apoptosis-activating factors are not entirely clear, although it is likely that IFN signaling is involved, given that Fas, TRAIL, and caspase-8 are known ISGs [70, 71].

Another mode of programmed cell death induced upon RIG-I activation is termed "pyroptosis," an immunogenic form of cell death occurring in response to activation of the inflammasome, a multi-protein holoenzyme comprised of capsase-1 oligomers, adaptor proteins known as ASC (Apoptosis-associated Speck with a Caspase-recruitment domain), and a molecular sensor of pathogens, such as RIG-I (Figure 3). RIG-I can interact, via its CARD domain, with the CARD domains of inflammasome components [72], resulting in auto-cleavage and activation of caspase-1 [29, 73], which then allows proteolysis of the pro-inflammatory cytokines interleukin (IL)-1β and IL-18 [73], which amplify inflammatory signaling in the local environment while activating natural killer (NK) cells and recruiting leukocytes to the affected tissue. Caspase-1 activation also results in cleavage of Gasdermin-D, removing the auto-inhibitory domain from Gasdermin-D to allow oligomerization at the plasma membrane and pore formation. Plasma membrane permeabilization by Gasdermin-D pores allows water to enter and swell the cell, a hallmark of necrosis. Once membrane integrity is lost, intracellular contents, including DAMPs, permeate the extracellular environment, inducing danger responses in neighboring cells, which amplifies the inflammatory response.

RIG-I signaling in tumor cells affects the complex tumor microenvironment

The capacity for RIG-I signaling to induce cell death, while inducing pro-inflammatory responses, makes therapeutic use of RIG-I mimetics a highly attractive option in cancers. A growing number of studies show that the molecular responses to RIG-I or RLR signaling are retained in tumor cells and in non-tumor cells of the tumor microenvironment, and support innate immune responses against tumor cells [34]. For example, RIG-I activation in ovarian cancer cells enables NK-mediated tumor cell killing in culture [36]. Further, RIG-I signaling within the tumor cell increases phagocytosis of the affected tumor cell by professional APCs, including macrophages and DCs, thus providing tumor antigens for presentation to lymphocytes [32]. At the same time, the IFN-enriched microenvironment generated by tumor cell RIG-I signaling increases expression of major histocompatibility complex (MHC)-II antigen presentation molecules in macrophages and DCs, which may further increase tumor antigen cross-presentation. In support of this idea, it is reported that DCs presented pancreatic cancer-derived

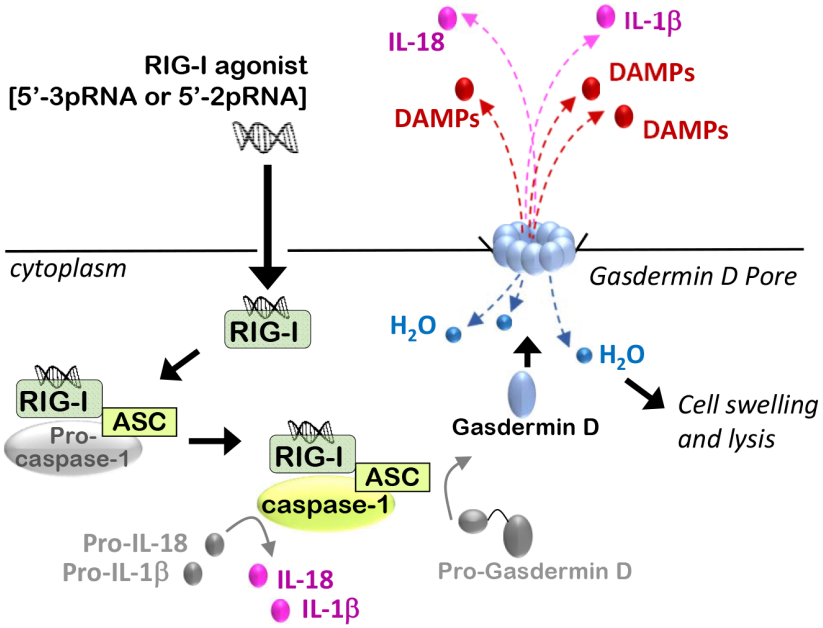

Figure 3: RIG-I activation induces immunogenic modes of programmed cell death. Activated RIG-I recruits the inflammasome adaptor protein ASC, which facilitates binding and oligomerization of Caspase-1, leading to caspase-1 auto-cleavage and activation. Caspase-1 cleaves protein precursors of IL-1β and IL-18 to generate their mature, pro-inflammatory isoforms, which are then secreted. Caspase-1 activity also drives cleavage of the auto-inhibitory domain from Gasdermin-D, liberation the amino-terminal pore-forming domain of Gasdermin-D to translocate to the plasma membrane and oligomerize, forming pores that initiate hypotonic cellular swelling and lysis, followed by release of DAMPs into the extracellular space, thus inducing an inflammatory response from surrounding cells.

antigens more robustly to T-cells if RIG-I signaling was activated in pancreatic cancer cells prior to their co-culture with DCs [32, 36]. Similar results were observed upon RIG-I activation ovarian cancer cells prior to co-culture with macrophages [74].

RIG-I mimetics are gaining traction as a possible cancer treatment in pre-clinical studies

Through direct activation of intrinsic immunity in cancer cells, and accompanying indirect activation of leukocytes in the TME, synthetic RIG-I mimetics are under investigation for cancer treatment in pre-clinical studies in hepatocellular carcinoma [75], leukemias [76], melanomas [27], prostate cancers [77] and others. RIG-I agonists that are stable and functional *in vivo* are under current development. For example, a minimal 5'-triphophosphorylated stem-loop RNA (SLR) sequence for intra-venous delivery to mice was recently reported [25]. The stem-loop structure enhances structural stability of the complex, a key determinant of RIG-I ligand potency. Delivery of SLR sequences to mice *in vivo* activated RIG-I signaling, IFN induction, and expression of genes required for potent anti-viral immunity, although this RIG-I mimetic has not yet been studied in tumors grown *in vivo*. A pre-clinical compound specific for RIG-I is RGT100 (Merck/Rigontec), currently in phase I clinical trials for treatment of advanced solid tumors and lymphomas (NCT03065023), although peer-reviewed preclinical reports for RGT100 were not identified, to our knowledge. Another compound which activates RIG-I by unknown mechanisms is SB-9200 [78], which is currently under investigation as an anti-viral agent, but has not yet been tested in the pre-clinical setting of cancer treatment.

In addition to RIG-I specific mimetics, synthetic RLR mimetics are being investigated in pre-clinical and early clinical studies. The compound Hiltonol [polyinosinic-polycytidylic acid stabilized with poly-l-lysine and carboxymethylcellulose (poly-ICLC)] [79, 80] was tested in combination with chemotherapy for patients with Stage IV anaplastic astrocytoma, resulting in increased overall survival (OS) to >8 years, versus the expected survival of two years on conventional chemotherapy alone [81]. Another trial tested poly-ICLC in combination with radiation and temozolomide in newly diagnosed adult glioblastoma patients. In these studies, intramuscular poly-ICLC increased OS to 18.3 months from 14.6 months [82–84]. Further, poly-ICLC is being tested as a tumor vaccine adjuvant in several cancer types, with a growing number of successes in Phase I and II clinical trials for gliomas [85], breast cancer [86], pancreatic cancer [87], ovarian cancer [88, 89], multiple myeloma [90], and others, highlighting the potential advances that Poly-ICLC may achieve across a spectrum of cancers. Although poly-ICLC potently activates MDA-5, it also activates Toll-like Receptor (TLR)-3, making the specific contributions of RLR signaling to the therapeutic effects of poly-ICLC, and to patient outcome, difficult to dissect.

The future of RIG-I agonists in cancer

Exciting innovations within the field of RIG-I agonists are emerging. For example, a powerful, bimodal application of RNAi-based silencing of intra-tumoral gene targets using a 5'-triphosphate modified dsRNA sequence would allow for RIG-I activation and simultaneous gene targeting. This approach was demonstrated in melanomas, using 5'-3p-siRNA sequences specific to the anti-apoptotic gene *BCL2*. Delivery of this construct to cells potently stimulated IFN production and NK activation, while enhancing tumor cell killing through Bcl-2 ablation [34]. This concept was validated using a 5'-3p-siRNA targeting transforming growth factor (TGF)-β in pancreatic cancer cells, resulting in tumor cell apoptosis, IFN induction, and enhanced CD8+ T cell responses [36]. A similar approach was used in models of non-small cell lung cancer, using 5'-3p-siRNA sequences against vascular endothelial growth factor (VEGF), resulting in reduced tumor angiogenesis while enhancing anti-tumor immunity [91]. Defining the most appropriate gene silencing target may be a difficult task, but the use of siRNA paves the pathway for targeting certain oncogenes (e.g., *MYC*) that are currently 'undruggable.'

Despite the potential success of RIG-I and RLR agonists, the immune system is powerful and incompletely understood, warranting cautious optimism and thorough examination of the caveats associated with innate immune activation, including possible on-target induction of autoimmunity, or induction of a cytokine 'storm' which could pose a threat to patient safety [92–94]. It is important to note that, since RIG-I is expressed in most cells of the human body, the consequences of RIG-I activation might be widespread, driving symptoms like fatigue, depression and cognitive impairment. In ICI-based therapies, these side-effects are generally managed by corticosteroid immunosuppression.

Delivery of small nucleotide sequences to tumor cells and leukocytes within the TME is another major obstacle to the widespread utility of RIG-I or RLR-based therapeutics in the cancer setting. Studies aimed at generating stable, specific and potent RIG-I ligands that retain functionality *in vivo* have been reported only recently. For example, a study employing a minimal 5'-triphophosphorylated stem-loop RNA (SLR) sequence delivered by intra-venous delivery to mice activated in RIG-I signaling, IFN induction, and expression of genes required for potent anti-viral immunity *in vivo*. A recently described 'conditional' RIG-I ligand, in which the 5'-triphosphorylated terminus of the RNA duplex remained shielded until release by predetermined molecular cues *in vivo*, could enhance delivery of RIG-I

agonist to tumors, and minimize RIG-I activation outside of the TME [95]. However, the efficacy of RIG-I ligands, including SLRs and conditional RIG-I ligands, not yet been tested in animal models of cancer [25].

CONCLUSION

Therapeutic RIG-I and RLR agonists are emerging as a novel approach to engage the immune system in the fight against cancer. Importantly, RIG-I signaling directly promotes tumor cell killing through three distinct modes of action: intrinsic apoptosis, extrinsic apoptosis, and pyroptosis. Further, simultaneous activation of the innate and adaptive arms of the immune system may generate durable therapeutic responses. The multi-faceted mechanisms by which RLR agonists eliminate cancer cells represent the well-rounded arsenal of weapons required to fight aggressive and metastatic cancers effectively.

Abbreviations

APC: antigen presenting cell; ASC: Apoptosis-associated Speck with a Caspase-recruitment domain; CARD: caspase activation and recruitment domain; CTD: carboxy-terminal domain; DAMP: danger associated molecular patterns; DC: dendritic cell; DR: death receptor; HIV: human immunodeficiency virus; ICI: immune checkpoint inhibitors; IFN: interferon; IFNAR: interferon α/β receptor; IKK: inhibitor of κB-kinase; IL: interleukin; IRF: interferon response factor; ISG: interferon stimulated genes; MAVS: mitochondrial anti-viral signaling; MDSC: myeloid derived suppressor cell; MDA-5 melanoma differentiation antigen-5; MHC: major histocompatibility complex; MOMP: mitochondrial outer membrane permeabilization; NF: nuclear factor; NK: natural killer; OS: overall survival; PCD: programmed cell death; Poly(I:C) polyinosinic-polycytidylic acid; Poly-ICLC polyinosinic-polycytidylic acid stabilized with poly-l-lysine and carboxymethylcellulose; PRR: pattern recognition receptor; RIG-I retinoic acid-inducible gene I; RLR: RIG-I-like receptor; STAT: Signal transducer and transcription factor; STING: Stimulator of Interferon Genes; TAM: tumor associated macrophage; TBK: tank binding kinase; TGF: Transforming growth factor; TLR: toll-like receptor; TME: tumor microenvironment; TNF: tumor necrosis factor; TRAIL: TNF-related apoptosis-inducing ligand; T_{Reg}: regulatory T-cells; VEGF: vascular endothelial growth factor; 5'-3pRNA: 5'-triphosphate RNA; 5'-2pRNA 5'-diphosphate.

Author contributions

D.E. and R.S.C. prepared the manuscript. D.E. and R.S.C have reviewed and agree to this information.

ACKNOWLEDGMENTS

We would like to acknowledge the shared resources at Vanderbilt University, Vanderbilt University Medical Center, and the Vanderbilt-Ingram Cancer Center that contributed to the studies reported herein.

CONFLICTS OF INTEREST

The authors declare no conflicts of interest with the materials described herein.

FUNDING

This work was supported by Specialized Program of Research Excellence (SPORE) grant NIH P50 CA098131 (VICC; to R. S. Cook), Cancer Center Support grant NIH P30 CA68485 (VICC; to R.S. Cook), CTSA UL1TR000445 (to R.S. Cook) from the National Center for Advancing Translational Sciences, W81XWH-161-0063 (to R.S. Cook) from the Congressionally Directed Medical Research Program.

REFERENCES

1. Pardoll DM. The blockade of immune checkpoints in cancer immunotherapy. Nat Rev Cancer. 2012; 12:252-264.
2. Hodi FS, O'Day SJ, McDermott DF, Weber RW, Sosman JA, Haanen JB, Gonzalez R, Robert C, Schadendorf D, Hassel JC, Akerley W, van den Eertwegh AJ, Lutzky J, et al. Improved survival with ipilimumab in patients with metastatic melanoma. N Engl J Med. 2010; 363:711-723.
3. Ellis PM, Vella ET, Ung YC. Immune Checkpoint Inhibitors for Patients With Advanced Non-Small-Cell Lung Cancer: A Systematic Review. Clin Lung Cancer. 2017; 18:444-459 e441.
4. Luen S, Virassamy B, Savas P, Salgado R, Loi S. The genomic landscape of breast cancer and its interaction with host immunity. Breast. 2016; 29:241-250.
5. Marincola FM, Jaffee EM, Hicklin DJ, Ferrone S. Escape of human solid tumors from T-cell recognition: molecular mechanisms and functional significance. Adv Immunol. 2000; 74:181-273.
6. Garrido F, Algarra I. MHC antigens and tumor escape from immune surveillance. Adv Cancer Res. 2001; 83:117-158.
7. Gatalica Z, Snyder C, Maney T, Ghazalpour A, Holterman DA, Xiao N, Overberg P, Rose I, Basu GD, Vranic S, Lynch HT, Von Hoff DD, Hamid O. Programmed cell death 1 (PD-1) and its ligand (PD-L1) in common cancers and their correlation with molecular cancer type. Cancer Epidemiol Biomarkers Prev. 2014; 23:2965-2970.
8. Takeuchi O, Akira S. Pattern recognition receptors and inflammation. Cell. 2010; 140:805-820.

9. Shalapour S, Karin M. Immunity, inflammation, and cancer: an eternal fight between good and evil. J Clin Invest. 2015; 125:3347-3355.
10. Okamoto M, Tsukamoto H, Kouwaki T, Seya T, Oshiumi H. Recognition of Viral RNA by Pattern Recognition Receptors in the Induction of Innate Immunity and Excessive Inflammation During Respiratory Viral Infections. Viral Immunol. 2017; 30:408-420.
11. Ishikawa H, Barber GN. STING is an endoplasmic reticulum adaptor that facilitates innate immune signalling. Nature. 2008; 455:674-678.
12. Ishikawa H, Ma Z, Barber GN. STING regulates intracellular DNA-mediated, type I interferon-dependent innate immunity. Nature. 2009; 461:788-792.
13. Chandra D, Quispe-Tintaya W, Jahangir A, Asafu-Adjei D, Ramos I, Sintim HO, Zhou J, Hayakawa Y, Karaolis DK, Gravekamp C. STING ligand c-di-GMP improves cancer vaccination against metastatic breast cancer. Cancer Immunol Res. 2014; 2:901-910.
14. Li T, Cheng H, Yuan H, Xu Q, Shu C, Zhang Y, Xu P, Tan J, Rui Y, Li P, Tan X. Antitumor Activity of cGAMP via Stimulation of cGAS-cGAMP-STING-IRF3 Mediated Innate Immune Response. Sci Rep. 2016; 6:19049.
15. Tang CH, Zundell JA, Ranatunga S, Lin C, Nefedova Y, Del Valle JR, Hu CC. Agonist-Mediated Activation of STING Induces Apoptosis in Malignant B Cells. Cancer Res. 2016; 76:2137-2152.
16. Demaria O, De Gassart A, Coso S, Gestermann N, Di Domizio J, Flatz L, Gaide O, Michielin O, Hwu P, Petrova TV, Martinon F, Modlin RL, Speiser DE, Gilliet M. STING activation of tumor endothelial cells initiates spontaneous and therapeutic antitumor immunity. Proc Natl Acad Sci U S A. 2015; 112:15408-15413.
17. Fu J, Kanne DB, Leong M, Glickman LH, McWhirter SM, Lemmens E, Mechette K, Leong JJ, Lauer P, Liu W, Sivick KE, Zeng Q, Soares KC, et al. STING agonist formulated cancer vaccines can cure established tumors resistant to PD-1 blockade. Sci Transl Med. 2015; 7:283ra252.
18. Konno H, Yamauchi S, Berglund A, Putney RM, Mule JJ, Barber GN. Suppression of STING signaling through epigenetic silencing and missense mutation impedes DNA damage mediated cytokine production. Oncogene. 2018; 37:2037-2051.
19. Xia T, Konno H, Ahn J, Barber GN. Deregulation of STING Signaling in Colorectal Carcinoma Constrains DNA Damage Responses and Correlates With Tumorigenesis. Cell Rep. 2016; 14:282-297.
20. Pepin G, Gantier MP. cGAS-STING Activation in the Tumor Microenvironment and Its Role in Cancer Immunity. Adv Exp Med Biol. 2017; 1024:175-194.
21. Yoneyama M, Kikuchi M, Natsukawa T, Shinobu N, Imaizumi T, Miyagishi M, Taira K, Akira S, Fujita T. The RNA helicase RIG-I has an essential function in double-stranded RNA-induced innate antiviral responses. Nat Immunol. 2004; 5:730-737.
22. Loo YM, Gale M Jr. Immune signaling by RIG-I-like receptors. Immunity. 2011; 34:680-692.
23. Goubau D, Schlee M, Deddouche S, Pruijssers AJ, Zillinger T, Goldeck M, Schuberth C, Van der Veen AG, Fujimura T, Rehwinkel J, Iskarpatyoti JA, Barchet W, Ludwig J, et al. Antiviral immunity via RIG-I-mediated recognition of RNA bearing 5'-diphosphates. Nature. 2014; 514:372-375.
24. Hornung V, Ellegast J, Kim S, Brzozka K, Jung A, Kato H, Poeck H, Akira S, Conzelmann KK, Schlee M, Endres S, Hartmann G. 5'-Triphosphate RNA is the ligand for RIG-I. Science. 2006; 314:994-997.
25. Linehan MM, Dickey TH, Molinari ES, Fitzgerald ME, Potapova O, Iwasaki A, Pyle AM. A minimal RNA ligand for potent RIG-I activation in living mice. Sci Adv. 2018; 4:e1701854.
26. Schlee M, Roth A, Hornung V, Hagmann CA, Wimmenauer V, Barchet W, Coch C, Janke M, Mihailovic A, Wardle G, Juranek S, Kato H, Kawai T, et al. Recognition of 5' triphosphate by RIG-I helicase requires short blunt double-stranded RNA as contained in panhandle of negative-strand virus. Immunity. 2009; 31:25-34.
27. Besch R, Poeck H, Hohenauer T, Senft D, Hacker G, Berking C, Hornung V, Endres S, Ruzicka T, Rothenfusser S, Hartmann G. Proapoptotic signaling induced by RIG-I and MDA-5 results in type I interferon-independent apoptosis in human melanoma cells. J Clin Invest. 2009; 119:2399-2411.
28. Liu LW, Nishikawa T, Kaneda Y. An RNA Molecule Derived From Sendai Virus DI Particles Induces Antitumor Immunity and Cancer Cell-selective Apoptosis. Mol Ther. 2016; 24:135-145.
29. Rintahaka J, Wiik D, Kovanen PE, Alenius H, Matikainen S. Cytosolic antiviral RNA recognition pathway activates caspases 1 and 3. J Immunol. 2008; 180:1749-1757.
30. Galluzzi L, Vitale I, Aaronson SA, Abrams JM, Adam D, Agostinis P, Alnemri ES, Altucci L, Amelio I, Andrews DW, Annicchiarico-Petruzzelli M, Antonov AV, Arama E, et al. Molecular mechanisms of cell death: recommendations of the Nomenclature Committee on Cell Death 2018. Cell Death Differ. 2018; 25:486-541.
31. Ramos HJ, Gale M Jr. RIG-I like receptors and their signaling crosstalk in the regulation of antiviral immunity. Curr Opin Virol. 2011; 1:167-176.
32. Duewell P, Steger A, Lohr H, Bourhis H, Hoelz H, Kirchleitner SV, Stieg MR, Grassmann S, Kobold S, Siveke JT, Endres S, Schnurr M. RIG-I-like helicases induce immunogenic cell death of pancreatic cancer cells and sensitize tumors toward killing by CD8(+) T cells. Cell Death Differ. 2014; 21:1825-1837.
33. Glas M, Coch C, Trageser D, Dassler J, Simon M, Koch P, Mertens J, Quandel T, Gorris R, Reinartz R, Wieland A, Von Lehe M, Pusch A, et al. Targeting the cytosolic innate immune receptors RIG-I and MDA5 effectively counteracts cancer cell heterogeneity in glioblastoma. Stem Cells. 2013; 31:1064-1074.

34. Poeck H, Besch R, Maihoefer C, Renn M, Tormo D, Morskaya SS, Kirschnek S, Gaffal E, Landsberg J, Hellmuth J, Schmidt A, Anz D, Bscheider M, et al. 5'-Triphosphate-siRNA: turning gene silencing and Rig-I activation against melanoma. Nat Med. 2008; 14:1256-1263.

35. van den Boorn JG, Hartmann G. Turning tumors into vaccines: co-opting the innate immune system. Immunity. 2013; 39:27-37.

36. Ellermeier J, Wei J, Duewell P, Hoves S, Stieg MR, Adunka T, Noerenberg D, Anders HJ, Mayr D, Poeck H, Hartmann G, Endres S, Schnurr M. Therapeutic efficacy of bifunctional siRNA combining TGF-beta1 silencing with RIG-I activation in pancreatic cancer. Cancer Res. 2013; 73:1709-1720.

37. Pichlmair A, Schulz O, Tan CP, Naslund TI, Liljestrom P, Weber F, Reis e Sousa C. RIG-I-mediated antiviral responses to single-stranded RNA bearing 5'-phosphates. Science. 2006; 314:997-1001.

38. Marques JT, Devosse T, Wang D, Zamanian-Daryoush M, Serbinowski P, Hartmann R, Fujita T, Behlke MA, Williams BR. A structural basis for discriminating between self and nonself double-stranded RNAs in mammalian cells. Nat Biotechnol. 2006; 24:559-565.

39. Solis M, Nakhaei P, Jalalirad M, Lacoste J, Douville R, Arguello M, Zhao T, Laughrea M, Wainberg MA, Hiscott J. RIG-I-mediated antiviral signaling is inhibited in HIV-1 infection by a protease-mediated sequestration of RIG-I. J Virol. 2011; 85:1224-1236.

40. Boelens MC, Wu TJ, Nabet BY, Xu B, Qiu Y, Yoon T, Azzam DJ, Twyman-Saint Victor C, Wiemann BZ, Ishwaran H, Ter Brugge PJ, Jonkers J, Slingerland J, Minn AJ. Exosome transfer from stromal to breast cancer cells regulates therapy resistance pathways. Cell. 2014; 159:499-513.

41. Ranoa DR, Parekh AD, Pitroda SP, Huang X, Darga T, Wong AC, Huang L, Andrade J, Staley JP, Satoh T, Akira S, Weichselbaum RR, Khodarev NN. Cancer therapies activate RIG-I-like receptor pathway through endogenous non-coding RNAs. Oncotarget. 2016; 7:26496-26515. https://doi.org/10.18632/oncotarget.8420.

42. Zeng Y, Wang PH, Zhang M, Du JR. Aging-related renal injury and inflammation are associated with downregulation of Klotho and induction of RIG-I/NF-kappaB signaling pathway in senescence-accelerated mice. Aging Clin Exp Res. 2016; 28:69-76.

43. Zhao L, Zhu J, Zhou H, Zhao Z, Zou Z, Liu X, Lin X, Zhang X, Deng X, Wang R, Chen H, Jin M. Identification of cellular microRNA-136 as a dual regulator of RIG-I-mediated innate immunity that antagonizes H5N1 IAV replication in A549 cells. Sci Rep. 2015; 5:14991.

44. Karlsen TA, Brinchmann JE. Liposome delivery of microRNA-145 to mesenchymal stem cells leads to immunological off-target effects mediated by RIG-I. Mol Ther. 2013; 21:1169-1181.

45. Barral PM, Sarkar D, Su ZZ, Barber GN, DeSalle R, Racaniello VR, Fisher PB. Functions of the cytoplasmic RNA sensors RIG-I and MDA-5: key regulators of innate immunity. Pharmacol Ther. 2009; 124:219-234.

46. Bork P, Koonin EV. An expanding family of helicases within the 'DEAD/H' superfamily. Nucleic Acids Res. 1993; 21:751-752.

47. Jankowsky E, Jankowsky A. The DExH/D protein family database. Nucleic Acids Res. 2000; 28:333-334.

48. Saito T, Hirai R, Loo YM, Owen D, Johnson CL, Sinha SC, Akira S, Fujita T, Gale M Jr. Regulation of innate antiviral defenses through a shared repressor domain in RIG-I and LGP2. Proc Natl Acad Sci U S A. 2007; 104:582-587.

49. Gack MU, Kirchhofer A, Shin YC, Inn KS, Liang C, Cui S, Myong S, Ha T, Hopfner KP, Jung JU. Roles of RIG-I N-terminal tandem CARD and splice variant in TRIM25-mediated antiviral signal transduction. Proc Natl Acad Sci U S A. 2008; 105:16743-16748.

50. Gack MU, Shin YC, Joo CH, Urano T, Liang C, Sun L, Takeuchi O, Akira S, Chen Z, Inoue S, Jung JU. TRIM25 RING-finger E3 ubiquitin ligase is essential for RIG-I-mediated antiviral activity. Nature. 2007; 446:916-920.

51. Gao D, Yang YK, Wang RP, Zhou X, Diao FC, Li MD, Zhai ZH, Jiang ZF, Chen DY. REUL is a novel E3 ubiquitin ligase and stimulator of retinoic-acid-inducible gene-I. PLoS One. 2009; 4:e5760.

52. Oshiumi H, Matsumoto M, Hatakeyama S, Seya T. Riplet/RNF135, a RING finger protein, ubiquitinates RIG-I to promote interferon-beta induction during the early phase of viral infection. J Biol Chem. 2009; 284:807-817.

53. Seth RB, Sun L, Ea CK, Chen ZJ. Identification and characterization of MAVS, a mitochondrial antiviral signaling protein that activates NF-kappaB and IRF 3. Cell. 2005; 122:669-682.

54. Kawai T, Takahashi K, Sato S, Coban C, Kumar H, Kato H, Ishii KJ, Takeuchi O, Akira S. IPS-1, an adaptor triggering RIG-I- and Mda5-mediated type I interferon induction. Nat Immunol. 2005; 6:981-988.

55. Meylan E, Curran J, Hofmann K, Moradpour D, Binder M, Bartenschlager R, Tschopp J. Cardif is an adaptor protein in the RIG-I antiviral pathway and is targeted by hepatitis C virus. Nature. 2005; 437:1167-1172.

56. Matsuda A, Suzuki Y, Honda G, Muramatsu S, Matsuzaki O, Nagano Y, Doi T, Shimotohno K, Harada T, Nishida E, Hayashi H, Sugano S. Large-scale identification and characterization of human genes that activate NF-kappaB and MAPK signaling pathways. Oncogene. 2003; 22:3307-3318.

57. Huang J, Liu T, Xu LG, Chen D, Zhai Z, Shu HB. SIKE is an IKK epsilon/TBK1-associated suppressor of TLR3- and virus-triggered IRF-3 activation pathways. EMBO J. 2005; 24:4018-4028.

58. Chariot A, Leonardi A, Muller J, Bonif M, Brown K, Siebenlist U. Association of the adaptor TANK with the

I kappa B kinase (IKK) regulator NEMO connects IKK complexes with IKK epsilon and TBK1 kinases. J Biol Chem. 2002; 277:37029-37036.

59. O'Neill LA, Bowie AG. Sensing and signaling in antiviral innate immunity. Curr Biol. 2010; 20:R328-333.

60. Panne D. The enhanceosome. Curr Opin Struct Biol. 2008; 18:236-242.

61. Schroder M, Baran M, Bowie AG. Viral targeting of DEAD box protein 3 reveals its role in TBK1/IKKepsilon-mediated IRF activation. EMBO J. 2008; 27:2147-2157.

62. Baum A, Garcia-Sastre A. Induction of type I interferon by RNA viruses: cellular receptors and their substrates. Amino Acids. 2010; 38:1283-1299.

63. Kovacsovics M, Martinon F, Micheau O, Bodmer JL, Hofmann K, Tschopp J. Overexpression of Helicard, a CARD-containing helicase cleaved during apoptosis, accelerates DNA degradation. Curr Biol. 2002; 12:838-843.

64. Kang DC, Gopalkrishnan RV, Wu Q, Jankowsky E, Pyle AM, Fisher PB. mda-5: An interferon-inducible putative RNA helicase with double-stranded RNA-dependent ATPase activity and melanoma growth-suppressive properties. Proc Natl Acad Sci U S A. 2002; 99:637-642.

65. Cui Y, Li M, Walton KD, Sun K, Hanover JA, Furth PA, Hennighausen L. The Stat3/5 locus encodes novel endoplasmic reticulum and helicase-like proteins that are preferentially expressed in normal and neoplastic mammary tissue. Genomics. 2001; 78:129-134.

66. Yoneyama M, Kikuchi M, Matsumoto K, Imaizumi T, Miyagishi M, Taira K, Foy E, Loo YM, Gale M Jr, Akira S, Yonehara S, Kato A, Fujita T. Shared and unique functions of the DExD/H-box helicases RIG-I, MDA5, and LGP2 in antiviral innate immunity. J Immunol. 2005; 175:2851-2858.

67. Komuro A, Horvath CM. RNA- and virus-independent inhibition of antiviral signaling by RNA helicase LGP2. J Virol. 2006; 80:12332-12342.

68. Rothenfusser S, Goutagny N, DiPerna G, Gong M, Monks BG, Schoenemeyer A, Yamamoto M, Akira S, Fitzgerald KA. The RNA helicase Lgp2 inhibits TLR-independent sensing of viral replication by retinoic acid-inducible gene-I. J Immunol. 2005; 175:5260-5268.

69. Venkataraman T, Valdes M, Elsby R, Kakuta S, Caceres G, Saijo S, Iwakura Y, Barber GN. Loss of DExD/H box RNA helicase LGP2 manifests disparate antiviral responses. J Immunol. 2007; 178:6444-6455.

70. de Veer MJ, Holko M, Frevel M, Walker E, Der S, Paranjape JM, Silverman RH, Williams BR. Functional classification of interferon-stimulated genes identified using microarrays. J Leukoc Biol. 2001; 69:912-920.

71. Leaman DW, Chawla-Sarkar M, Jacobs B, Vyas K, Sun Y, Ozdemir A, Yi T, Williams BR, Borden EC. Novel growth and death related interferon-stimulated genes (ISGs) in melanoma: greater potency of IFN-beta compared with IFN-alpha2. J Interferon Cytokine Res. 2003; 23:745-756.

72. Yu HB, Finlay BB. The caspase-1 inflammasome: a pilot of innate immune responses. Cell Host Microbe. 2008; 4:198-208.

73. Poeck H, Bscheider M, Gross O, Finger K, Roth S, Rebsamen M, Hannesschlager N, Schlee M, Rothenfusser S, Barchet W, Kato H, Akira S, Inoue S, et al. Recognition of RNA virus by RIG-I results in activation of CARD9 and inflammasome signaling for interleukin 1 beta production. Nat Immunol. 2010; 11:63-69.

74. Kubler K, Gehrke N, Riemann S, Bohnert V, Zillinger T, Hartmann E, Polcher M, Rudlowski C, Kuhn W, Hartmann G, Barchet W. Targeted activation of RNA helicase retinoic acid-inducible gene-I induces proimmunogenic apoptosis of human ovarian cancer cells. Cancer Res. 2010; 70:5293-5304.

75. Hou J, Zhou Y, Zheng Y, Fan J, Zhou W, Ng IO, Sun H, Qin L, Qiu S, Lee JM, Lo CM, Man K, Yang Y, et al. Hepatic RIG-I predicts survival and interferon-alpha therapeutic response in hepatocellular carcinoma. Cancer Cell. 2014; 25:49-63.

76. Li D, Gale RP, Liu Y, Lei B, Wang Y, Diao D, Zhang M. 5'-Triphosphate siRNA targeting MDR1 reverses multi-drug resistance and activates RIG-I-induced immune-stimulatory and apoptotic effects against human myeloid leukaemia cells. Leuk Res. 2017; 58:23-30.

77. Kawaguchi Y, Miyamoto Y, Inoue T, Kaneda Y. Efficient eradication of hormone-resistant human prostate cancers by inactivated Sendai virus particle. Int J Cancer. 2009; 124:2478-2487.

78. Jones M, Cunningham ME, Wing P, DeSilva S, Challa R, Sheri A, Padmanabhan S, Iyer RP, Korba BE, Afdhal N, Foster GR. SB 9200, a novel agonist of innate immunity, shows potent antiviral activity against resistant HCV variants. J Med Virol. 2017; 89:1620-1628.

79. Zhu X, Nishimura F, Sasaki K, Fujita M, Dusak JE, Eguchi J, Fellows-Mayle W, Storkus WJ, Walker PR, Salazar AM, Okada H. Toll like receptor-3 ligand poly-ICLC promotes the efficacy of peripheral vaccinations with tumor antigen-derived peptide epitopes in murine CNS tumor models. J Transl Med. 2007; 5:10.

80. Salem ML, El-Naggar SA, Kadima A, Gillanders WE, Cole DJ. The adjuvant effects of the toll-like receptor 3 ligand polyinosinic-cytidylic acid poly (I:C) on antigen-specific CD8+ T cell responses are partially dependent on NK cells with the induction of a beneficial cytokine milieu. Vaccine. 2006; 24:5119-5132.

81. Salazar AM, Levy HB, Ondra S, Kende M, Scherokman B, Brown D, Mena H, Martin N, Schwab K, Donovan D, Dougherty D, Pulliam M, Ippolito M, et al. Long-term treatment of malignant gliomas with intramuscularly administered polyinosinic-polycytidylic acid stabilized with polylysine and carboxymethylcellulose: an open pilot study. Neurosurgery. 1996; 38:1096-1103; discussion 1103-1094.

82. Rosenfeld MR, Chamberlain MC, Grossman SA, Peereboom DM, Lesser GJ, Batchelor TT, Desideri S,

Salazar AM, Ye X. A multi-institution phase II study of poly-ICLC and radiotherapy with concurrent and adjuvant temozolomide in adults with newly diagnosed glioblastoma. Neuro Oncol. 2010; 12:1071-1077.

83. Stupp R, Hegi ME, Mason WP, van den Bent MJ, Taphoorn MJ, Janzer RC, Ludwin SK, Allgeier A, Fisher B, Belanger K, Hau P, Brandes AA, Gijtenbeek J, et al. Effects of radiotherapy with concomitant and adjuvant temozolomide versus radiotherapy alone on survival in glioblastoma in a randomised phase III study: 5-year analysis of the EORTC-NCIC trial. Lancet Oncol. 2009; 10:459-466.

84. Grossman SA, Ye X, Piantadosi S, Desideri S, Nabors LB, Rosenfeld M, Fisher J. Survival of patients with newly diagnosed glioblastoma treated with radiation and temozolomide in research studies in the United States. Clin Cancer Res. 2010; 16:2443-2449.

85. Okada H, Butterfield LH, Hamilton RL, Hoji A, Sakaki M, Ahn BJ, Kohanbash G, Drappatz J, Engh J, Amankulor N, Lively MO, Chan MD, Salazar AM, et al. Induction of robust type-I CD8+ T-cell responses in WHO grade 2 low-grade glioma patients receiving peptide-based vaccines in combination with poly-ICLC. Clin Cancer Res. 2015; 21:286-294.

86. Dillon PM, Petroni GR, Smolkin ME, Brenin DR, Chianese-Bullock KA, Smith KT, Olson WC, Fanous IS, Nail CJ, Brenin CM, Hall EH, Slingluff CL Jr. A pilot study of the immunogenicity of a 9-peptide breast cancer vaccine plus poly-ICLC in early stage breast cancer. J Immunother Cancer. 2017; 5:92.

87. Mehrotra S, Britten CD, Chin S, Garrett-Mayer E, Cloud CA, Li M, Scurti G, Salem ML, Nelson MH, Thomas MB, Paulos CM, Salazar AM, Nishimura MI, et al. Vaccination with poly(IC:LC) and peptide-pulsed autologous dendritic cells in patients with pancreatic cancer. J Hematol Oncol. 2017; 10:82.

88. Tsuji T, Sabbatini P, Jungbluth AA, Ritter E, Pan L, Ritter G, Ferran L, Spriggs D, Salazar AM, Gnjatic S. Effect of Montanide and poly-ICLC adjuvant on human self/tumor antigen-specific CD4+ T cells in phase I overlapping long peptide vaccine trial. Cancer Immunol Res. 2013; 1:340-350.

89. Sabbatini P, Tsuji T, Ferran L, Ritter E, Sedrak C, Tuballes K, Jungbluth AA, Ritter G, Aghajanian C, Bell-McGuinn K, Hensley ML, Konner J, Tew W, et al. Phase I trial of overlapping long peptides from a tumor self-antigen and poly-ICLC shows rapid induction of integrated immune response in ovarian cancer patients. Clin Cancer Res. 2012; 18:6497-6508.

90. Rapoport AP, Aqui NA, Stadtmauer EA, Vogl DT, Xu YY, Kalos M, Cai L, Fang HB, Weiss BM, Badros A, Yanovich S, Akpek G, Tsao P, et al. Combination immunotherapy after ASCT for multiple myeloma using MAGE-A3/Poly-ICLC immunizations followed by adoptive transfer of vaccine-primed and costimulated autologous T cells. Clin Cancer Res. 2014; 20:1355-1365.

91. Yuan D, Xia M, Meng G, Xu C, Song Y, Wei J. Anti-angiogenic efficacy of 5'-triphosphate siRNA combining VEGF silencing and RIG-I activation in NSCLCs. Oncotarget. 2015; 6:29664-29674. https://doi.org/10.18632/oncotarget.4869.

92. Buers I, Nitschke Y, Rutsch F. Novel interferonopathies associated with mutations in RIG-I like receptors. Cytokine Growth Factor Rev. 2016; 29:101-107.

93. Lee-Kirsch MA. The Type I Interferonopathies. Annu Rev Med. 2017; 68:297-315.

94. Trinchieri G. Type I interferon: friend or foe? J Exp Med. 2010; 207:2053-2063.

95. Palmer CR, Jacobson ME, Fedorova O, Pyle AM, Wilson JT. Environmentally Triggerable Retinoic Acid-Inducible Gene I Agonists Using Synthetic Polymer Overhangs. Bioconjug Chem. 2018; 29:742-747.